

Reservoir Characterization of the Middle  
Pennsylvanian Cleveland Sandstone, Cleveland Field  
Unit, Pawnee County, Oklahoma

By

CURTIS MARTIN RODDY

Bachelor of Science in Geology

Oklahoma State University

Stillwater, Oklahoma

2012

Submitted to the Faculty of the  
Graduate College of the  
Oklahoma State University  
in partial fulfillment of  
the requirements for  
the Degree of  
MASTER OF SCIENCE  
July, 2014

Reservoir Characterization of the Middle Pennsylvanian Cleveland Sandstone,  
Cleveland Field Unit,  
Pawnee County, Oklahoma

Thesis Approved:

Dr. James O. Puckette

---

Thesis Adviser

Dr. Gary F. Stewart

---

Dr. John W. Shelton

---

Name: Curtis Roddy

Date of Degree: July 2014

Title of Study: RESERVOIR CHARACTERIZATION OF THE MIDDLE PENNSYLVANIAN CLEVELAND SANDSTONE, CLEVELAND FIELD UNIT, PAWNEE COUNTY, OKLAHOMA.

Major Field: Geology

Abstract:

The Cleveland Field Unit has produced an estimated 50 MMBO since its discovery in 1904. Wireline data from old oil fields is sparse and has a resolution much lower than that of modern conventional wireline logs. Consequently, oil-in-place calculations commonly are underestimated. By use of data from cores, borehole-image logs, and modern well-logs, in-place oil and gas volumes can be estimated more accurately.

The purpose of this study was to re-evaluate a mature oil and gas field by use of high-resolution reservoir data in a manner that estimates oil and gas volumes and accurately identifies bypassed "pay". This thesis presents data obtained from the Middle Pennsylvanian (Desmoinesian) Cleveland Sandstone in what is now the Cleveland Field Unit. The Cleveland Sandstone is composed of four distinct depositional units, and these units range in thickness from 5 ft. to 100 ft. Oil-and-gas-bearing zones, commonly interstratified with siltstone and shale, have been discounted because the values recorded by vintage wireline logs led to an under-calculation of in-place oil volumes due to the low resolution of those wireline tools (gamma-ray, induction, and micro-log). This study is thought to have potential application in other mature oil and gas fields producing from fluvial/deltaic depositional systems in the Mid-Continent.

## TABLE OF CONTENTS

Chapter	Page
I. Introduction .....	1
Purpose of Research.....	2
Study Area .....	4
General Methods.....	4
Previous Investigations .....	8
II. Geologic Setting .....	11
Regional Stratigraphy .....	11
Regional Structure .....	13
Local Structure.....	16
III. Stratigraphic Framework .....	19
IV. Petrography and Sedimentology.....	24
Introduction.....	24
Characterization of Rock-Stratigraphic Units (Zones) .....	26
Cleveland “A” Zone.....	26
Cleveland “B” Zone.....	30
Cleveland “C” Zone.....	33
Cleveland “D” Zone.....	37
Associations of Electrofacies and Depositional Setting .....	42
VI. Petrophysical Analysis.....	46
Introduction.....	46
Availability of Data.....	47
Methods and Calculations.....	47
Interpretation of Data from Cores.....	48
Mineralogy and Grain Size .....	48
Grain Density .....	50
Porosity and Permeability .....	51
Petrophysical Attributes and Integration of Data from Analysis of Cores .....	58

Shale Volume .....	58
Porosity .....	60
Water Saturation .....	62
Chapter	Page
VII. Petroleum Geology and Reservoir Geometry .....	65
Reservoir Geometry Thickness and Distribution.....	65
Net Pay, Petroleum-bearing Sandstone.....	66
Estimation of Reserves .....	67
VIII. Discussion and Conclusions.....	73
Discussion.....	73
Conclusions.....	78
REFERENCES .....	79
APPENDICES .....	81
Appendix A: Core Sample Acquisition Procedures .....	81
Appendix B: Laser Particle-Size Analysis (LPSA) Results .....	83
Appendix C: Pickett Plot, Cleveland Sand Interval.....	86
Appendix D: Well Data .....	88
Appendix E: Cross-Section Location Map and Cross-Sections .....	90
Appendix F: Petrophysical Evaluation of the J.A Jones No.58 .....	100

## LIST OF TABLES

Table	Page
5.1 Summary of average core porosity and permeability .....	51
5.2 Summary of average porosity and permeability, J.A Jones No.58.....	55
5.3 Summary of average porosity and permeability, Frazee No.22.....	55
5.4 Summary of average porosity and permeability, Van Eman No.16 .....	55
5.5 Summary of petrophysical analysis .....	64
6.1 Summary of cut-offs for net pay maps .....	66

## LIST OF FIGURES

Figure	Page
1.1) Geologic Provinces of Oklahoma.....	3
1.2) Map of study area .....	6
1.3) Key vintage-wireline log, Cleveland Sandstone .....	7
1.4) Cleveland Sandstone reference log with depositional interpretation .....	10
2.1) Stratigraphic nomenclature, Desmoinesian formations.....	12
2.2) Regional representative log of Cleveland Sandstone interval.....	14
2.3) Regional structural map of the Checkerboard Limestone .....	15
2.4) Local structural map of the Checkerboard Limestone .....	16
2.5) Rose plot of fractures, Cleveland Sandstone.....	17
2.6) Cross-section depicting the structure of the Cleveland Sandstone.....	18
3.1) Cleveland Sandstone, representative log depicting internal stratigraphy.....	21
3.2) Northeast-to-southwest gamma-ray cross-section through the study area .....	22
3.3) Map of line of cross-section in Figure 3.2.....	23
4.1) Location map of cores examined.....	25
4.2) Core photographs, Cleveland “A” zone .....	26
4.3) Core photographs, Cleveland “A” zone .....	27
4.4) Photomicrograph, Cleveland “A” zone .....	28
4.5) Photomicrograph, Cleveland “A” zone (detail of part of Figure 4.4) .....	28

4.6)	XRD diffractogram, Cleveland "A zone" .....	29
4.7)	Core photographs, Cleveland "B" zone .....	30
4.8)	Core photographs, Cleveland "B" zone .....	31
4.9)	Photomicrograph, Cleveland "B" zone .....	32
4.10)	Photomicrograph, Cleveland "B" zone (detail of part of figure 4.9) .....	32
4.11)	Core photographs, Cleveland "C" zone .....	33
4.12)	XRD diffractogram, Cleveland "C" zone.....	34
4.13)	Core photographs, Cleveland "C" zone .....	35
4.14)	Photomicrograph, Cleveland "C" zone .....	36
4.15)	Photomicrograph, Cleveland "C" zone (detail of part of figure 4.14) .....	36
4.16)	Core photographs, Cleveland "D" zone .....	37
4.17)	Photomicrograph, Cleveland "D" zone .....	38
4.18)	Photomicrograph, Cleveland "D" zone (detail of part of figure 4.18) .....	38
4.19)	XRD diffractogram, Cleveland "D" zone .....	39
4.20)	Core photographs, Cleveland "D" zone .....	40
4.21)	Photograph of entire core from J.A Jones No.58 .....	41
4.22)	Cleveland interval Electrofacies, SP log .....	44
4.23)	Wireline-log suite with core photographs, J.A Jones No.58 .....	45
5.1)	Pie chart with average composition of Cleveland from XRD analysis.....	49
5.2)	Cross-plot, grain density versus porosity .....	50
5.3)	Cross-plot, permeability versus porosity, Cleveland "A" zone.....	52



5.4)	Cross-plot, permeability versus porosity, Cleveland “B” zone.....	52
5.5)	Cross-plot, permeability versus porosity, Cleveland “C” zone.....	53
5.6)	Cross-plot, permeability versus porosity, Cleveland “D” zone.....	53
5.7)	Core-plug photograph, Van Eman No.16.....	56
5.8)	Core-plug photograph, Van Eman No.16 (enlargement of figure 5.7) .....	56
5.9)	Core-plug photograph, Van Eman No.16 (enlargement of figure 5.8) .....	57
5.10)	Composite gamma-ray histogram, Cleveland Sandstone interval.....	59
5.11)	Cross-plot, total core porosity versus total porosity .....	61
6.1)	Gross thickness map, Cleveland Sandstone .....	68
6.2)	Net pay map, Cleveland “A” zone .....	69
6.3)	Net pay map, Cleveland “B” zone.....	70
6.4)	Net pay map, Cleveland “C” zone.....	71
6.5)	Net pay map, Cleveland “D” zone .....	72
7.1)	Spectrascan image, J.A Jones No. 58.....	77

## CHAPTER I

### **Introduction**

The initial discovery of oil and gas in rocks known as Cleveland Sandstone was in 1904, near the town of Cleveland, Pawnee County, Oklahoma (Campbell, 1997). Of all geologic provinces in Oklahoma (Figure 1.1), the Cherokee Platform is the most productive of oil from the Cleveland stratigraphic interval. The majority of this exploration was conducted in the early 1900's, using cable-tool drilling rigs. Before the middle 1900's, the "boom" of Cleveland exploration was over in order to exploit deeper reservoirs (Bartlesville Sandstone, Simpson, and Arbuckle). As a result, very little modern data exists on the Cleveland reservoir. It is known that the Cleveland Sandstone has produced an estimated 50 MMBO during primary and secondary production, with the majority of petroleum having been produced by 1935. Today the Cleveland Sandstone is a target for secondary recovery in many mature oil fields within the Cherokee Platform region.

Classifications of some of the rock-stratigraphic units cited in this thesis are informal. Among the publications relevant to this study, usage of names of rock-stratigraphic and time-stratigraphic units is inconsistent. The names of subsurface rock-stratigraphic units herein are those shown by Jordan (1957), whose work is thought to be reliable.

## Purpose of Research

The purpose of this study was to acquire, analyze, and interpret data about the Cleveland Sandstone in northeastern Oklahoma to properly characterize the reservoir in the Cleveland field. Prior investigations into the Cleveland Sandstone were based primarily on wireline logs recorded before 1950, and drillers' descriptions of rock samples obtained while drilling. Recently Mid-Con Energy, LLC initiated a drilling and data-acquisition program targeting the Cleveland Sandstone for the purpose of recovery by waterflood. The primary objectives of this study are to:

1. Refine stratigraphic correlations within the Cleveland interval and identify lithofacies from conventional cores and borehole-image logs to modern conventional wireline logs to vintage logs, as quality of data allows.
2. Apply results of petrophysical analyses to parts of the study area where data is not readily available.
3. Estimate depositional environment for each lithofacies within subdivisions of the Cleveland Sandstone.
4. Estimate the current and original oil-in-place by using capillary-pressure data and relative permeability data obtained from whole-core analyses.
5. Develop an analog for exploitation of Pennsylvanian sandstones on the Cherokee Platform.

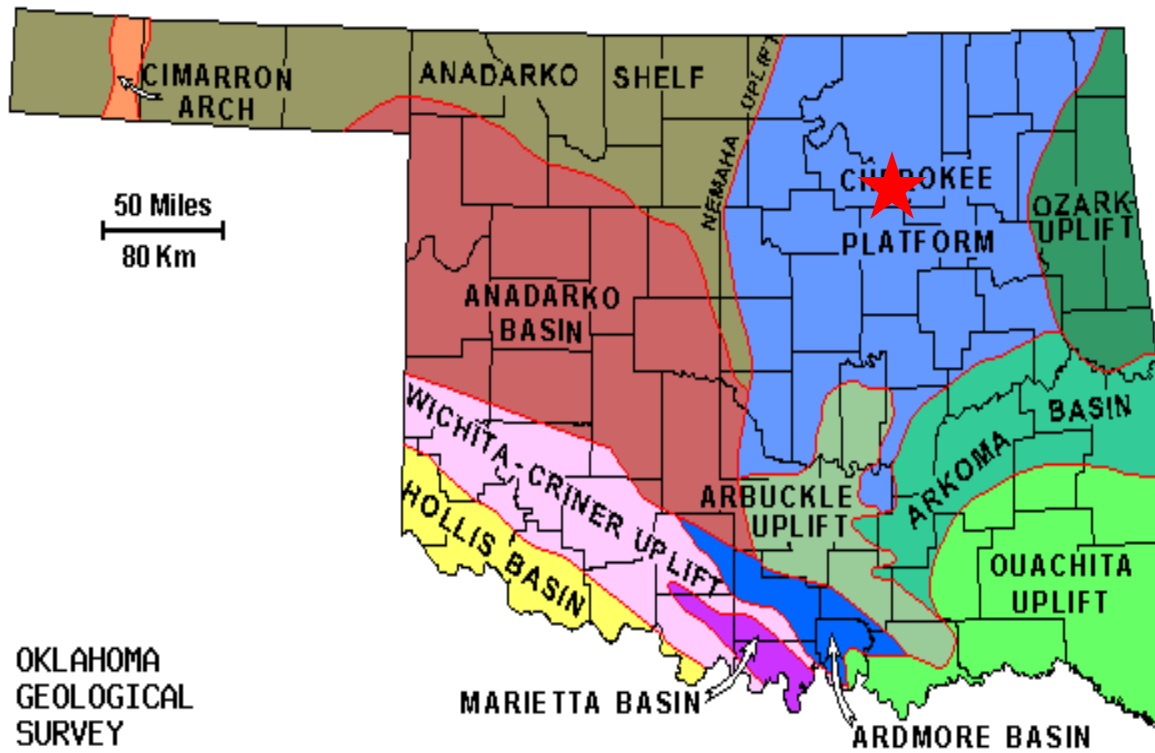


Figure 1.1: Geologic provinces of Oklahoma (modified after Campbell, 1997), showing the relation of the Cherokee Platform to the other geological provinces in Oklahoma. Red star represents the approximate location of the study area.

## **Study Area**

This study focuses on the Cleveland Field Unit of Pawnee County, Oklahoma. The Cleveland Field Unit is in Township 21 North, Range 8 East, in northeastern Oklahoma and consists of 1,760 acres (Figure 1.2). Within this unit, all Pennsylvanian formations in the subsurface have been unitized in order to produce the remaining oil reserves more efficiently by secondary-recovery methods. The Cleveland Field Unit was chosen for this study because of the immense amount of data available and the lengthy history of the field. Data available include conventional wireline logs (gamma ray, spontaneous potential, resistivity, density, and neutron), borehole image logs (Baker Atlas Star © or Weatherford Compact Micro-Imager ©), whole cores, thin sections, and bit cuttings.

## **General Methods**

The primary source of data for field-wide evaluation of the Cleveland Sandstone is wireline logs. The study area contains 204 wells with approximately 400 conventional wireline logs (gamma ray, spontaneous potential, resistivity, density, and neutron), and the majority of these wireline logs were recorded before 1950 (referred to herein as “vintage logs”). Because of the poor resolution of some logs (for example, see Figure 1.3), vintage logs were used only for calculations of elevations of lithostratigraphic marker beds and for thicknesses of some rock-stratigraphic units.

Wireline logs were used in the construction of eight cross sections, utilizing Petra® for assistance in the mechanics of their construction. Wireline-log data was also evaluated by use of Hydrocarbon Data System’s HDS 2000® petrophysical evaluation software. Structural geologic and thickness maps were prepared in order to describe the geometry and distribution of the Cleveland Sandstone and its internal rock-stratigraphic units across the Cleveland Field Unit. The top and base of the Cleveland Sandstone are easily identifiable in both vintage and modern wireline logs. In order to distinguish rock-stratigraphic units within the Cleveland

stratigraphic interval, only modern wireline logs were used. These modern logs have much better vertical resolution than vintage logs and provide uniform data of almost uniform quality across the field. Three borehole image logs were used. Resolution of these borehole image logs is much greater than that of conventional wireline logs; in most cases, vertical resolution is accurate to two inches. Correlation by borehole-image logs and core lithofacies was superior to correlation by conventional wireline logs.

Whole cores of the entire Cleveland Formation from three wells were obtained: Mid-Con Energy No. 16 Van Eman (T.21N, R.8E, Sec.30), Mid-Con Energy No.58 J.A. Jones (T.21N, R.8E, Sec.20), and Mid-Con Energy No.22 Frazee (T.21N, R.8E, Sec.29) (These cores were integrated with wireline and borehole-image logs in order to calibrate and correlate features in core to the logs.) The cores were sampled for routine core analysis, as well as X-ray diffraction analysis, thin section-petrography, capillary pressure, laser particle-size analysis, and relative permeability. This data aided in developing a hypothesis for the depositional setting of each lithofacies and calculating oil-in-place volumes within the Cleveland Sandstone. Samples were prepared by Core Lab laboratories and by Mid-Con Energy geology and engineering staff.

Approximately 20 thin-sections were analyzed using a Leica DM EP polarizing microscope. Of these thin sections, 10 were analyzed by point-counting. For each thin section point-counted, 100 points were inspected to determine authigenic and detrital mineral constituents, porosity, and type of cement. X-ray diffraction analysis of powdered samples from core plugs was completed by using a Phillips PW3020 X-ray diffractometer.

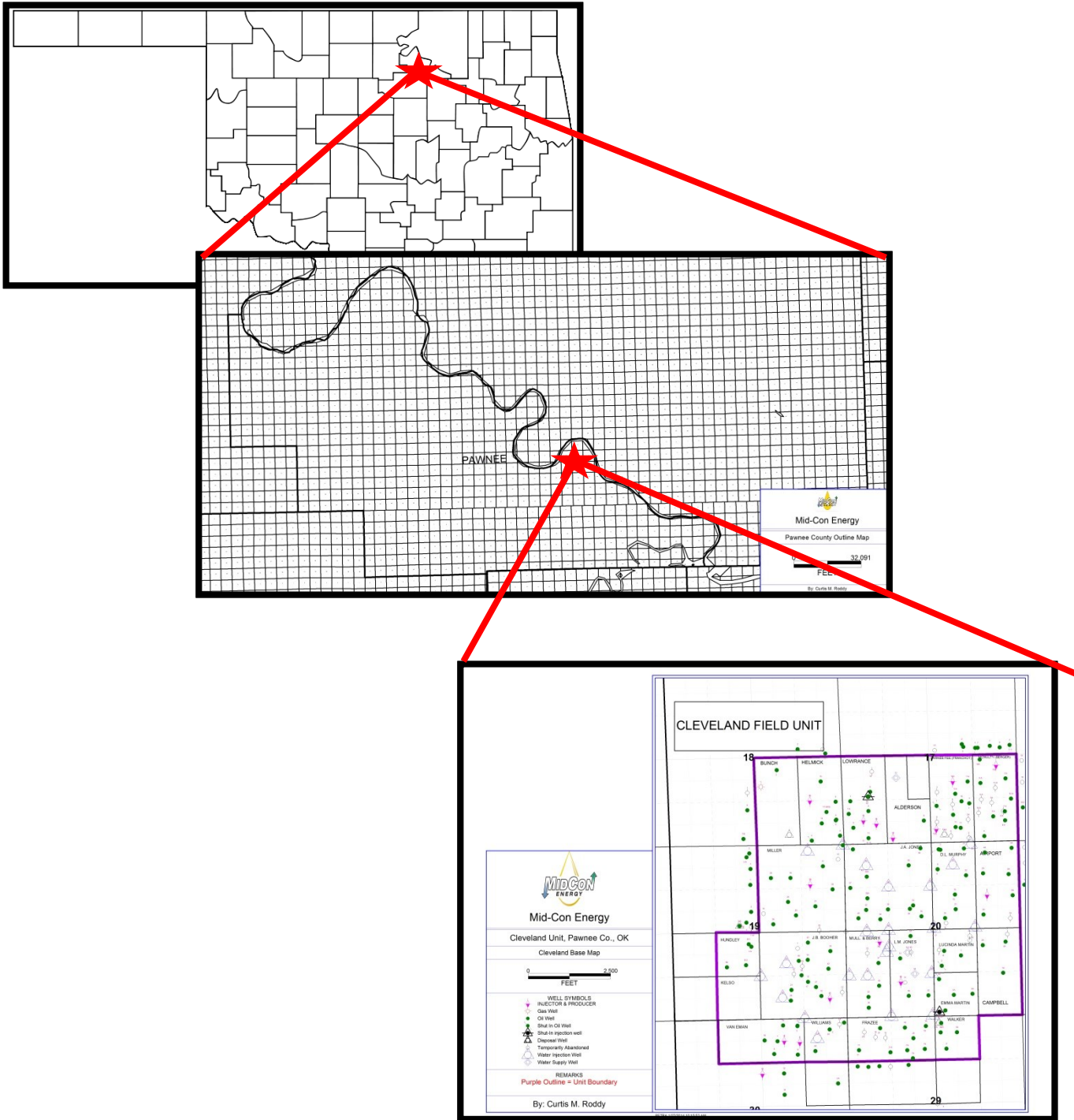


Figure 1.2: Maps of Oklahoma, Pawnee Co., Oklahoma and the Cleveland Field Unit. This succession of maps is intended to highlight the area in which this study was conducted. The Cleveland Field Unit is located in T.21N, R.8E, Pawnee Co., Oklahoma.

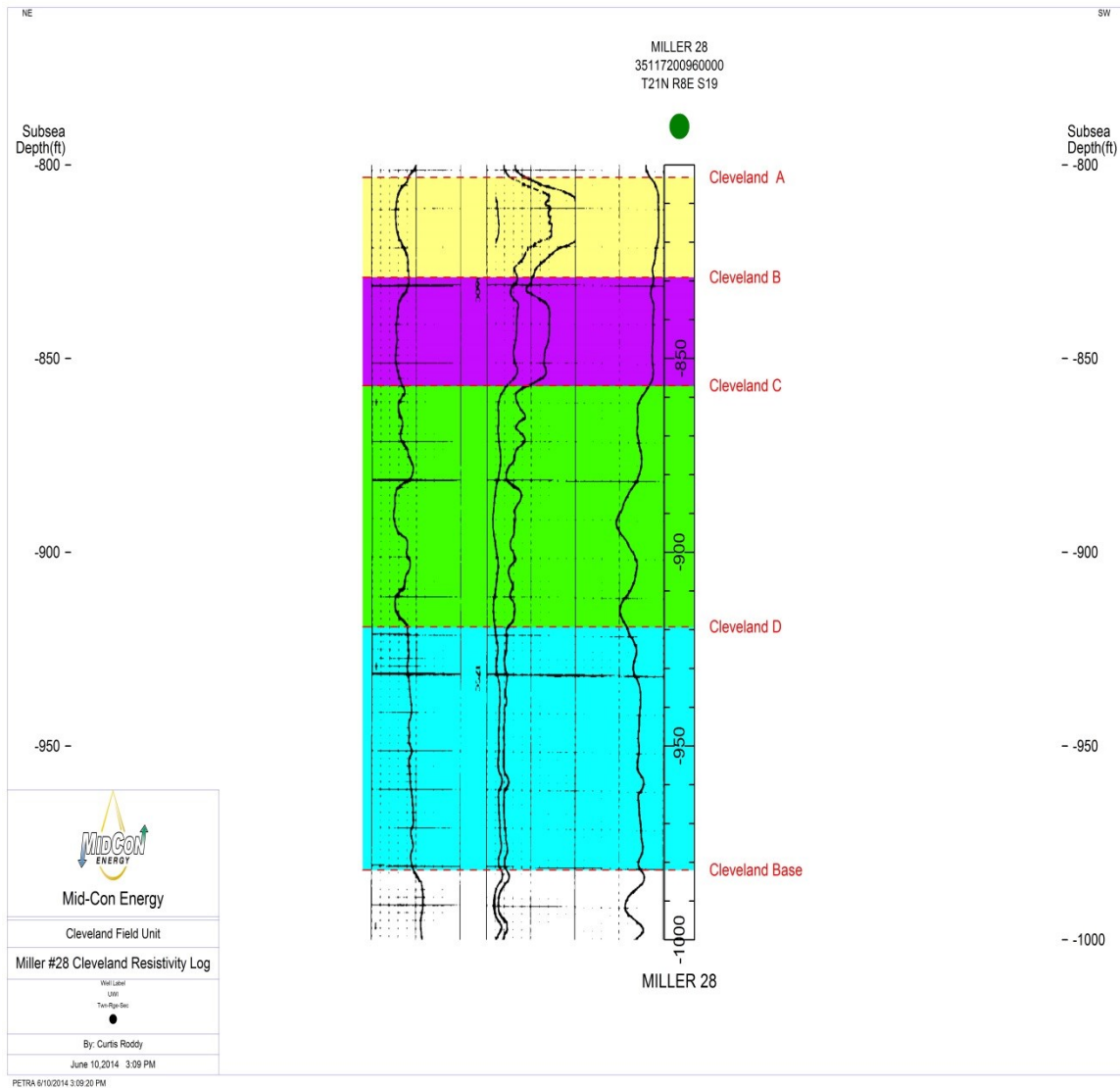


Figure 1.3: Spontaneous potential and resistivity logs from the Miller #28 (T.21N, R.8E, Sec.19) as an example of a wireline log that has poor resolution. The “A” (yellow) and “B” (magenta) zones appear to be the only zones above an oil/water contact. Modern, higher resolution logs most commonly show a higher resistivity and demonstrate that much of the “C” (green) zone is above its respective oil/water contact.



## **Previous Investigations**

The Cleveland Sandstone has produced large quantities of oil and gas within northern Oklahoma. The shallow depth of the Cleveland in this area and its development early in the 20<sup>th</sup> century has resulted in very little published literature on this interval, with information on it commonly in generalized studies of Pennsylvanian strata in the Cherokee Platform region (Clare, 1963, pp. 29-30).

The Cleveland Sandstone was described by Clare (1963) as being dull white to gray, coarse-grained, micaceous, calcareous sandstone. Campbell (1997) provided a detailed interpretation of the Cleveland Sandstone's depositional environment based on characteristics of gamma-ray and spontaneous-potential curves. The lower zone was described by Campbell as being of marine origin and the upper zone was interpreted as fluvial-deltaic. The marine origin of the "lower Cleveland" was based on glauconite in drill samples. Baker (1958) described the "lower Cleveland" as being a delta-front (shallow-marine) deposit and the "upper Cleveland" as a delta-plain deposit (Figure 1.4). The source of the Cleveland Sandstone has been widely accepted as having been the Ouachita uplift (Rascoe and Adler, 1983). This is based on the presence of Lower Pennsylvanian type siliciclastics. Krumme (1981) mapped the general thickness of the Cleveland Sandstone regionally as a series of channels, ranging in thickness from 10' to 160'. This study area was mapped by Krumme as being part of the "Kiefer" channel in northeastern Oklahoma. The Kiefer channel generally flowed from southeast to northwest.

The majority of the modern literature related to the Cleveland Sandstone describes it in the area west of the Nemaha uplift in the region commonly referred to as the "Anadarko Basin". There it is much deeper (typically from 5,000 ft. to 10,000 ft.) than on the Cherokee Platform of Oklahoma (typically 1,500 ft. to 3,000 ft. deep). The only modern literature relating to the Cleveland Sandstone in the Cherokee Platform region was published by Krystinik and Lupo (2011), who describe the environments of the Cleveland Sandstone as deltaic and incised

valleys, separated by baffles. The incised valleys compose two-thirds of the Cleveland Sandstone and tend to be the best petroleum reservoirs. Using seismic maps, Krystinik and Lupo (2011) have been able to differentiate between the upper Cleveland deltaic reservoirs above the incised-valley unit. In differentiating between these reservoirs it was possible to target only the oil-bearing reservoirs with horizontal wells (Krystinik and Lupo, 2011; Krystinik, 2013).

Arco Oil and Gas Co./  
RDT Properties, Inc.  
no. 55 J. A. Jones  
SE SE NW Sec. 20, T. 21 N., R. 8 E.

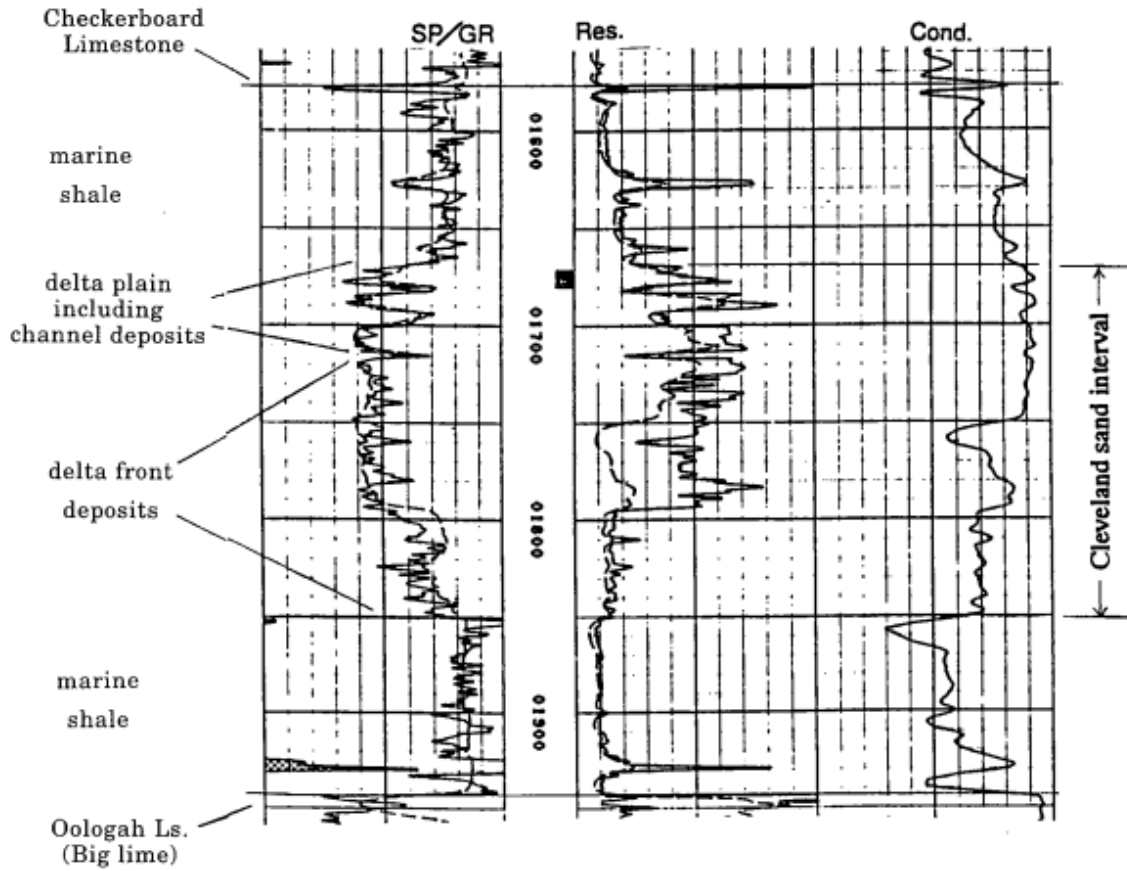


Figure 1.4: Cleveland Sandstone reference log depicting an interpretation of the depositional environment for the Cleveland Sandstone interval. The log is composed of spontaneous potential (SP) and gamma-ray (GR) curves in the left-hand track and resistivity and conductivity curve in the right-hand track (from Campbell, 1997).

## CHAPTER II

### Geologic Setting

#### Regional Stratigraphy

Though the boundary between the Upper and Middle Pennsylvanian is often not well defined in Oklahoma true Cleveland Sandstone is included in the Skiatook Group, above the Nuyaka Creek Shale. The informal Cleveland sandstone in the subsurface is often Middle Pennsylvanian Series (Desmoinesian) (Hemish, 1989; Tulsa Geological Society, 1989; Cole, 1967; Heckel, 1991; Fay, 1987; Campbell, 1997) (Figure 2.1). In northeastern Oklahoma, the majority of wells are drilled through the Cleveland Sandstone to the Bartlesville Sandstone or older formations. Therefore, data that can be used to map the Cleveland Sandstone on a regional scale is abundant. The Cleveland Sandstone is within the stratigraphic interval between the Checkerboard Limestone (above) and the “Big Lime” (below) (Figure 2.1). The Checkerboard is extensive and easily identifiable in both wireline (Figure 2.2) and drillers’ logs. Therefore, the Checkerboard is a convenient marker for mapping the Cleveland Sandstone regionally (Figure 2.3) (Campbell, 1997). Within the region, the Cleveland varies from less than 100 ft. thick to approximately 700 ft. thick (Krumme, 1981). The Cleveland Sandstone is divided informally into upper and lower zones. The “Upper Cleveland” can easily be identified by the sharp contrast in porosity (greater than 10% density-porosity units) and gamma ray (less than 85 API), compared to the overlying shale; it has a serrated blocky-shaped gamma-ray signature (Figure 2.2).

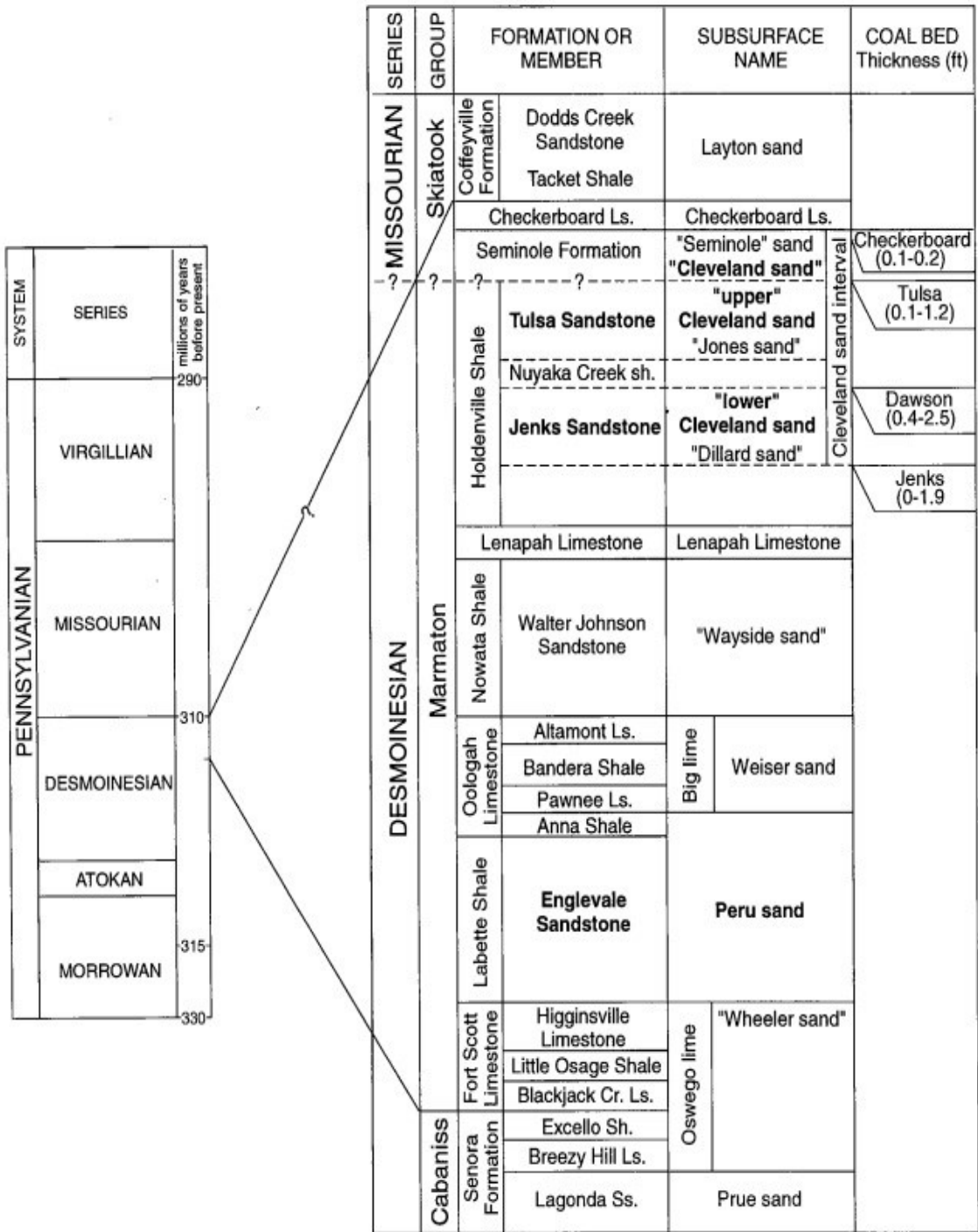


Figure 2.1 Stratigraphic nomenclature of the Pennsylvanian Marmaton Group and adjacent strata (from Campbell, 1997).

In some areas, the “Lower Cleveland” is separated from the “Upper Cleveland” by shale. The “Lower Cleveland” has an apparent serrated-funnel-shaped gamma-ray signature, but the base is characteristically sharp, as defined by marked sharp changes in porosity, gamma-ray, and resistivity.

## **Regional Structure**

The Cherokee Platform is bounded to the west by the Nemaha uplift, to the east by the Ozark Mountains, and to the south by the Arkoma basin. The Cushing structure with culminations along it (Bennison, 1964) represents the most significant structural feature in the region. Surface-expressed, closed anticlines (e.g., Shamrock and Dropright domes), along with groups of more gentle folds (Powers, 1933), are characteristics of the region. As a result of the importance anticlines have played in oil and gas exploration, the anticlines in the region have been carefully described. The most obvious trend observed in northeastern Oklahoma anticlines reflects the underlying fault trends, the most common of which is southwest-northeast to south-southwest - north-northeast (Powers, 1933). Tectonic activity, which occurred post-Arbuckle, post-Simpson, pre-Woodford, post-Osage, and post-Permian (and pre-Quaternary) times (Campbell, 1997; Eardley, 1951; Powers, 1933), has influenced thicknesses and trends of Pennsylvanian reservoirs in the region, primarily by movement along strike-slip faults. Faults displacing Pennsylvanian strata in the region generally have throws of less than 30 ft. (Powers, 1933).

JONES 57  
35117234210000  
MID-CON ENERGY  
T21N R8E S20

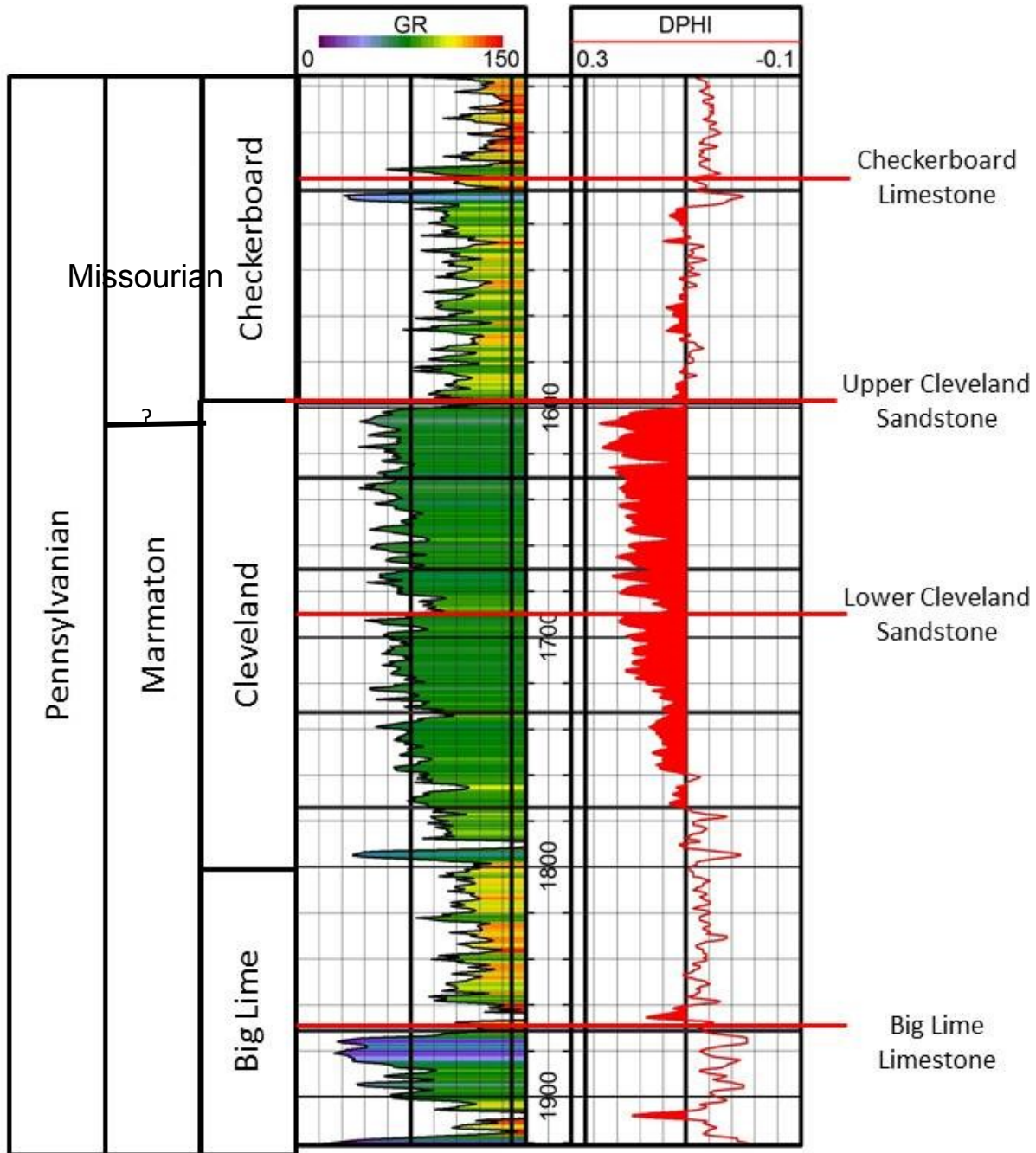


Figure 2.2: Representative log of the upper part of the Marmaton Group, Cleveland Field Unit (J.A Jones #57, Mid-Con Energy, and T.21N, R.8E, Sec.20). This well is adjacent to the J.A Jones #55 (T.21N, R.8E, Sec.20; Figure 1.4). Gamma-ray is measured in API units and DPHI (Density porosity) is measured in porosity units. Green dot at top of well log represents symbol for oil well.

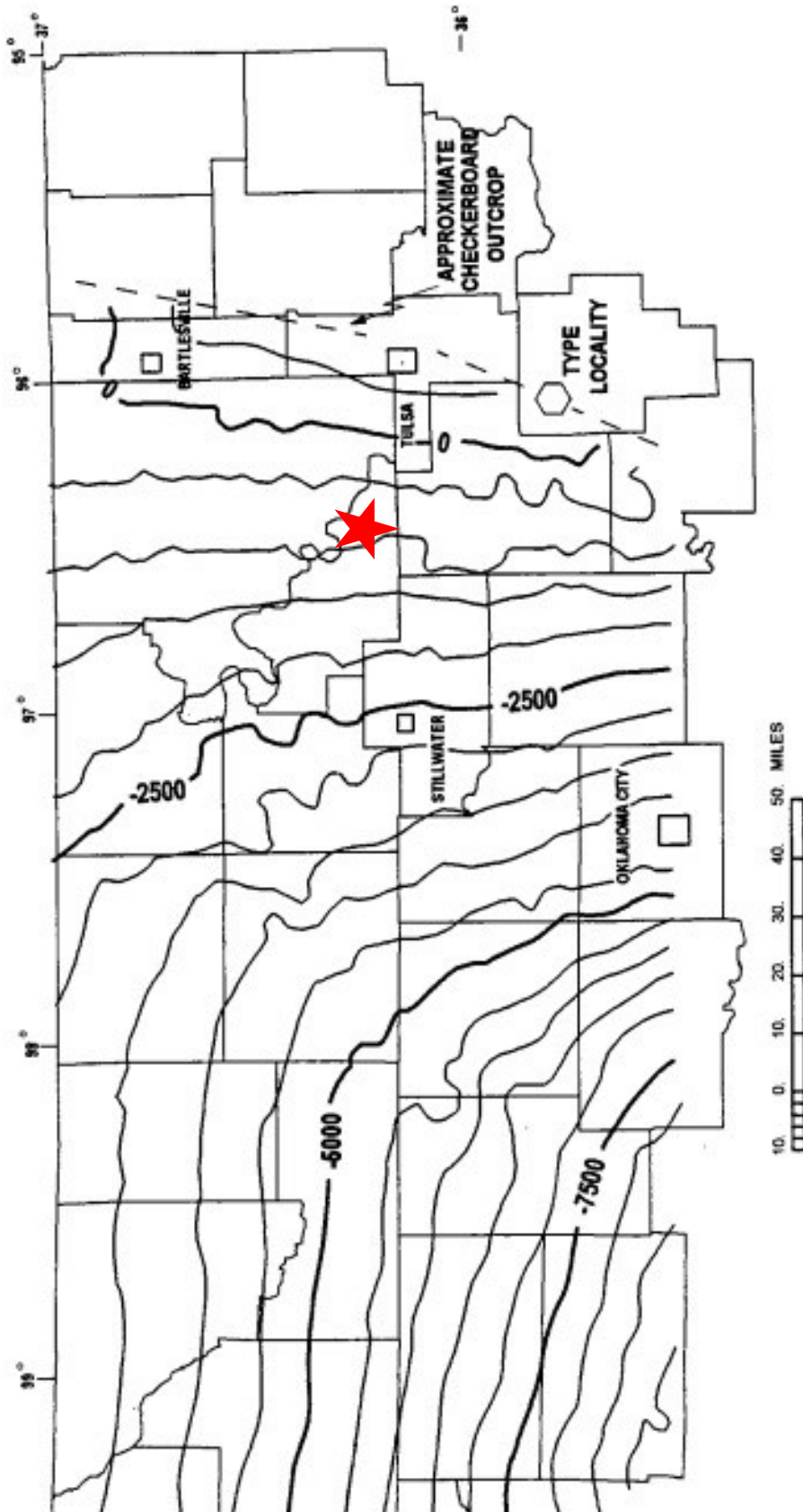


Figure 2.3: Regional structure of the Missourian Checkerboard Limestone, showing gentle overall dip to the west in Pawnee Co. The Checkerboard is a laterally extensive limestone that is easily mapped across the Cherokee Platform. Sea-level datum, C.I. = 500ft. Red star marks the approximate location of this study. (Modified from Campbell, 1997.)



## Local Structure

A structural contour map of the top of the Checkerboard Limestone (Figure 2.4) shows the local, prominent anticlinal structure of the Cleveland Field Unit, commonly referred to as the “Cleveland dome.” The Checkerboard Limestone was selected to map because of its proximity to the Cleveland zone and because it is easily identifiable throughout the region and field

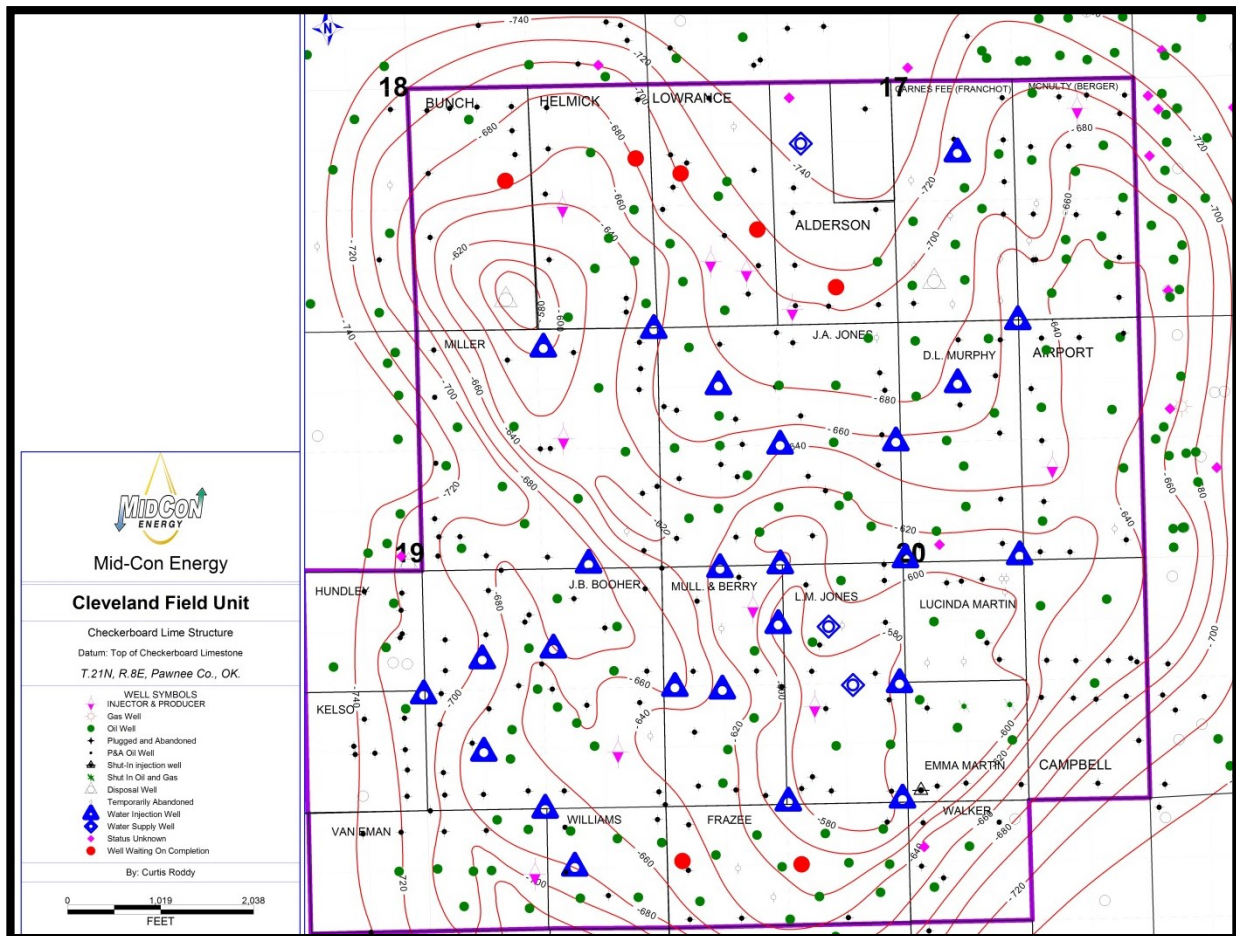


Figure 2.4: Structural contour map of the top of the Checkerboard Limestone, Cleveland Field Unit, T.21N, R.8E, defining “Cleveland dome.” Subsea elevations. C.I. 20 ft.

Pre-Pennsylvanian formations within the Cleveland Field Unit show the same domal configuration shown by the Checkerboard Limestone. This anticlinal fold is reflected in the subsurface rocks.

. The structural dip in the study area ranges from 20 ft. to 100 ft. per mile. The magnitude of the dip increases as depth decreases. Analysis of compact micro-imaging (CMI) logs indicates an east-northeast trend of fractures in the field area (Figure 2.5). The trend of the fractures allows an estimate of the stress field, with the fractures oriented normal to the minimum principal stress ( $\sigma_{\min}$ , or  $P_{\min}$  in Figure 2.5).

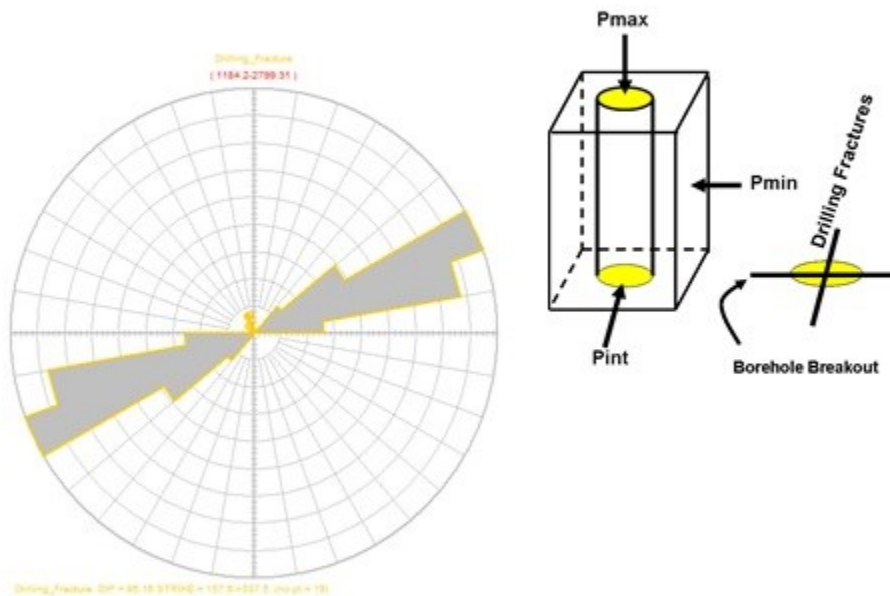


Figure 2.5: Rose plot of fracture orientation taken from Weatherford Image (CMI) Logs, Mid-Con Energy, Frazee #22 located in T.21N, R.8E, Sec.30. Interpretation of this log by M. Grace (2014).



## CHAPTER III

### Stratigraphic Framework

The Cleveland Sandstone has been divided traditionally into two distinct stratigraphic units (zones) in areas on the Cherokee Platform, the upper and the lower Cleveland (Figure 2.2; Campbell, 1997 and Krystinik, 2011). These divisions are informal and are based on general observations from wireline logs in the region. Within the study area for this thesis, the Cleveland Sandstone has been divided vertically into four distinct subdivisions. Figure 3.1 is a representative log of the Cleveland stratigraphic interval; it shows the local internal stratigraphic nomenclature.

The Cleveland “A” and “B” zones thin from west-to-east across the field and are absent in some areas. The Cleveland “C” and “D” zones are present throughout the field and show no distinct thickening or thinning patterns. Figure 3.2 is a northeast-to-southwest stratigraphic cross-section across the study area (Figure 3.3). This cross-section depicts the localized thickening and thinning described above. Divisions of the Cleveland stratigraphic interval are based on evidence documented from cores correlated with wireline-log signatures. These zones were established using observations from core examination, together with correlation of wireline logs, in order to establish the local distribution of each of the four zones ad-hoc stratigraphic units.

The Cleveland "A" was cored only in one well (Mid-Con Energy, Van Eman No.16) and is not present in either of the other two cored wells. Cleveland "B", "C", and "D" zones are in all three cores collected from within the study area. The overlying sandy shale and underlying shale were cored in all three wells.

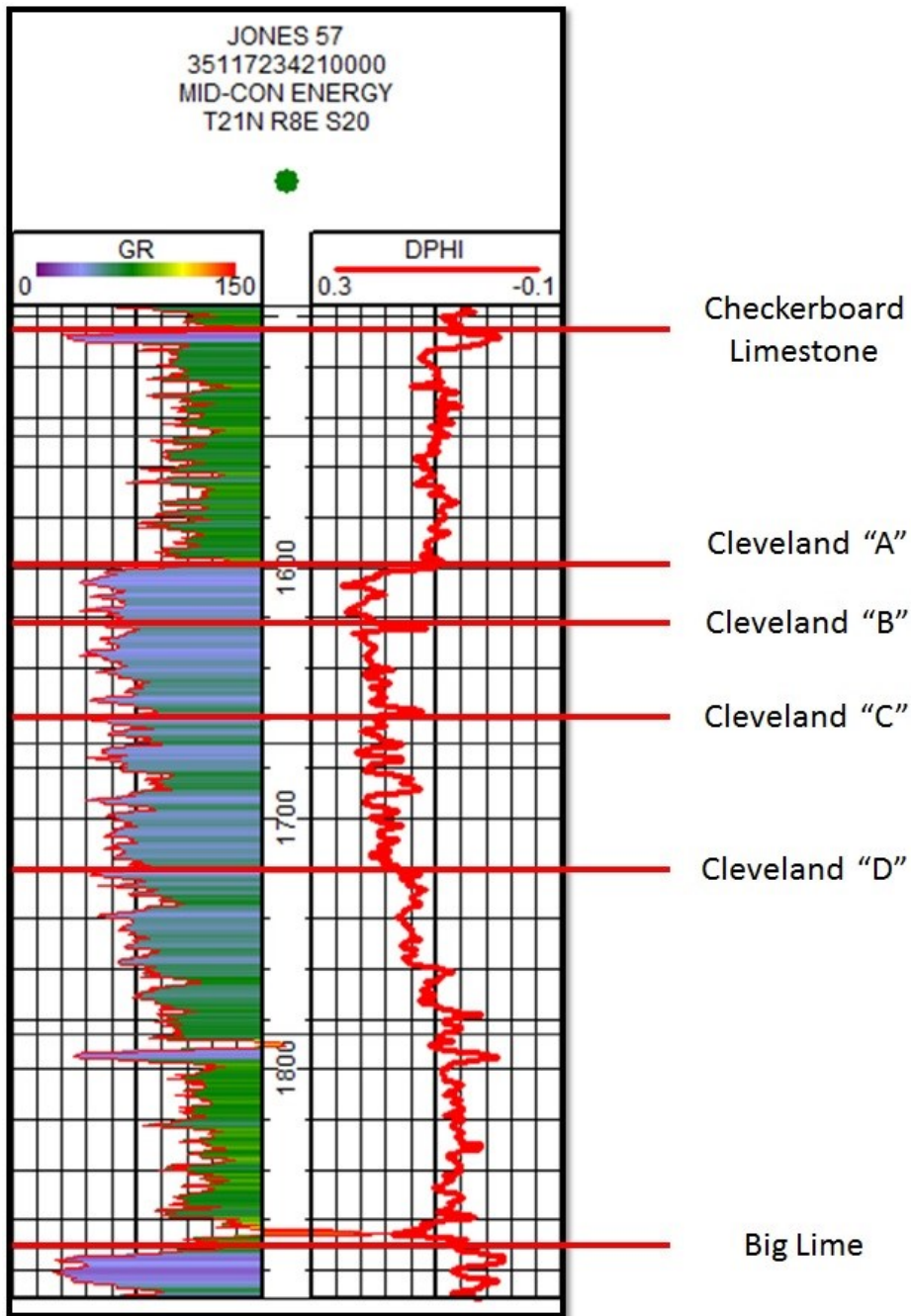


Figure 3.1: Representative wireline log of the Cleveland Sandstone log, with subunits of the Cleveland Sandstone identified. The zone boundaries were chosen based on changes in porosity and gamma-ray values.

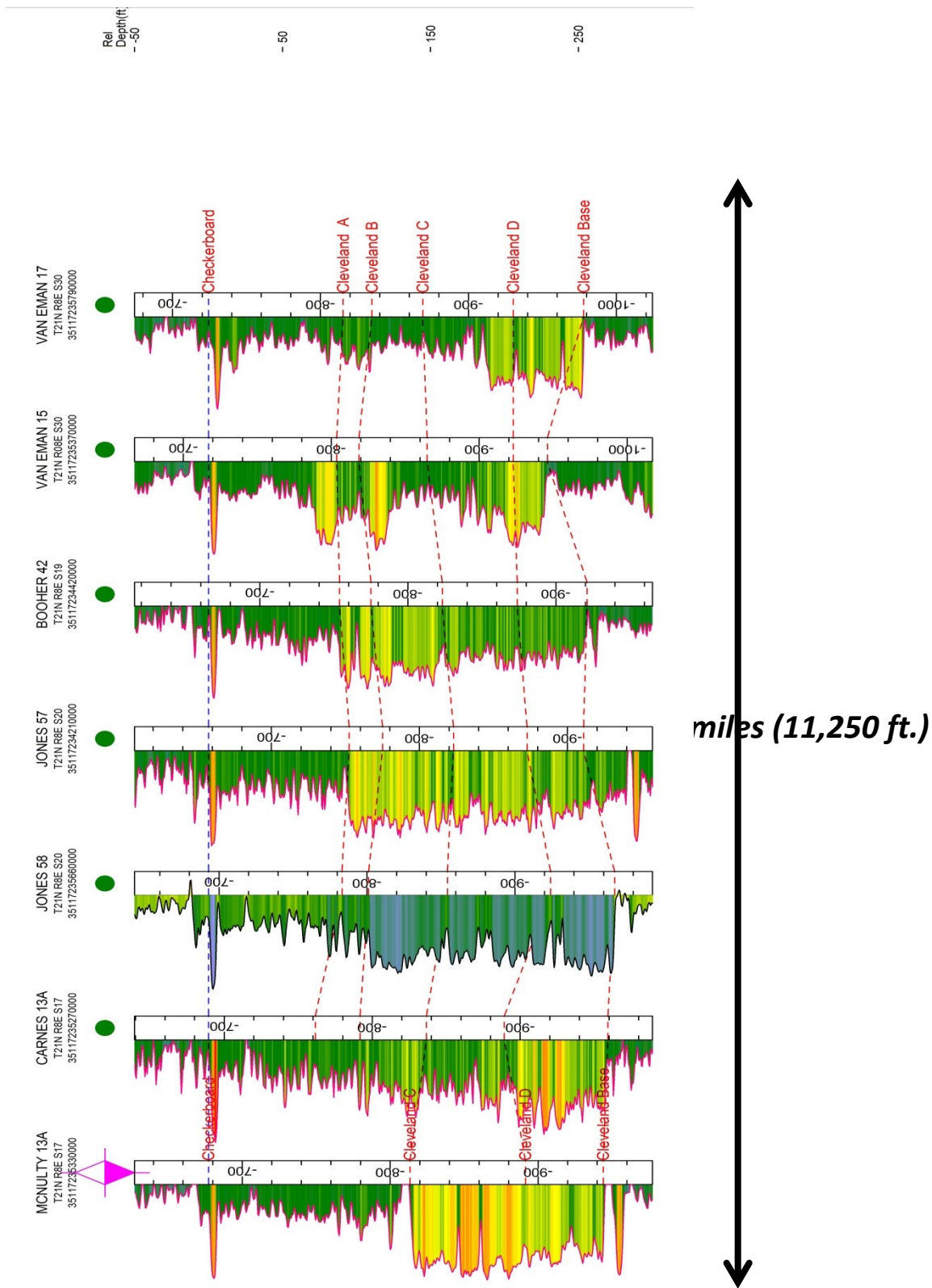


Figure 3.2: Northeast-southwest stratigraphic cross-section (gamma-ray) across the study area. The Cleveland Sandstone interval is between the Checkerboard Limestone above and the “Big Lime”. The line of section is shown in Figure 3.3. Green symbols represent oil-producing wells; pink and white diamond represents a well that is both an oil producer and a water-injection well.

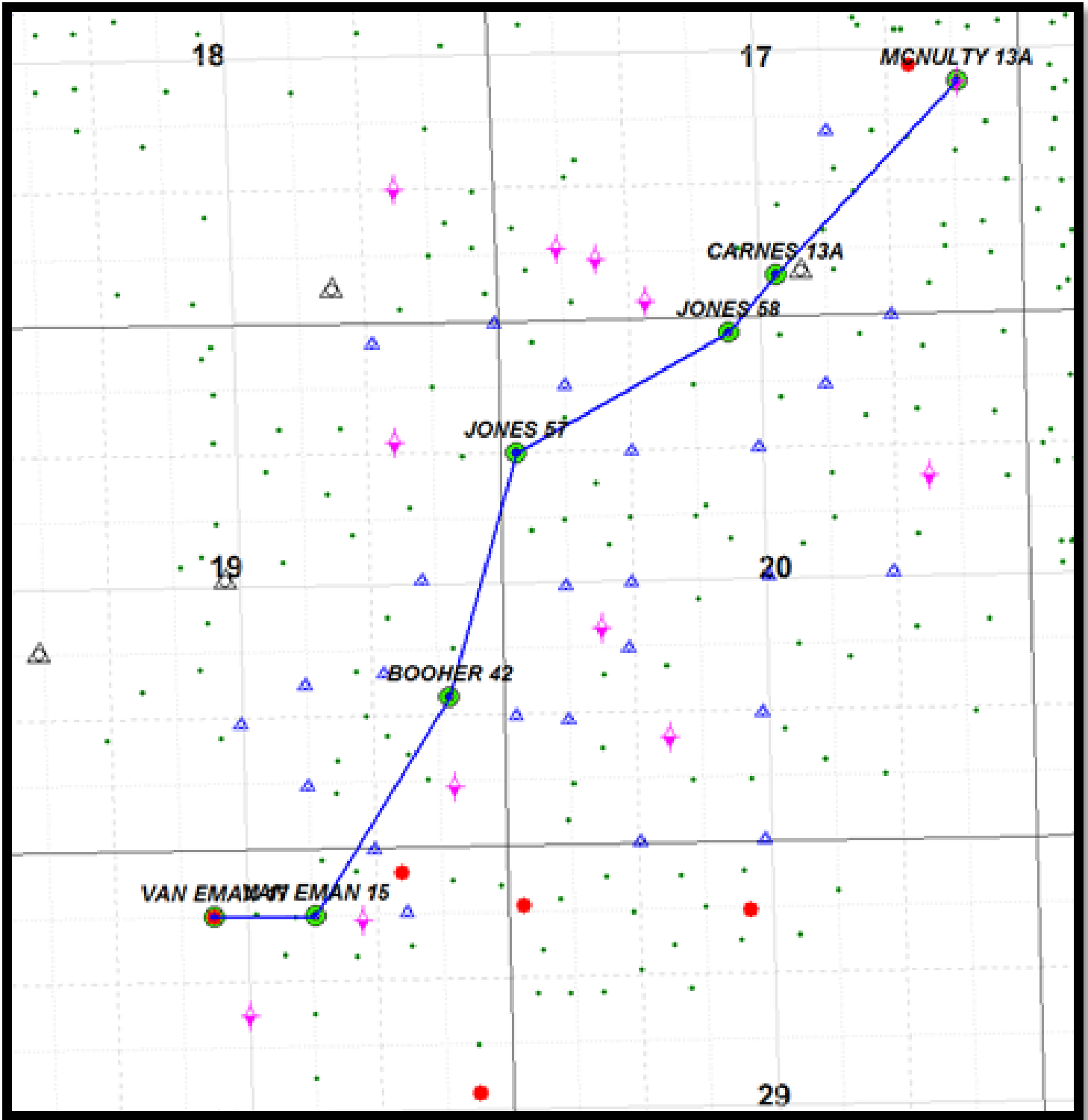


Figure 3.3: Line of stratigraphic cross-section shown in Figure 3.2. The wells are located in Sec. 17, 19, 20, and 30, T.21N, R.8E, Pawnee Co., Oklahoma.



## CHAPTER IV

### **Petrography and Sedimentology**

#### **Introduction**

The Cleveland Sandstone has been interpreted as having been deposited in a river-dominated deltaic setting (Campbell et al., (1997). Campbell described the Cleveland Sandstone of the Cleveland Field Unit as having been deposited in two distinct depositional environments: the “Lower Cleveland” as delta-front deposits and the “Upper Cleveland” as channel-fill deposits. Research reported herein indicates that the Cleveland may have been deposited during four depositional episodes.

In order to describe the depositional setting more accurately and to establish a high-resolution stratigraphic model, the Cleveland in three wells within the study area was cored and analyzed. Locations of these wells are shown in Figure 4.1. These cores were inspected for depositional variations related to grain size, sedimentary structures, mineralogy, texture, and color. The descriptions recorded were then used to determine zone boundaries of the four discrete stratigraphic units in the Cleveland sand. Wireline logs, thin-sections, x-ray diffraction analysis (XRD), isopach maps, and cross sections were sources of information to verify boundaries of stratigraphic units that compose the Cleveland Sandstone. These ad hoc units, designated as Cleveland A-D, show evidence of good correlation from core to wireline logs and thin-sections.

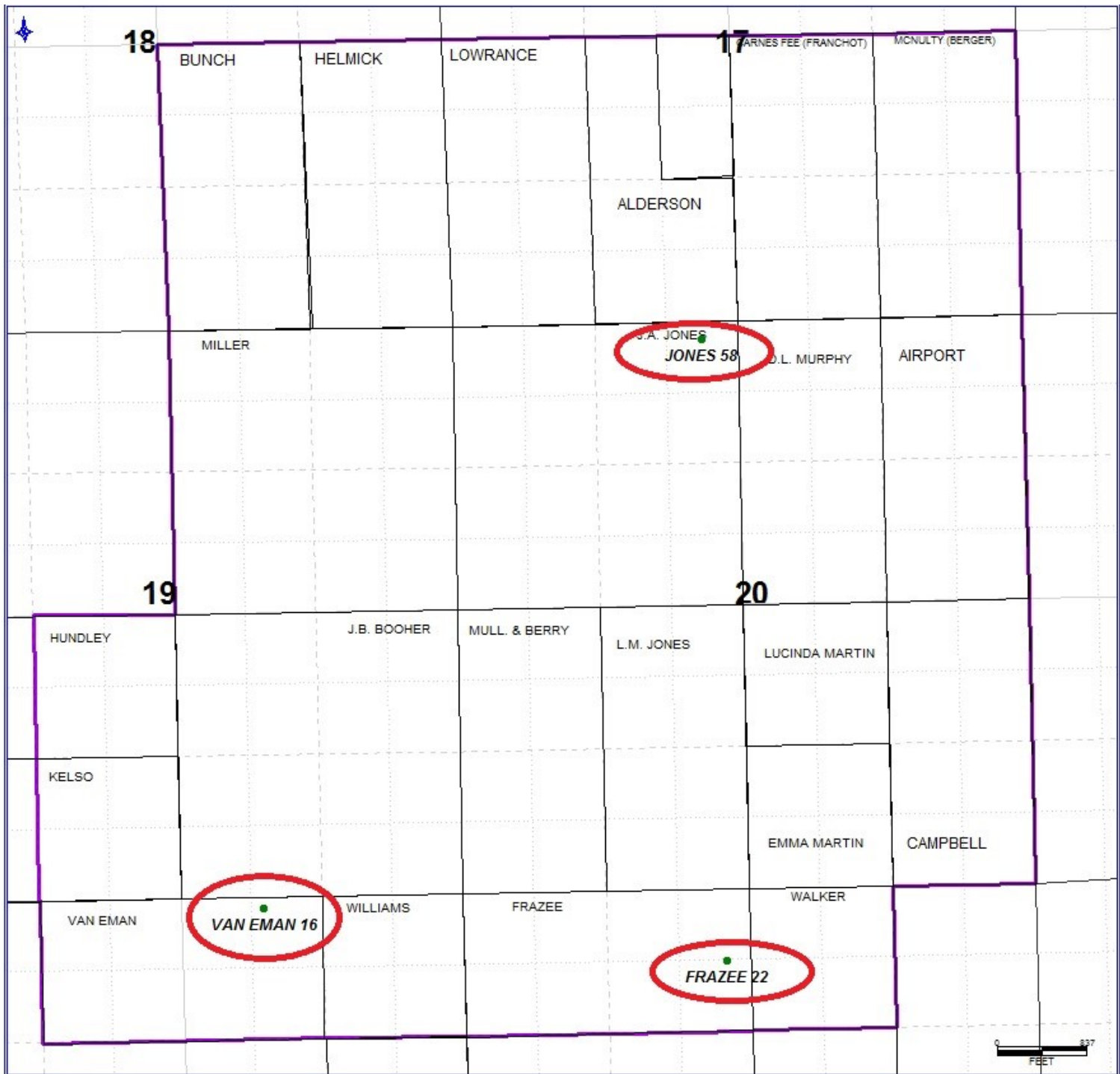


Figure 4.1: Map of the study area, showing the locations of the three wells, from which cores were obtained and described for this study. These wells were cored through the entire Cleveland interval, along with shales above and below the Cleveland sandstone bodies. These wells are located in Sections. 20, 29, and 30, T.21N, R.8E, respectively.

## Characterization of Rock-Stratigraphic Units (Zones)



Figure 4.2: Core photographs of Cleveland “A” Sandstone. Mid-Con Energy, J.A Jones #58 (1581-1583 ft.) (T.21N, R.8E, Sec.20, Pawnee Co., Oklahoma). Left: Plain light. Right: Ultraviolet light. Interbedded to interlaminated, very fine-grained sandstone, and siltstone. Contacts mostly are planar (horizontal), but some beds-laminae show small-scale cross-bedding (ripple bedding).

### *Cleveland “A” Zone*

The “A” zone is composed primarily of gray to light-gray, fine- to very fine-grained, silty sandstone, with interbeds or interlaminae of shale (Figures 4.2 and 4.3). Bed thickness ranges from 0.5 in. to 3 ft. Average bed thickness increases with depth. Small-scale cross-bedding (commonly ripple bedding) is common.

In thin-sections, discontinuous laminations are composed primarily of organic material (Figures 4.4. and 4.5). In fact, organic material is scattered throughout the sandstone. Based on point-count examination of four thin-sections from the “A” unit, the average porosity is 13.7%. Sandstone shown in Figure 4.4 has average thin-section porosity of 10%, whereas the core plug

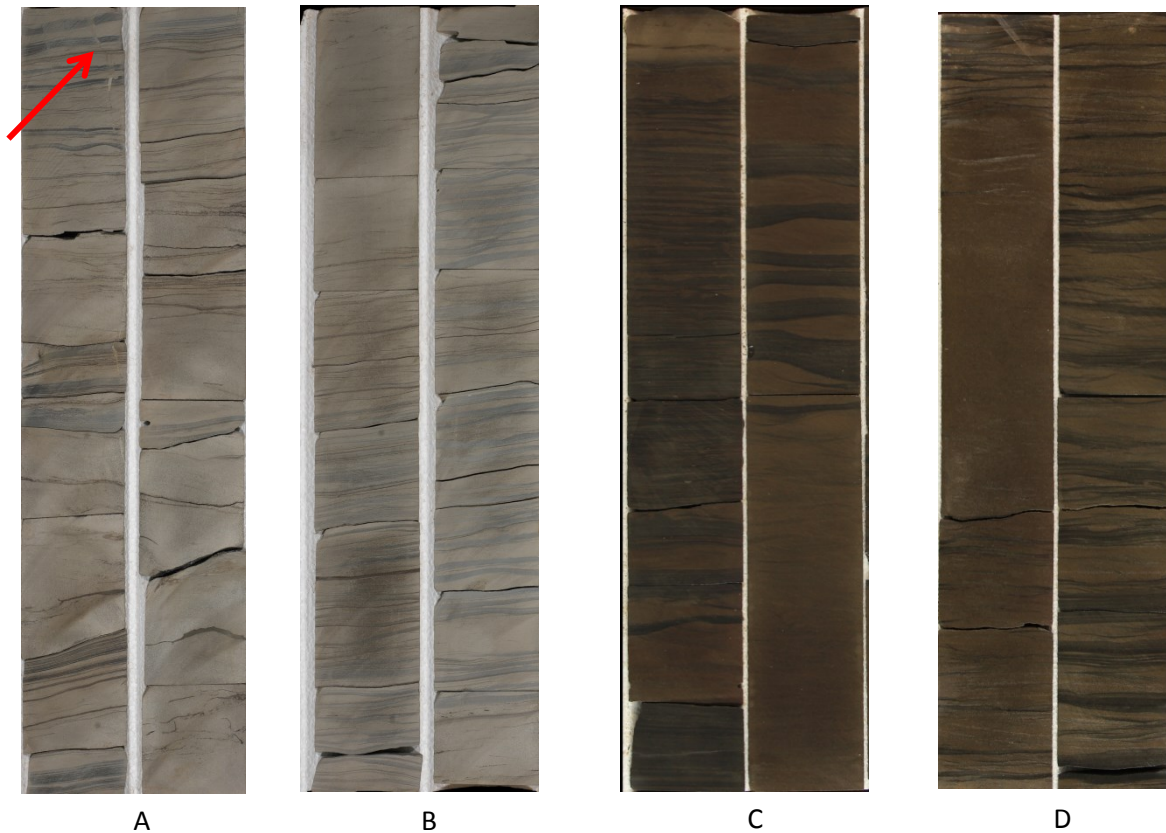
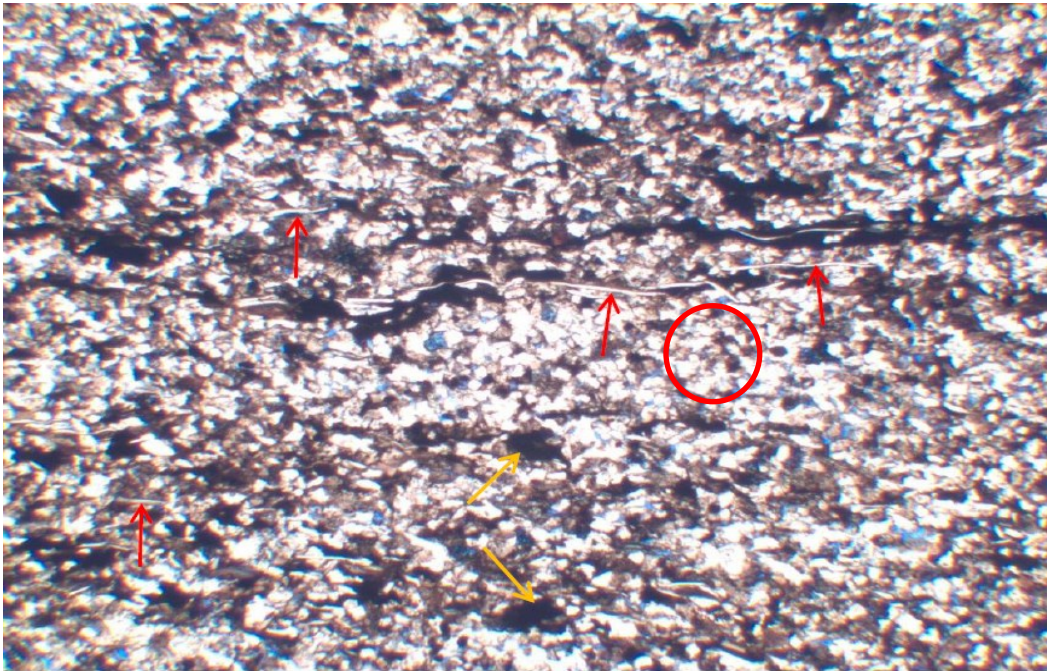


Figure 4.3: Photographs of cores from the Cleveland “A” zone. Photographs A and B: Van Eman No.16. Photographs C and D: J.A Jones No.58. See Figure 4.1 for locations of wells.

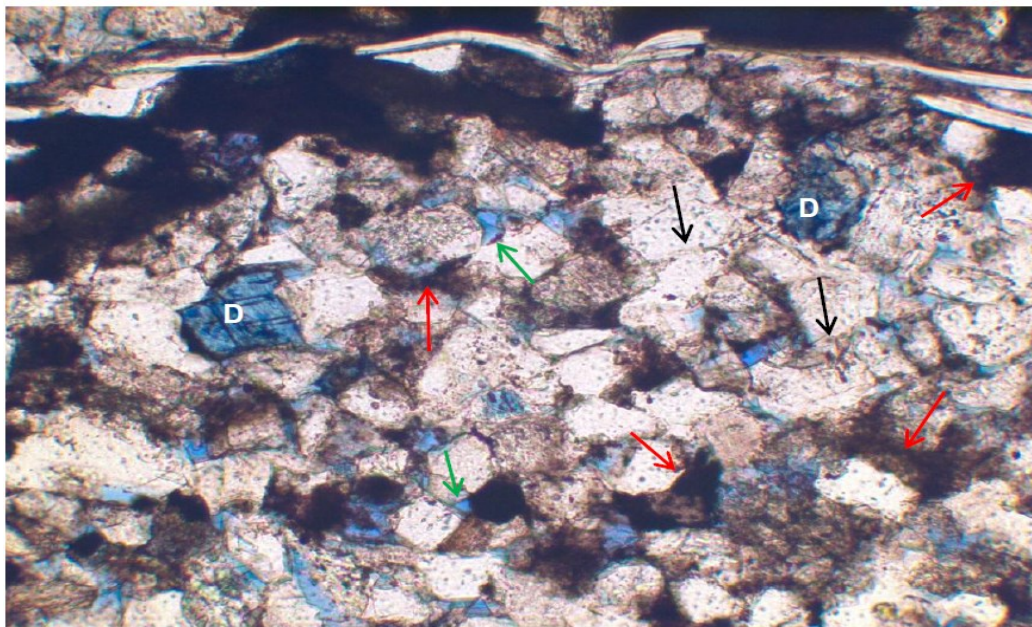
- A: 1610 ft. to 1614 ft. MD: Alternating beds of gray, silty sandstone and shale. A silica-filled vertical fracture (red arrow) is approximately 1/8 in. wide and 6 in. long.
- B: 1620 ft. to 1624 ft. MD: Gray to dark gray, silty sandstone interbedded with shale and silt- stone drapes. Oil staining is scattered. Bedding is planar to inclined.
- C: 1569 to 1573 MD: Brown to dark brown sandstone interbedded with shale. Sand is oil-stained throughout interval; bedding is predominantly planar.
- D: 1589 to 1593 MD: Brown to dark brown, oil-stained sandstone interbedded with shale. Bedding is predominantly planar.

A



0.50 mm

B



0.10 mm

- A) Figure 4.4: Thin-section photomicrograph from Cleveland Sandstone, Van Eman No.16 (T.21N, R.8E, Sec. 30) at 1,620.8 ft. Red arrows point to long, discontinuous muscovite flakes that are parallel to laminae visible in the core. Yellow arrows point to organic material scattered throughout the framework. Blue pattern in the thin section indicates porosity.
- B) Figure 4.5: The position of this image is indicated by the red circle in Figure 4.4. Red arrows indicate organic material and deformed rock fragments. Dolomite cement (D, stained blue) seems to have replaced grains within the framework. Green arrows indicate primary porosity; the remaining porosity almost certainly is secondary porosity due to dissolution of grains.

from the same depth has average porosity of 13.2%. Average porosity in thin-sections generally is within 5% of the helium porosity measured from core plugs.

The most common constituent within the “A” unit is quartz (Figures 4.4 and 4.5), averaging 62% of the total point-count. The rest of the fabric is composed mainly of plagioclase feldspar, mica flakes, rock fragments, organic material, and dolomite cement. Sandstone in the “A” unit, actually in the entire Cleveland, is classified as arkosic quartzarenite. .

To verify the observations made in thin-section, X-ray diffraction analysis was performed on end-trims from adjacent core plugs

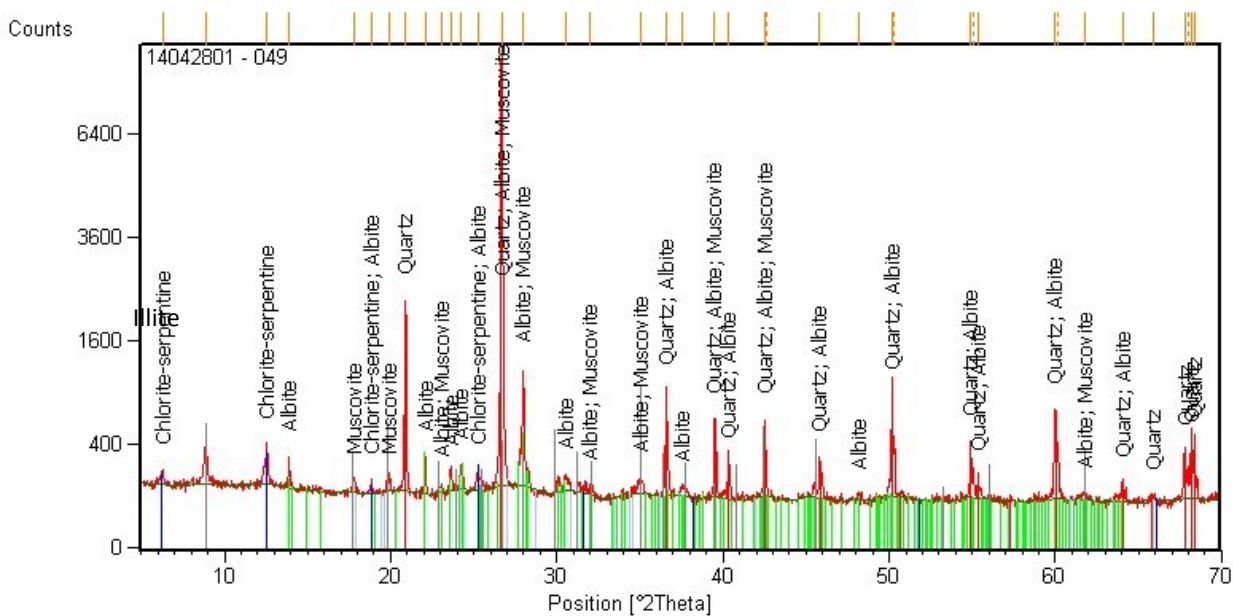


Figure 4.6: X-ray diffractogram from the Cleveland Sandstone, 1708.5 ft. MD. From this graph the conclusion is that most of the “A” sandstone is composed of quartz, muscovite, and albite. Attempts to extract clay from the XRD sub-samples were unsuccessful.

## Cleveland "B" Zone



Figure 4.7: Core photography of Cleveland "B" Sandstone. Mid-Con Energy, J.A Jones #58 (1581-1583 ft.) (T.21N, R.8E, Sec.20, Pawnee Co., Oklahoma). Left: Plain light. Right: Ultraviolet light. Thin bed of shale-sandstone interbedded with shale clasts in massive to planar-bedded, fine-grained sandstone.

The "B" zone is composed primarily of gray to brown, very-fine to fine-grained, well sorted sandstone. Sedimentary features include medium-scale cross-beds, shale rip-up clasts, soft-sediment deformation, massive beds with randomly oriented organic filaments, scours, truncations, interbeds, and root traces (Figure 4.9).

The "B" zone is composed of quartz, with feldspar and minor constituents that include kaolinite, mica, and dolomite cement. Figure 4.10 shows evidence of tight packing of grains in the "B" zone. Porosity seems to be largely secondary, owing to dissolution of feldspar and other framework constituents. Some of these secondary pores are filled by dolomite.

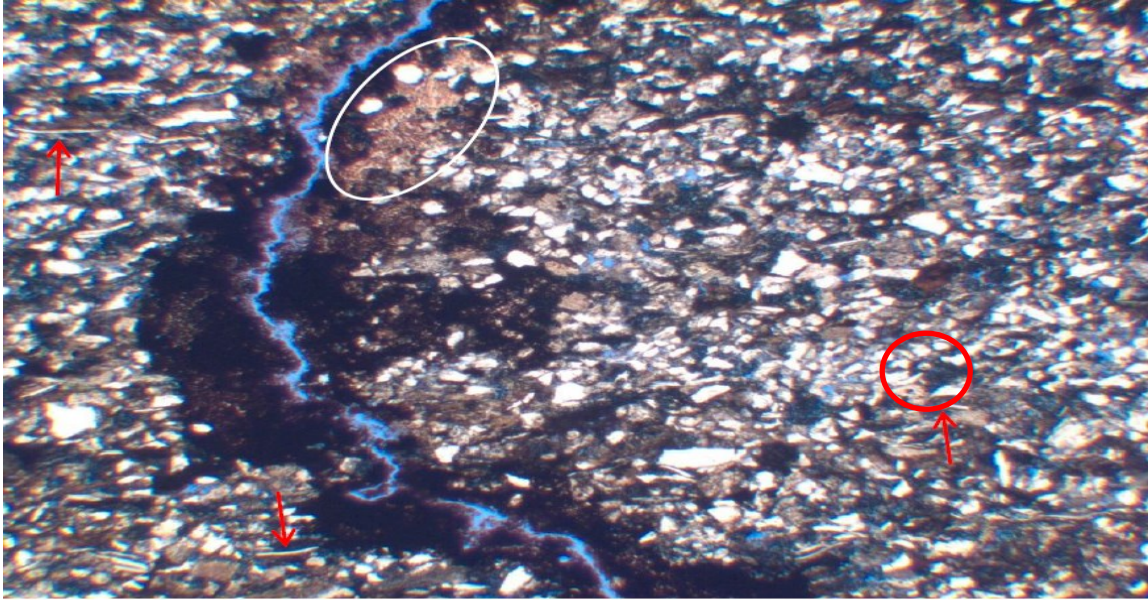


Figure 4.8: Photographs of the Cleveland “B” zone. Photo A: Mid-Con J.A Jones No.58. Photos B and C: Mid-Con Van Eman No.16. See Figure 4.1 for locations of wells. Cores are 3.5 inches in width.

- A: 1619 to 1623 ft. MD: Dark brown sandstone with thin beds of siltstone irregularly developed throughout the section. Distinct hydrocarbon odor and yellow glow under ultraviolet light. Small clasts of clay (1/8 in. diameter) are present, along with larger shale rip-up clasts.
- B: 1630 to 1634 ft. MD: Dark gray to light gray sandstone with interbedded siltstone, predominantly planar-bedded. In ultraviolet light this section has a faint yellow glow, possibly evidence of residual oil stain.
- C: 1640 to 1644 ft. MD: Dark gray to light gray, silty sandstone with interbedded shale and

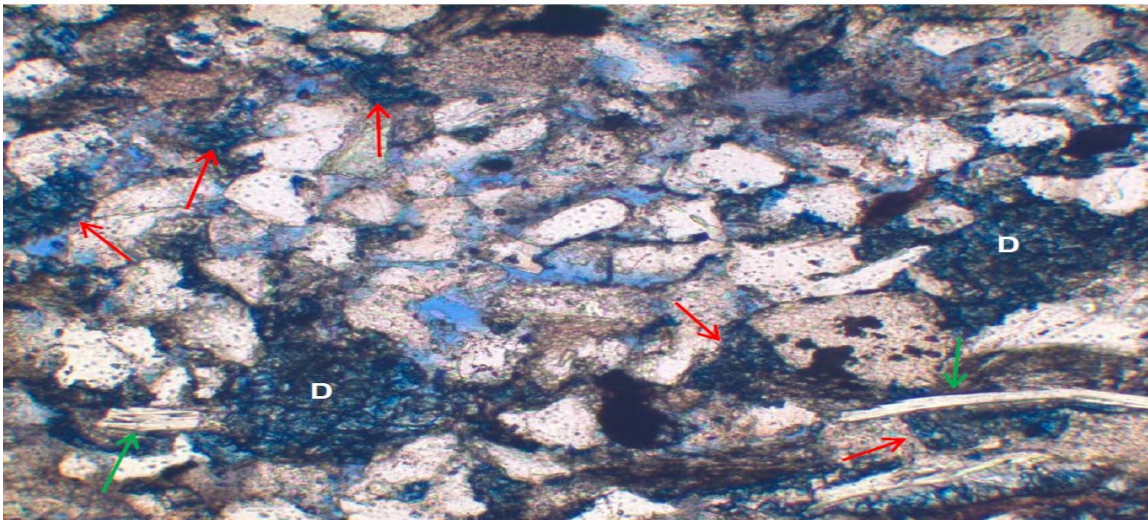


A



0.50 mm

B



0.10 mm

A) Figure 4.9: Thin-section photomicrograph from the Van Eman #16 (T.21N, R.8E, Sec.30) at 1,658.7 ft. The most prominent feature is the fracture, which may be sampling- induced. Carbonate cement (white ellipse) is present in an isolated part of the thin-section. Muscovite flakes (red arrows) are parallel to the bedding. Pore space is also present in this thin-section and is indicated by blue stain.

B) Figure 4.10: Location of sample from which this image was taken is indicated in Figure 4.9 by a red circle. Muscovite flake is shown by green arrow. Pores (blue) probably are secondary, from dissolution of grains. Dolomite cement (D, blue).

### Cleveland "C" Zone



Figure 4.11: Core photography of Cleveland "C" Sandstone. Mid-Con Energy, J.A Jones #58 (1643-1644 ft.) (T.21N, R.8E, Sec.20, Pawnee Co., Oklahoma). Left: Plain light. Right: Ultraviolet light. Very fine- to fine-grained sandstone. Sedimentary structures (massive to planar bedding) are largely obscured by oil staining.

The "C" unit is predominantly very fine- to fine-grained sandstone, light to dark brown and moderately to well sorted. Grains are loosely cemented, primarily with silica and secondarily with dolomite. In the core, the "C" unit is massive-bedded, with some planar and cross-bedding, and partly interbedded with shale and siltstone. This sandstone contains shale rip-up clasts, along with soft-sediment deformation, especially in the lowermost part.

Quartz and feldspar are the major constituents of the "C" unit. Dolomite cement in the "C" sandstone seems to be more highly crystallized than dolomite cement in the "A" and "B" units. Both primary porosity and secondary porosity are present, with the secondary porosity having formed from the dissolution of feldspar grains and calcite cement.

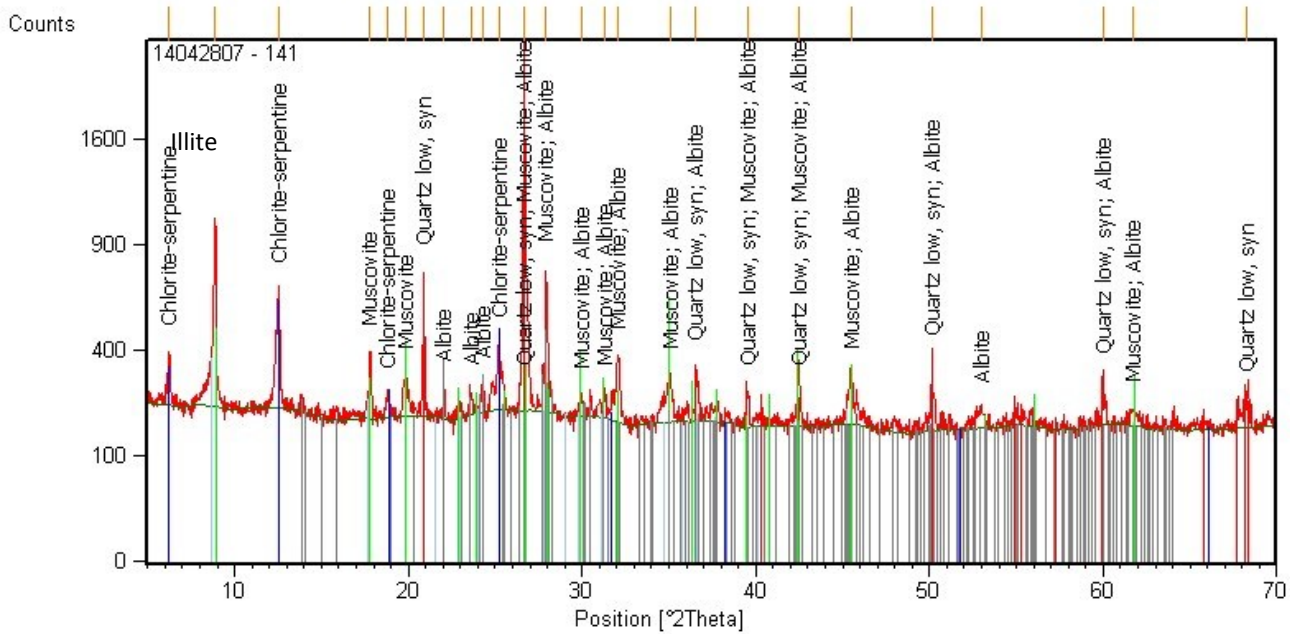
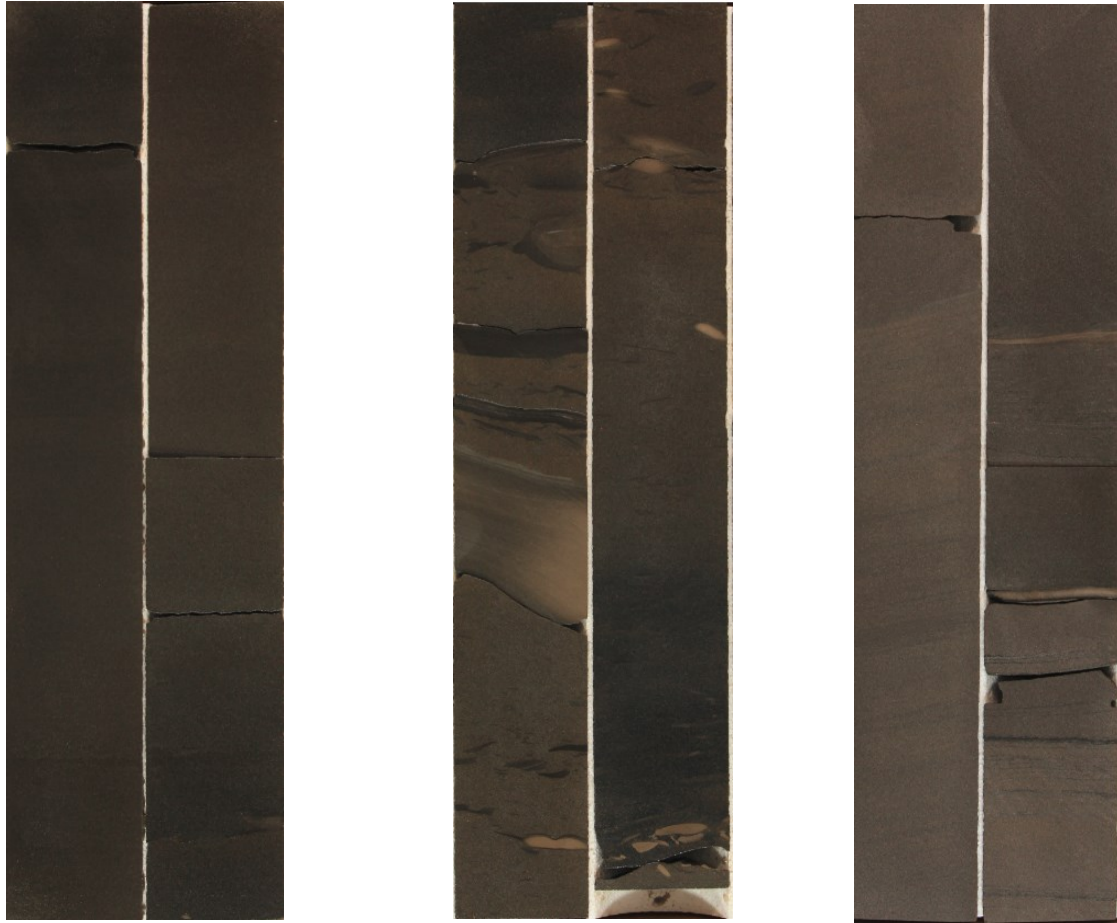


Figure 4.12: X-ray diffractogram from the Cleveland Sandstone 1799 ft. MD. From this graph the conclusion is that most of the “C” sand is composed of quartz, muscovite, and albite. Attempts to extract clay from the XRD sub-samples were unsuccessful.



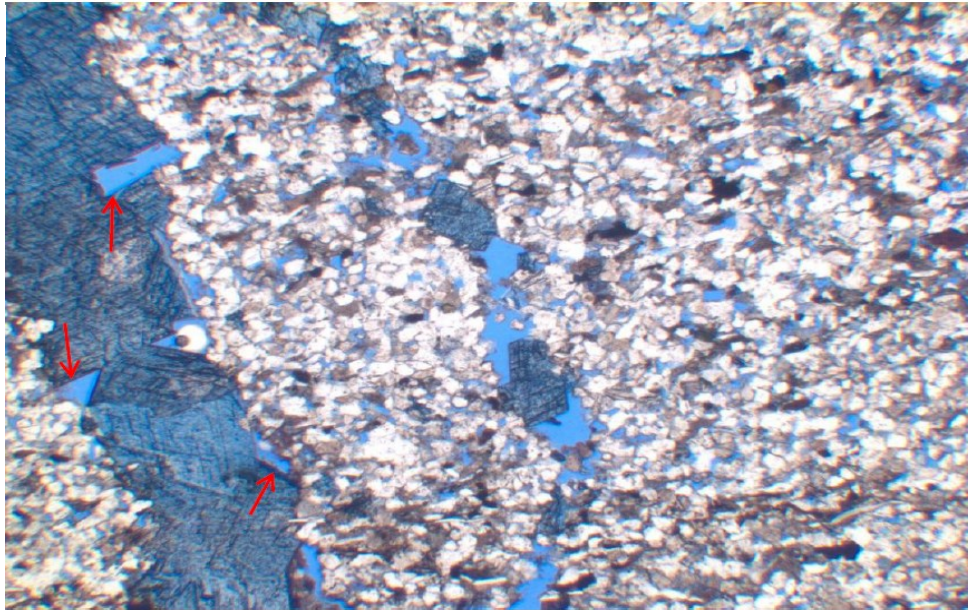
A

B

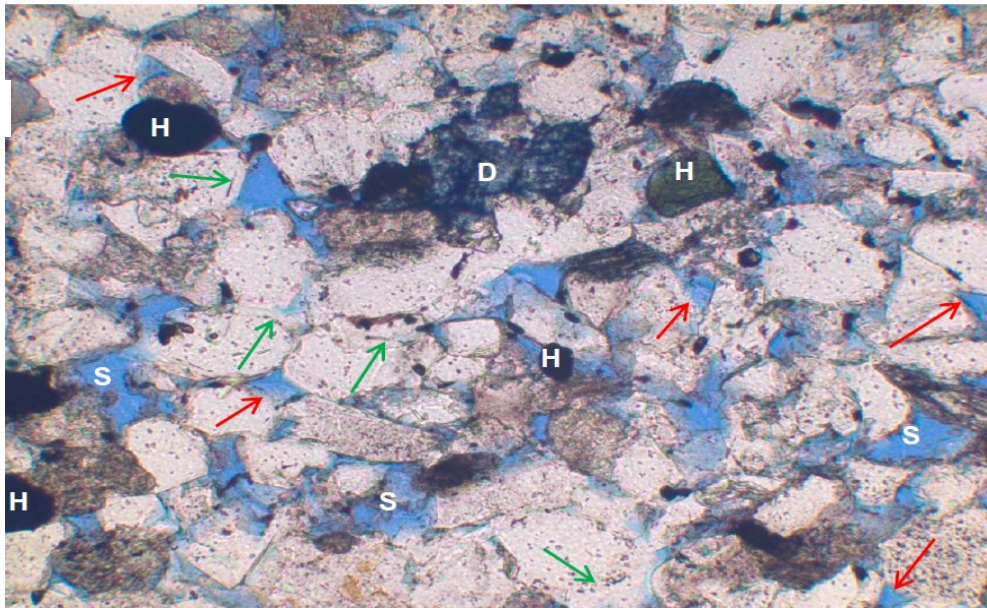
C

Figure 4.13: Core photographs from the Cleveland “C” zone. Photos A and B are from the J.A Jones #58. Photo C was taken from the Frazee #22, see figure 4.1 for well locations. Cores are 3.5 inches in width.

- A: 1645 to 1649 ft. MD: Dark brown to brown, fine grained, well sorted sandstone. Massive sandstone with small (1-3mm) clay clasts but no obvious sedimentary structures.
- B: 1650 to 1654 ft. MD: Dark brown to light brown, very fine-grained sandstone. Shale rip-up clasts and shale laminae. Possible erosional contact at 1651.5 ft. Clay clasts, scattered throughout the section, appear to be compacted.
- C: 1747 to 1751 ft. MD: Brown to light brown, very fine-grained sandstone. Very faint horizontal planar laminae.

**A**

0.50 mm

**B**

0.10 mm

A) Figure 4.14: Thin-section photomicrograph from the Van Eman #16 (T.21N, R.8E, Sec.30) at 1,717.7 ft. The most prominent features in this thin-section are two fractures. The fracture on the left is filled with dolomite (stained blue), leaving only trace amounts of pore space. The smaller fracture is partially filled by dolomite crystals.

B) Figure 4.15: This photograph shows the general granular fabric of the "C" unit. Grains are very fine to fine in size, moderately sorted, and tightly packed. The grains show irregular to long contacts. Green arrows indicate quartz overgrowths, identified primarily from "dust rims." As in the other units, dolomite cement (D) is present. The majority of the porosity is secondary porosity (S) owing to dissolution of grains. Heavy minerals (H) are also present.

### Cleveland "D" Zone

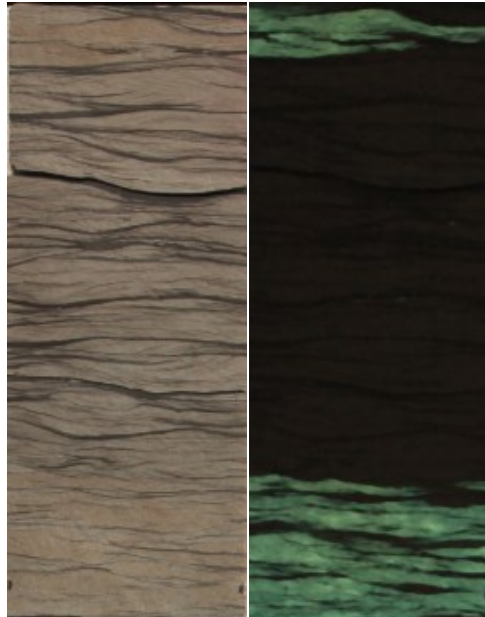
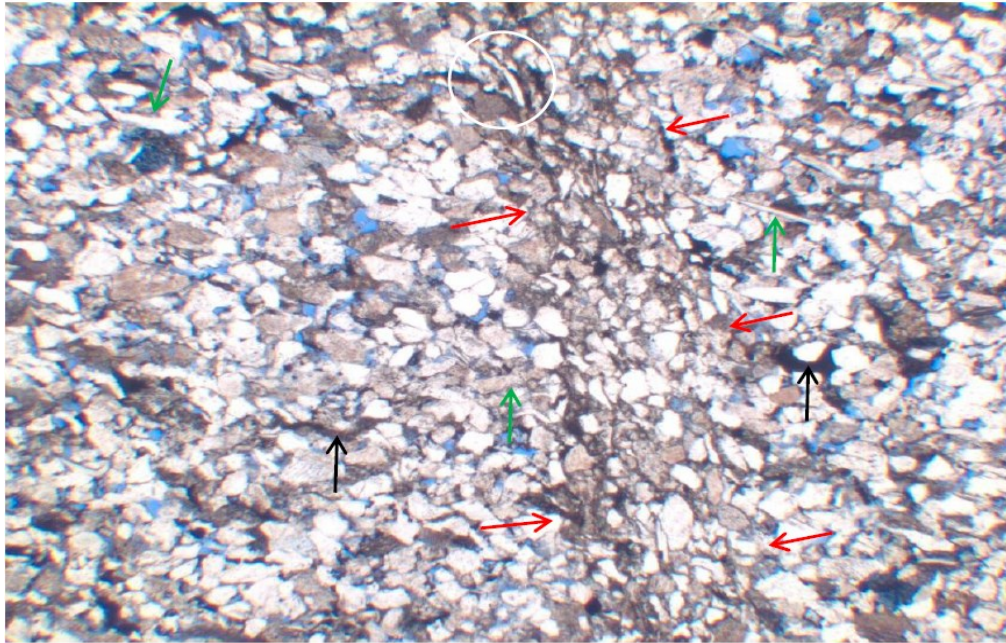


Figure 4.16: Core photography of Cleveland "D" Sandstone. Mid-Con Energy, Frazee #22 (1815-1816 ft.) (T.21N, R.8E, Sec.29). Left: Plain light. Right: Ultraviolet light. Interlaminae of shale in very fine-grained sandstone, with flaser-like bedding. Cores are 3.5 inches in width.

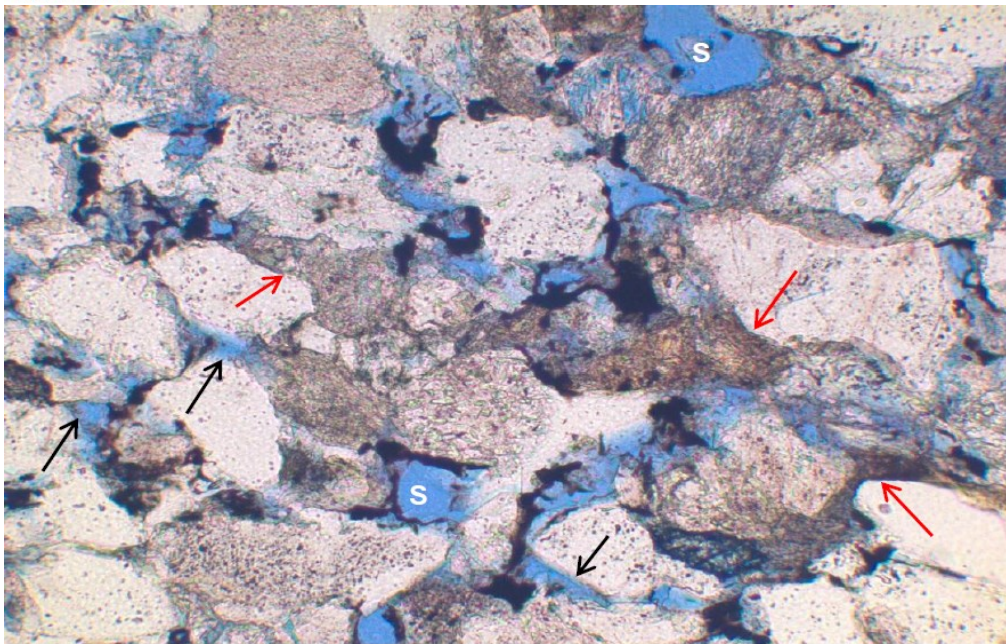
Texture of the "D" unit is predominantly that of very fine- to lower medium-grained sand. This sandstone is light brown to gray and moderately sorted. Grains are cemented by silica and dolomite. Common sedimentary structures are flaser bedding and associated ripple beds along with planar bedding surfaces, soft sediment deformed beds, and shale rip-up clasts. Quartz and feldspar are the most abundant constituents of the "D" unit. Dolomite cement in the "D" sandstone is similar to that in the "C" sandstone in being more highly crystallized than dolomite cement in "A" and "B" sandstones. Figure 4.17 shows what appears to have been root trace, Micas and other ductile grains have been deformed, most likely by compaction during burial. The "D" unit contains more rock fragments than the overlying Cleveland Sandstone units.

A



0.50 mm

B



0.10 mm

- A) Figure 4.17: Thin-section photomicrograph from the Van Eman No.16 at 1,761.8 ft. Red arrows indicate a possible “vertical” root trace. One mica flake (white circle) is almost perpendicular to bedding and parallel to the possible root. Rock fragments and organic material are more abundant than in the “C” unit. Porosity (blue) is both secondary and primary.
- B) Figure 4.18: Most of the framework in this thin-section is composed of quartz with some feldspar. Rock fragments appear to have been deformed (red arrows). Scattered black material is interpreted as being oil residue. Black arrows indicate primary porosity; secondary porosity is indicated by “S”.

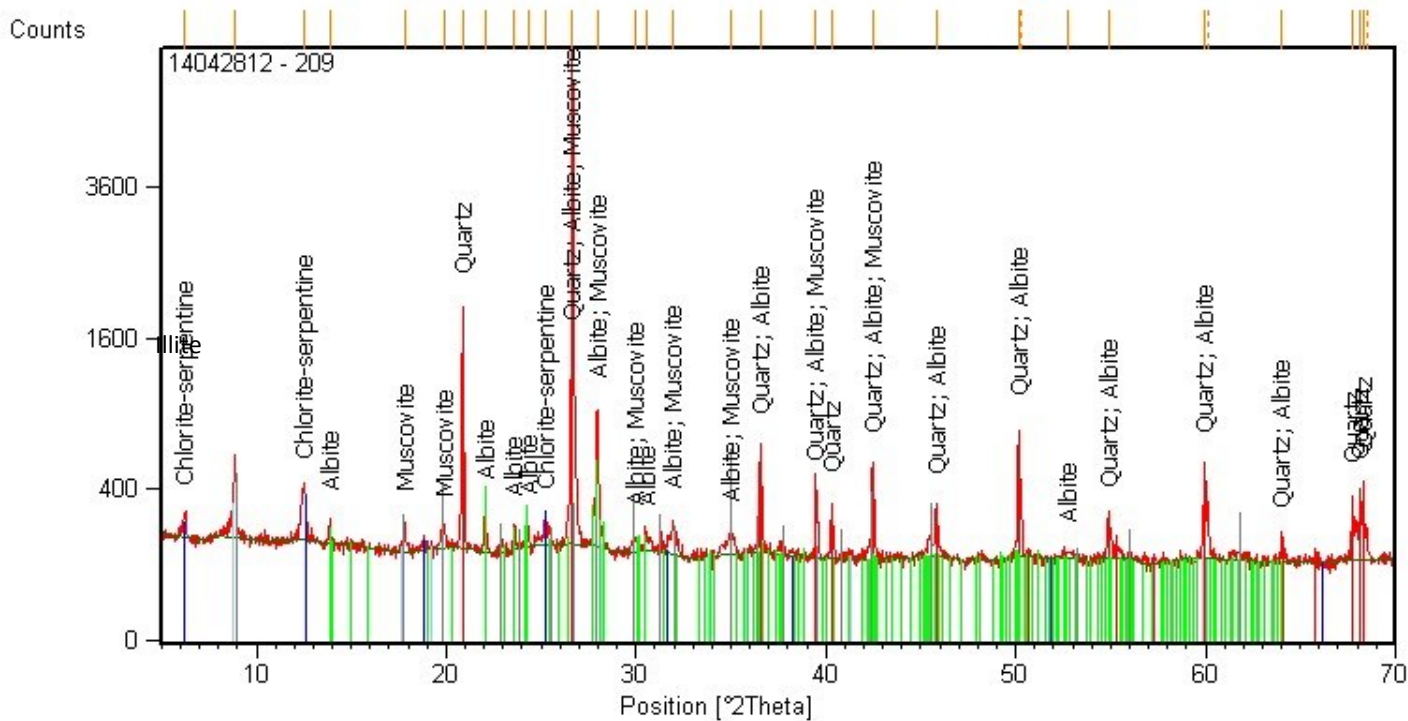


Figure 4.19: XRD diffractogram from the “D” zone at 1731.5 ft. (J.A Jones No. 58). This graph shows the majority of the “D” sand is composed of quartz, muscovite, and albite. Attempts to extract clay from the XRD sub-samples were unsuccessful, but the dominant clay appears to be illite with a lesser amount of chlorite.



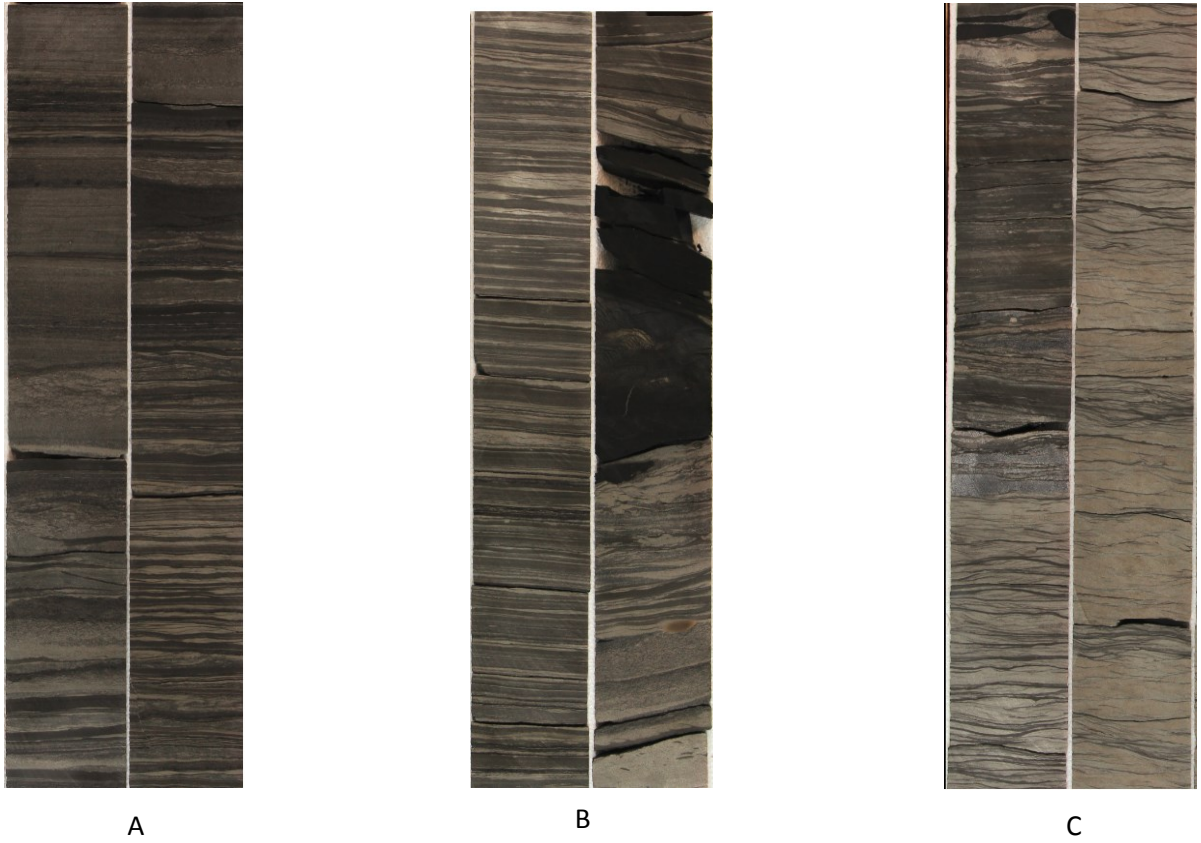


Figure 4.20: Core photographs from the Cleveland “D” zone. Photos A and B are from the J.A Jones #58. Photo C was taken from the Frazee #22, see Figure 4.1 for well locations.

- A: 1652 to 1656 ft. MD: Interbedded-interlaminated very fine-grained sandstone and shale. Sandstone is light brown; shale is dark black to light gray. Bedding is dominantly planar, between the two lithologies, with internally cross-stratified sandstone.
- B: 1662 to 1666 ft. MD: Interbedded to interlaminated sandstone and shale, as well as a 1-ft. bed of coal. Sandstone is light brown; shale is black. Bedding ranges from planar laminae to cross-bedding. Clay clasts present, but not abundant.
- C: 1815 to 1819 MD: Interbedded sandstone and siltstone, with thin but prominent shaly sandstone bed at top of photograph. Shale is black; sandstone is gray to light brown; siltstone is light brown to black. Laminae in siltstone are commonly inclined, reflecting ripple-like structure.

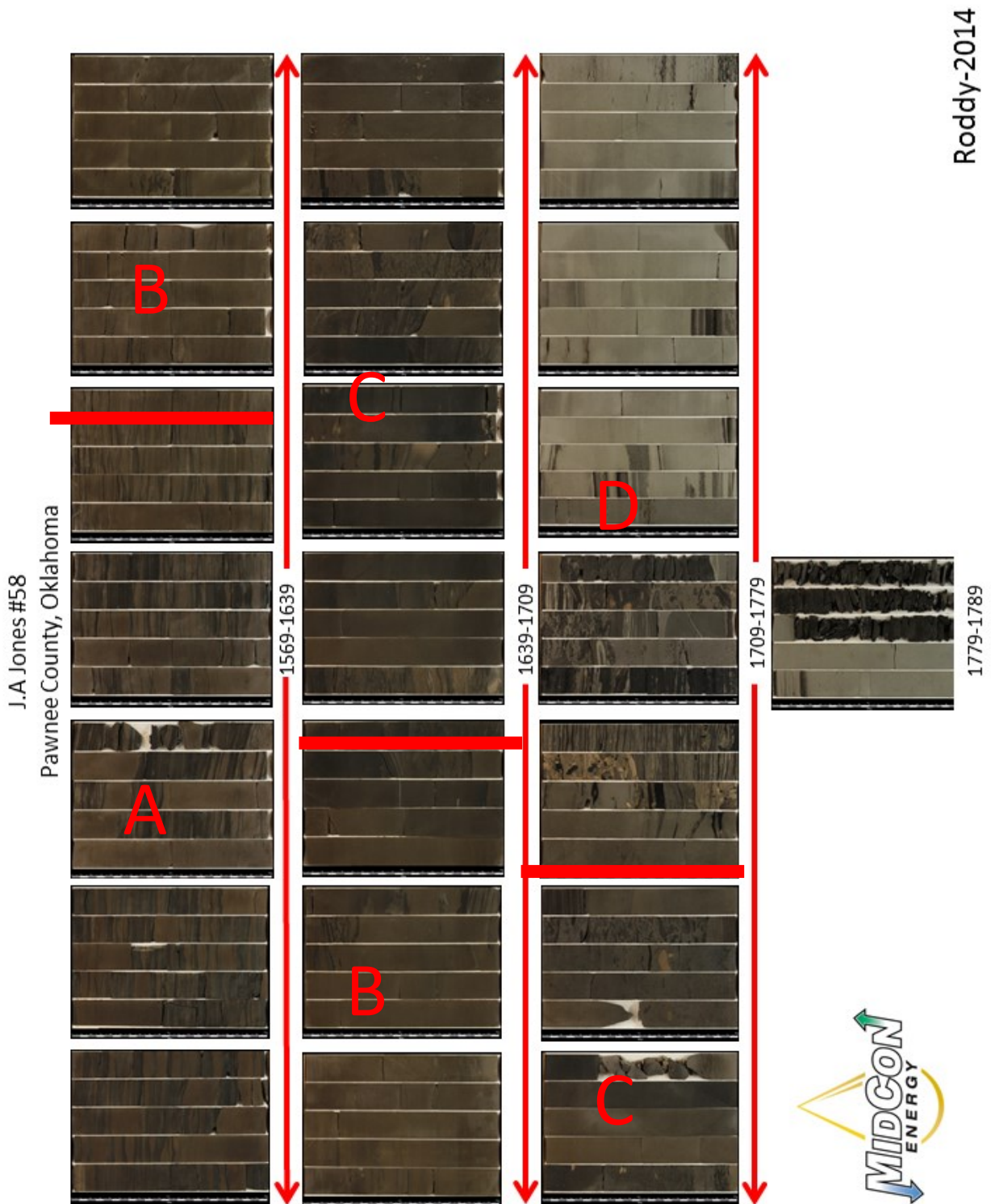


Figure 4.21: Photograph of the entire J.A Jones No. 58 core including the A, B, C, and D zones.

## **Associations of Electrofacies and Depositional Environments**

To predict with confidence the reservoir geometry of units that compose the Cleveland Sandstone, boundaries of internal rock-stratigraphic units must be correlated accurately. Calibrated-to-core gamma-ray, spontaneous-potential, and density-porosity curves were used to identify boundaries of rock-stratigraphic units within the Cleveland interval. Figure 4.22 illustrates the spontaneous-potential and density-porosity signatures of boundaries of each of the four units of the Cleveland Sandstone, as well as the depositional environment interpreted from each zone. Depositional environments were inferred from observations made during examination and analysis of cores, from micro-image logs, and signature analysis of spontaneous-potential and gamma-ray curves.

The “D” unit has a “blocky” (cylindrical) SP signature and is interpreted as having been deposited in a channel-fill environment, probably a delta distributary, given its relatively fine-grained texture and sharp base.

Because boundaries among the units are associated with interbedded-interlaminated, very fine-grained sandstone and shale, the deltaic complex probably did not migrate completely out of the study area during deposition of the Cleveland; these units of interbedded, interlaminated sandstone and shale probably are the record of interdistributary-tidal flat-delta front (fringe) environments. Both the “C” and “B” units, which show somewhat serrated blocky wireline signatures, seem to be interpreted best as channel-fill material. The C unit probably is a multistoried (two genetic units) distributary-channel deposit. The B unit is coarser than the other units; it almost certainly was deposited upstream from the depositional tracts for the C and D units. The “A” unit is the record of transition from a delta to a shallow-marine setting, it may have formed in prodelta/tidal-flat/delta-front environments. Whereas the “B”, “C”, and “D” units are predominantly sandstones, the “A” unit consists of shale and sandstones.

Unlike the base of the Cleveland interval, the top of the unit (and of the Cleveland Sandstone) commonly is gradational. A good “rule of thumb” for determining the upper boundary for the “A” unit, is this: where the density porosity is 10% or more and the gamma-ray deflection is less than 120 API units.

JONES 58  
 35117235660000  
 T21N R8E S20

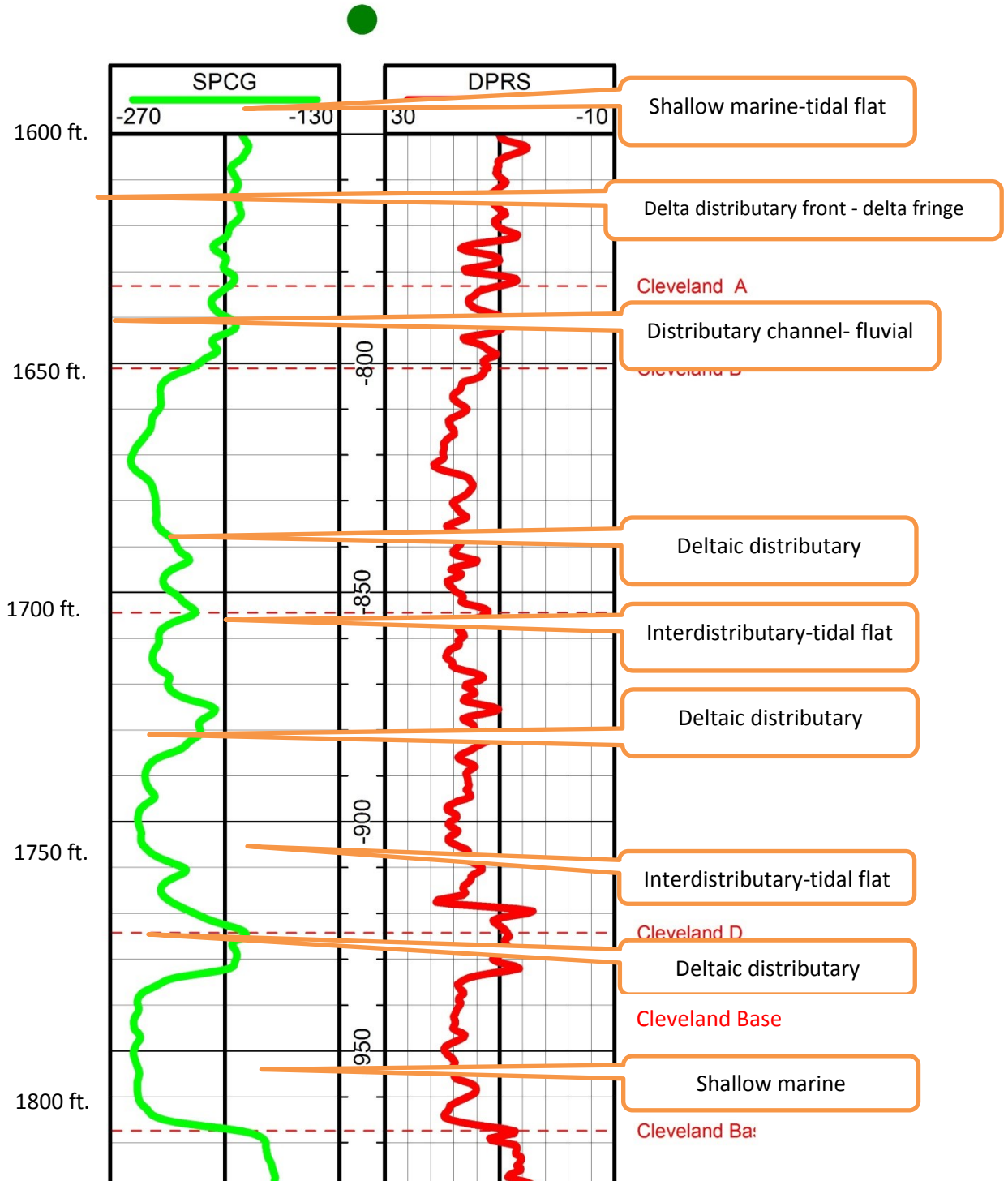


Figure 4.22: Wireline log from: Mid-Con Energy, J.A Jones No. 58, Sec. 20, T.21N, R.8E. Representative spontaneous potential (bright green) and density porosity (bright red) log signatures. The interpreted depositional environments (electrofacies) are shown for each zone is shown.

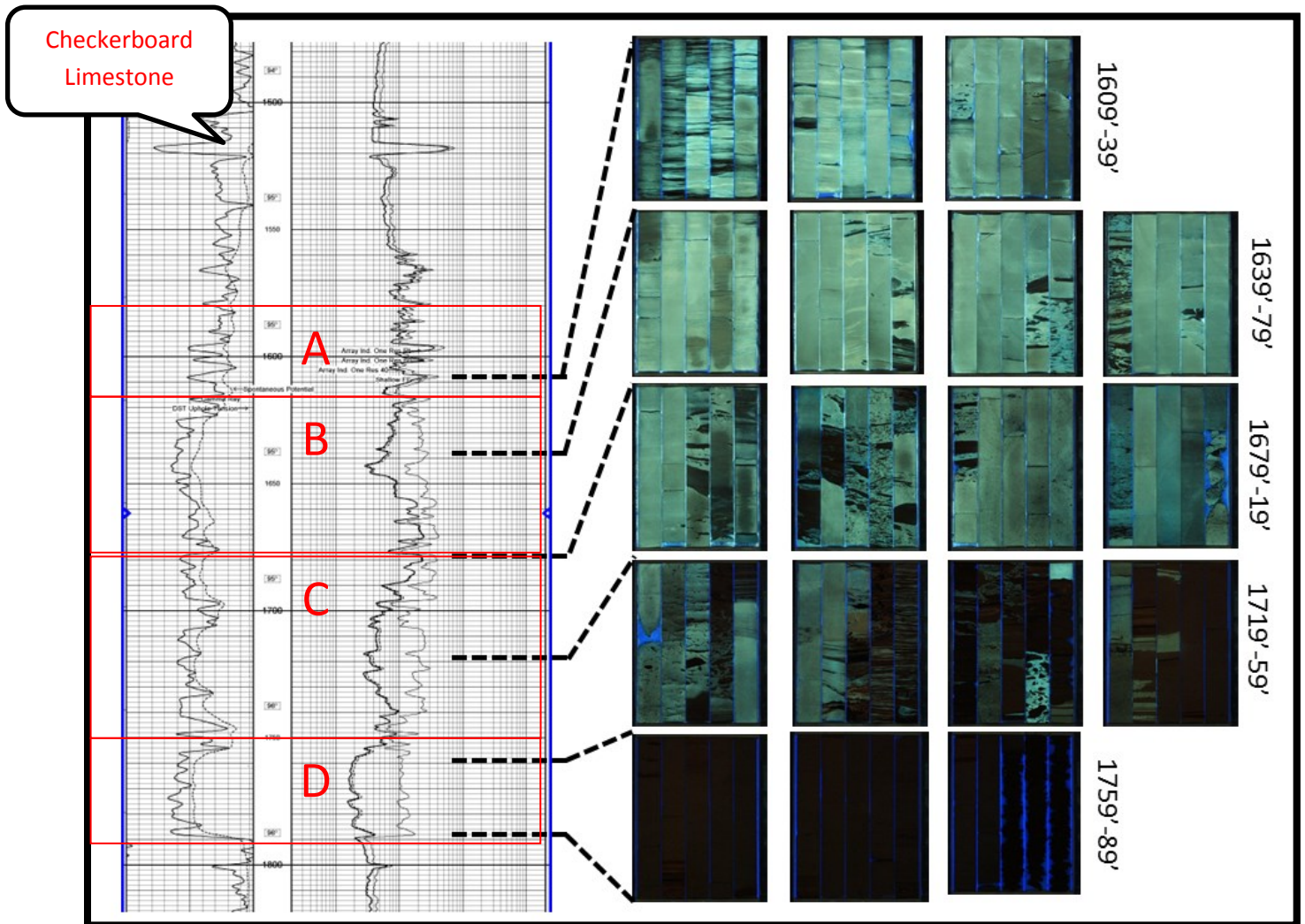


Figure 4.23: Basic log suite of the J.A Jones No.58 (T.21N, R.8E, Sec.20), showing the entire Cleveland Sandstone and the Checkerboard Limestone above. Core photographs were depth-shifted to match the wireline logs. Photographs were taken under ultraviolet light, which accentuates laminae (especially in the “A” unit), clay rip-up clasts in the “B” and “D” units and the presence of oil and gas (yellow color).

## CHAPTER V

### **Petrophysical Analysis**

#### **Introduction**

Many complexities come with developing a century-old oil field. Wireline-log data from old oil fields commonly is sparse and has a resolution much lower than that of modern conventional wireline logs. Bootle et al. (2009) notes that the average vertical resolution for conventional wireline logging tools is 5 ft. This poor vertical resolution is the result of heterogeneities (sandy shale, thinly bedded formations, clay-rich sand, etc.) within the formation in question as well as the past state of technology and is manifested in the form of suppressed resistivity, “lazy” density-neutron curves, and a “spikey” gamma-ray curve (Passey et al. ,2006), leading to miscalculation of volumes of oil-in-place.

A comprehensive petrophysical study of the Cleveland Sandstone of the Cleveland Field Unit, initiated by Mid-Con Energy LLC., became a vital part of this study and also of Mid-Con Energy’s efforts to study the potential of waterflooding the Cleveland Sandstone.

The primary objectives of this evaluation were:

1. Correlate core data with wireline log data.
2. Assess petrophysical uncertainties in estimating oil/water saturations, original oil/water saturations, and residual water saturations in order to make more accurate estimates.
3. Develop a porosity/permeability correlation for predicting permeability in areas where data from core is not available.

### **Availability of Data**

Wireline logs were available from 204 wells within the study area (Figure 5.1). Of these 204 wells, only 40 wells have modern well-logs. For this study, only modern well logs were used for petrophysical analysis of the Cleveland Sandstone. The older vintage logs were excluded in order to ensure uniformity of data, as well as to make certain that all the wireline logs analyzed were accompanied with digital (LAS) data. Only two wireline-logging companies were used for all of the modern logs. Water samples from wells that are open only in the Cleveland Sandstone were taken in order to measure resistivity of the water and to determine accurate water saturations.

### **Methods and Calculations**

Petrophysical analysis of the Cleveland sand was divided into two major activities:

- 1) Core Analysis: Cores acquired from the Van Eman No.16, J.A Jones No.58 and Frazee No.22 were sent to Core Labs Inc. for routine and special core analysis (X-ray diffraction, capillary pressure, relative permeability, LPSA, etc.). Routine analysis includes measurement of porosity, permeability, water saturation, oil saturation, and grain density. A detailed workflow for core data analysis is shown in Appendix A.



2) Analysis of Wireline Data: The forty well logs analyzed are composed of the standard triple combination curves (resistivity, neutron porosity, density porosity, gamma ray, spontaneous potential, microlog, and caliper). The logs were calibrated to core data. Data obtained from these curves was used to generate petrophysical parameters, using HDS Petrophysical evaluation software. This evaluation includes calculations of porosity, permeability, shale volume, hydrocarbon volume, and water saturation. A porosity-permeability function was developed; this ensured that uniform porosity-permeability calculation was applied to the Cleveland in the entire field. It also rendered a more accurate depiction of the actual porosity and permeability in areas where cores are not available. This improvement in estimated-porosity and permeability resulted from use of a shale-corrected effective- porosity equation and from the Timur equation for estimation of permeability (Roller, C., 2014, Private Communication.)

## **Interpretation of Data from Cores**

### *Mineralogy and Grain Size*

As described previously, the Cleveland Sandstone is composed primarily of quartz with feldspar. X-ray diffraction (XRD) tests of 22 core-plug samples and 50 bit-cutting samples from 12 wells in the Cleveland Field were used to test the results of thin-section analysis and to measure the percentage of clay in the sandstone. Core plugs and bit-cutting samples were used for XRD analysis, to provide a larger sample size and to sample a larger part of the study area. Clay minerals have adverse effects on petrophysical measurements, interpretations, and conclusions because clays are associated with under-estimated resistivity measurements. The results of X-ray diffraction of core plugs show that clays mainly are chlorite, illite, and kaolinite possibly being marked by chlorite or muscovite (Figures 4.6, 4.12, and 4.19) with trace amounts of kaolinite and illite. Figure 5.1 shows the mineral composition, including abundance of clay

minerals, based on the XRD analysis of bit cuttings. The largest discrepancy between the XRD (bit cuttings and core plugs) and thin-section data is the amount of pyrite. The point count estimates from thin-section examination estimated a much higher percentage of pyrite than that from the XRD analysis.

LPSA (laser particle size analysis) tests were also run in order to gain a quantitative understanding of the grain-size distribution in the Cleveland Sandstone. LPSA results show that the majority of the samples measured are fine to very fine-grained, with minor amounts of medium-size grains. (Appendix B).

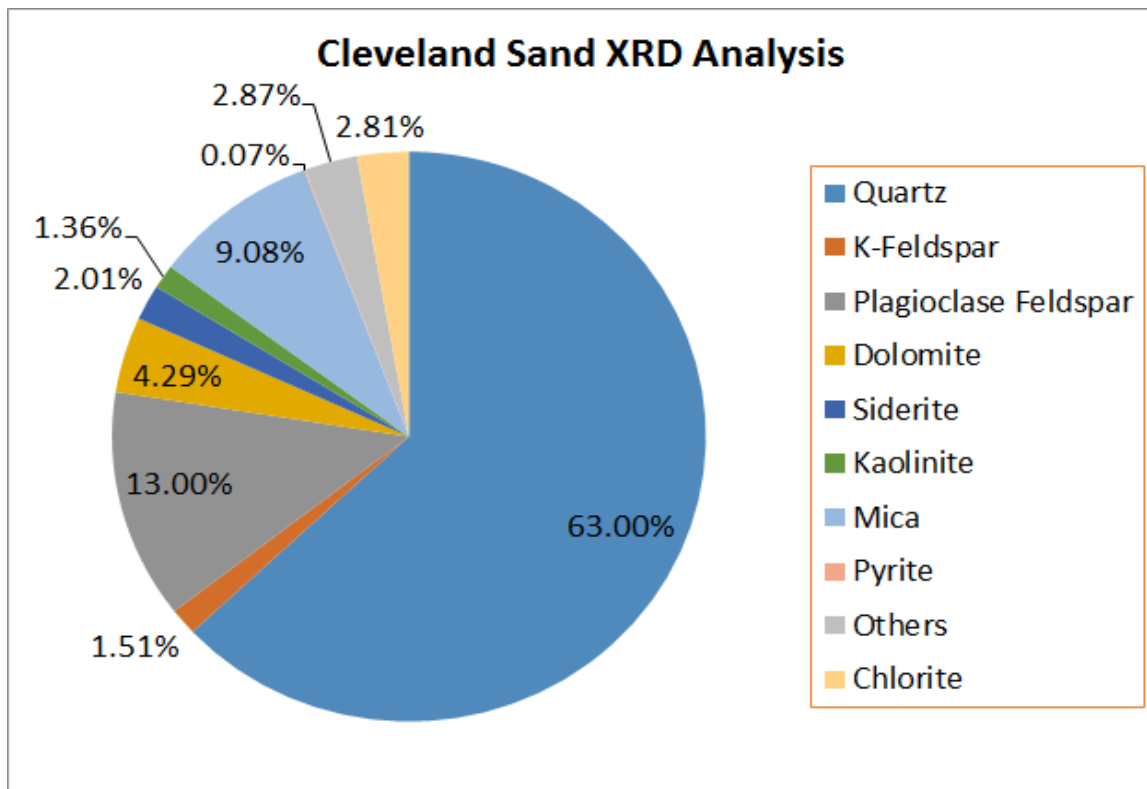


Figure 5.1: Pie chart representing the average mineral composition of Cleveland Sandstone. These samples were measured from drill cuttings, acquired from seven wells within the Cleveland Field Unit (T.21N, R.8E, Pawnee Co., Oklahoma).

## Grain Density

Grain density of 498 core samples from three wells was measured. Grain density was calculated by measuring grain volume and weight of dry core-plug samples. Grain density was plotted by well against measured porosity (Figure 5.2). Grain density varied from 2.47 to 2.88 g/cm<sup>3</sup>; the average was 2.68 g/cm<sup>3</sup>. Figure 5.2 shows the relationship between core-derived grain density and log-derived porosity from bulk-density logs.

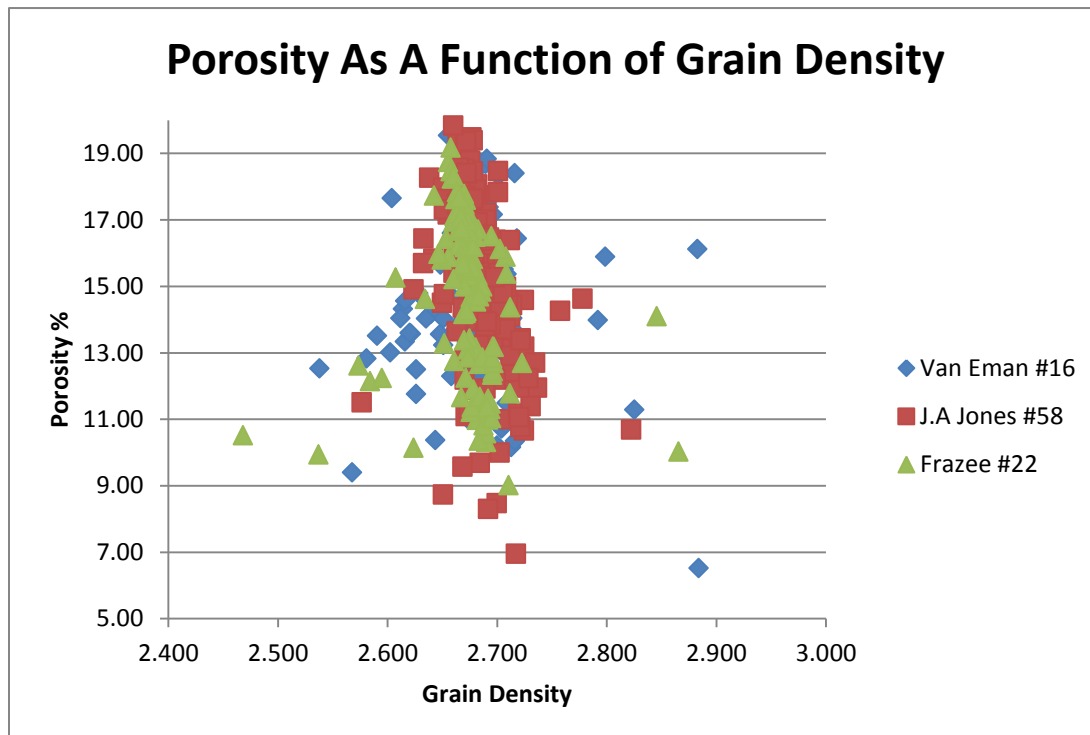


Figure 5.2: Porosity as a function of grain density. Data obtained from 498 core plug samples, from three wells in the Cleveland Field Unit.

## Porosity and Permeability

Permeability and porosity were measured for 402 core plugs were taken, from the three wells cored in the Cleveland Field Unit. Permeability (as well as porosity, capillary pressure, etc.) should be measured at effective confining pressures, which are related to the triaxial stresses in the formation. The equation shown below (Equation 5.1) was used to calculate effective stress.

$$\sigma_{eff}^{iso} = 0.59\sigma_v - 0.53P_{pore}$$

$$\sigma_{eff}^{iso} = 0.59(1 \frac{psi}{ft}) * 1,800 ft.) - 0.53(0.433 \frac{psi}{ft}) * 1,700 ft.$$

Equation 5.1: Effective stress (confining pressure – fluid pressure). Stress Model Equation. (From Roller, C., 2014, Private Communication.)

Based on the equation above, Klinkenberg permeability ( $K_{klink}$ ) and air permeability ( $K_{air}$ ) were computed at a net confining pressure of 600 psi.

Measurements of porosity and permeability obtained from cores are summarized in Table 5.1. Overall, the porosity-permeability relationships are rather consistent in all four zones of the Cleveland Sandstone (Figures 5.3-5.6). The porosity-permeability correlations for the Cleveland have an average  $R^2$  value of 0.685. The  $R^2$  value of the “A” zone is .498, which reduces the average  $R^2$  value significantly.

Zone	Porosity Range (%)	Klinkenberg Permeability Range (mD)	Average Porosity (%)	Average Permeability (mD)
A	6.52-16.90	.025-18.9	13.35	3.02
B	6.26-20.83	0.015-605	16.71	62.88
C	8.10-18.60	0.005-65.3	15.19	12.29
D	6.95-19.84	.005-85.5	14.95	8.6

Table 5.1: Summary of porosity and permeability measured from cores of the Cleveland Sandstone, J. A Jones No.58, Frazee No.22, and Van Eman No.16.

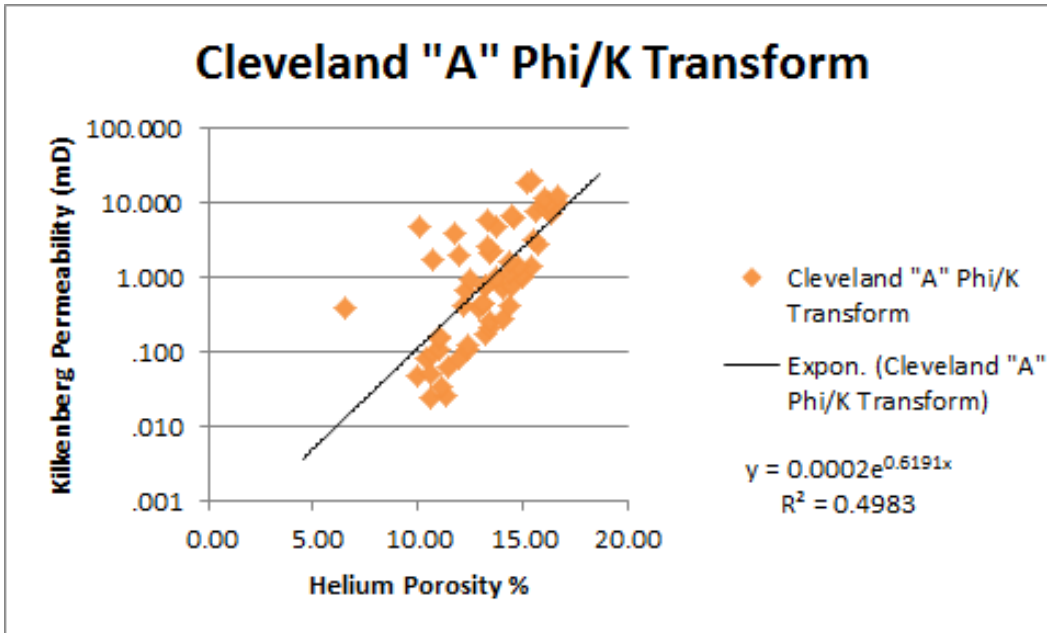


Figure 5.3: Porosity-permeability transform, Cleveland "A" zone. Data included in this graph was acquired from the Cleveland Field Unit, T.21N, R.8E, Pawnee Co., Oklahoma. Porosity and permeability measurements depicted above are from 61 core plugs from the Cleveland "A" zone.

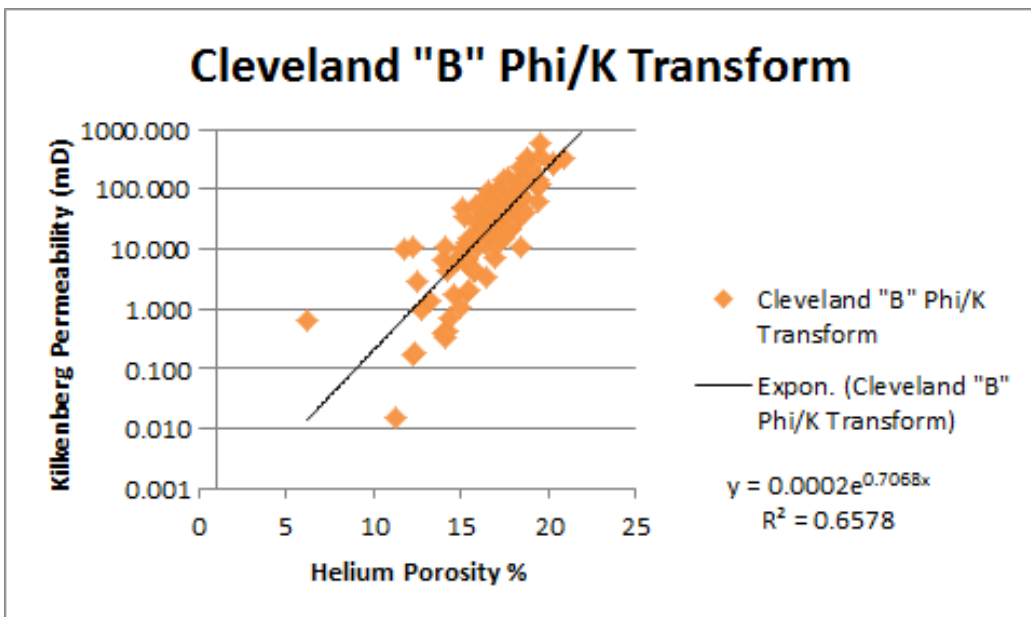


Figure 5.4: Porosity-permeability transform for the Cleveland "B" zone. Data included in this graph was acquired from the Cleveland Field Unit, T.21N, R.8E, Pawnee Co., Oklahoma. Porosity and permeability measurements depicted above are from 130 core plugs from the Cleveland "B" zone.

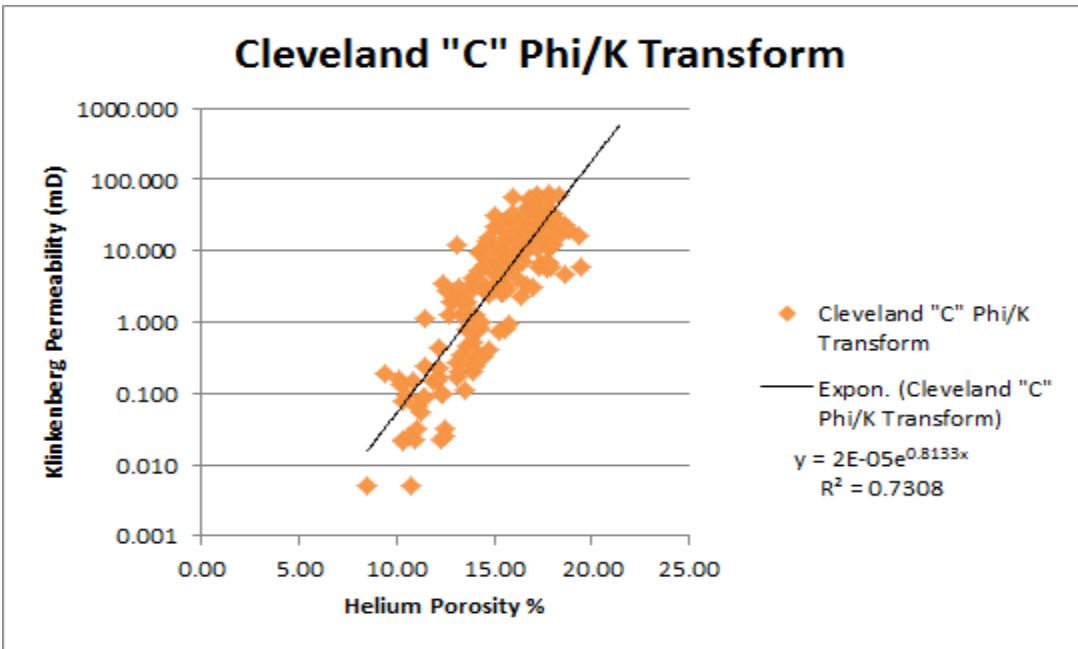


Figure 5.5: Porosity-permeability transform for the Cleveland "C" zone. The data included in this graph was acquired from the Cleveland Field Unit, T.21N, R.8E, Pawnee Co., OK. The porosity and permeability measurements depicted above are from 202 core plugs from the Cleveland "C" zone.

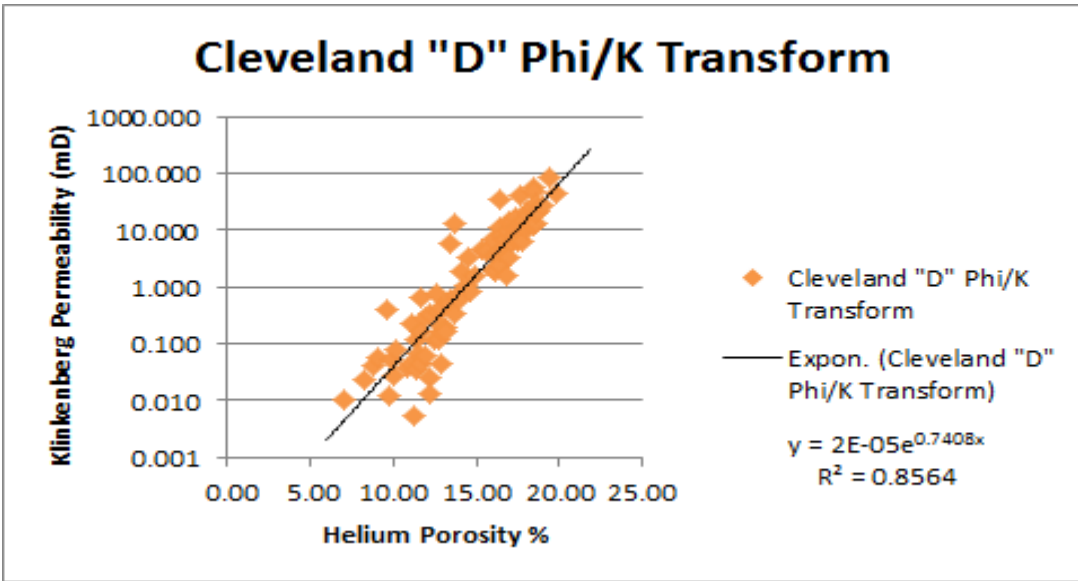


Figure 5.6: Porosity-permeability transform, Cleveland "D" zone. Data included in this graph was acquired from the Cleveland Field Unit, T.21N, R.8E, Pawnee Co., Oklahoma. Porosity and permeability measurements depicted above are from 101 core plugs from the Cleveland "D" zone.

Table 5.2 summarizes core-data analysis from the J.A. Jones No. 58 well. Most of the rock sampled for core analysis from the J.A. Jones No. 58 is clean “homogenous” sandstone with “uniform” bedding.

One hundred-thirty feet of Cleveland Sandstone were cored in the Mid-Con Energy Frazee No. 22 well. As in the other cored wells in the field, samples for analysis are of consistent lithology and of uniform bedding. Table 5.3 is a summary of the data. The Lower R2 values may be attributed to the larger volume of shale rip-up clasts, especially in the “D” zone.

Summary of core-analysis data from the Mid-Con Energy Van Eman No. 16 well is given in Table 5.4. The largest macroscopic difference, in comparison of the Van Eman No. 16 core to the other cores, is the abundance of fractures, most of which are in the “C” zone. The fractures seem to be limited in vertical extent. Figures 5.7-5.9 show some examples of fractures in core plugs of the Cleveland in the Van Eman No. 16.

Zone	Average Porosity	Average Klinkenberg Permeability	R <sup>2</sup>
A	13.83%	3.0 mD	0.7584
B	17.55%	52.67 mD	0.8867
C	15.89%	13.72 mD	0.8714
D	15.53%	9.12 mD	0.8426

Table 5.2: Summary of porosity and permeability measured from samples of the J. A Jones No.58 core, Cleveland Sandstone.

Zone	Average Porosity	Average Klinkenberg Permeability	R <sup>2</sup>
A	Not Present		
B	16.57%	60.10 mD	0.76
C	14.61%	19.82 mD	0.8214.
D	11.87%	0.217	0.3815

Table 5.3: Summary of porosity and permeability measured from samples of the Frazee No.22 core, Cleveland Sandstone.

Zone	Average Porosity	Average Klinkenberg Permeability	R <sup>2</sup>
A	11.58%	3.14 mD	0.2488
B	16.34%	82.62 mD	0.8665
C	15.11%	6.48 mD	0.7218
D	16.57%	15.20 mD	0.7097

Table 5.4: Summary of porosity and permeability measured from samples of the Van Eman No.16 core, Cleveland Sandstone.



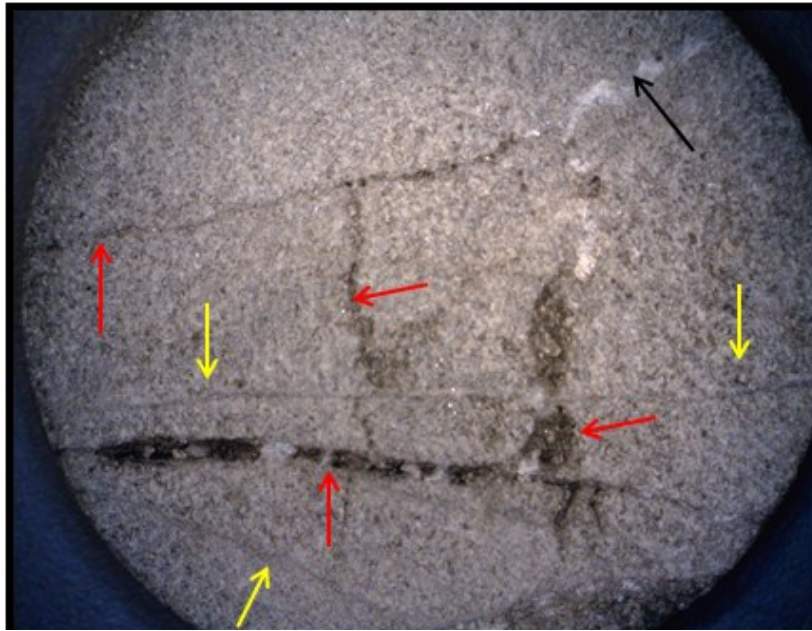


Figure 5.7: Photo of the end of a core plug, Van Eman No.16 at 1683 ft. (core depth). Yellow arrows indicate calcite-sealed fractures. Black arrow indicate partly sealed fractures propped open by euhedral calcite crystals. Red arrows indicate partly open fractures.



Figure 5.8: Enlargement of part of Figure 5.7. Black arrows point to a partly sealed fracture. Aperture of the fracture is approximately 1 mm. It is propped open by euhedral calcite crystals.

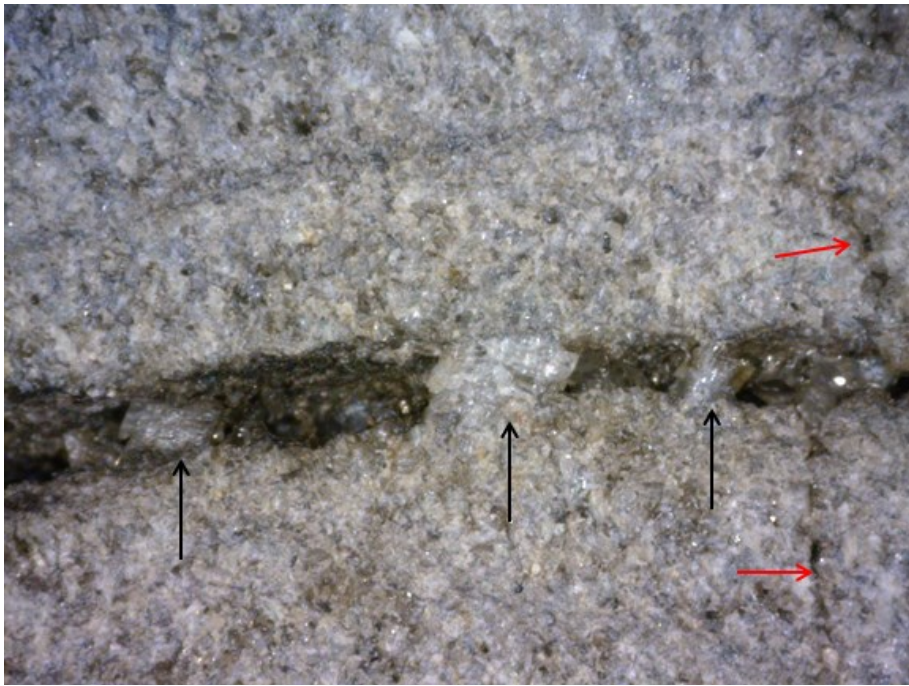


Figure 5.9: Enlargement of Figure 5.8. Black arrows point to a partly sealed fracture. Red arrows point a much narrower vertical fracture that is partly open.

Based on the core analysis, zone “A” is the least porous and permeable, with average porosity ranging from 11.6 to 13.8% and permeability of approximately 3 mD. Porosity in the “D” zone ranges from 11.9 to 16.6%, and average permeability ranges from 0.2 to 15.2 mD. Lower permeability in these units is due to overall smaller grain size, along with associated silt and clay particles. As discussed in Chapter IV, the “B” and “C” zones vary less in lithology than the “A” and “D” zones. Maximum permeability in the “B” zone is 605 mD; overall the average is 63 mD. The porosity ranges from 16.3 to 17.6%, and the permeability ranges from 52.7 to 82.6 mD. The high permeability is important during fracturing and water flooding of the Cleveland Sandstone. The values for the “C” zone are 14.6 to 15.9%; average porosity and 6.5 to 19.8 mD average permeability.

## **Petrophysical Attributes and Integration of Data from Analysis of Cores**

Petrophysical attributes of the Cleveland Sandstone and the procedure (workflow) for their determination, to be utilized in this study, are thought to be of much value in areas where only partial suites of requisite petrophysical data are available. This becomes especially important in mature oil fields, like the Cleveland Field, where the majority of the data consists solely of resistivity and spontaneous-potential logs. By acquiring cores from a reservoir of interest, measuring attributes of the rock, and then extrapolating from core-porosity measurements, older porosity logs can be calibrated; this procedure results in more accurate estimation of porosity and permeability. Having an assortment of porosity, resistivity, SP, and gamma-ray logs allows for development of reliable estimates of the most essential components of a suite of petrophysical attributes: shale volume, total porosity, effective porosity, and water saturation. These statistics can then be integrated with information about reservoir deposition and geometry to assess reservoir quality and estimate oil in-place

### **Shale Volume**

Volumes of shale can be calculated by a variety of methods and algorithms. The preferred method of estimating volume of shale in clastic rocks is based on information derived from the gamma-ray log. In addition to approximating shale volume from other wireline logs, shale volume can be calculated by different empirical formulae. The preferred method for shale volume calculation is given in equation 5.2 below

$$V_{Sh} = \frac{(GR_{shale} - GR_{log})}{(GR_{shale} - GR_{sandstone})}$$

Equation 5.2: Calculation of volume of shale. This calculation was used in part to measure the volume of shale within the Cleveland Sandstone in the study area. (Asquith, 2004, p. 31)

This equation is the foundation for other shale volume calculations (e.g., Clavier, Larinov, Steiber, Konen; J. Kulha, personal communication). The  $GR_{sh}$  and  $GR_{Sand}$  measurements typically are derived by plotting the GR (API) values on a histogram and selecting boundaries of 100% sandstone and 100% shale (Figure 5.10). This method inherently has flaws (nearly all sands have a small percentage of shale or clay present), but plotting gamma-ray measurements on a histogram, with almost any office/geological software packages, has practical value.

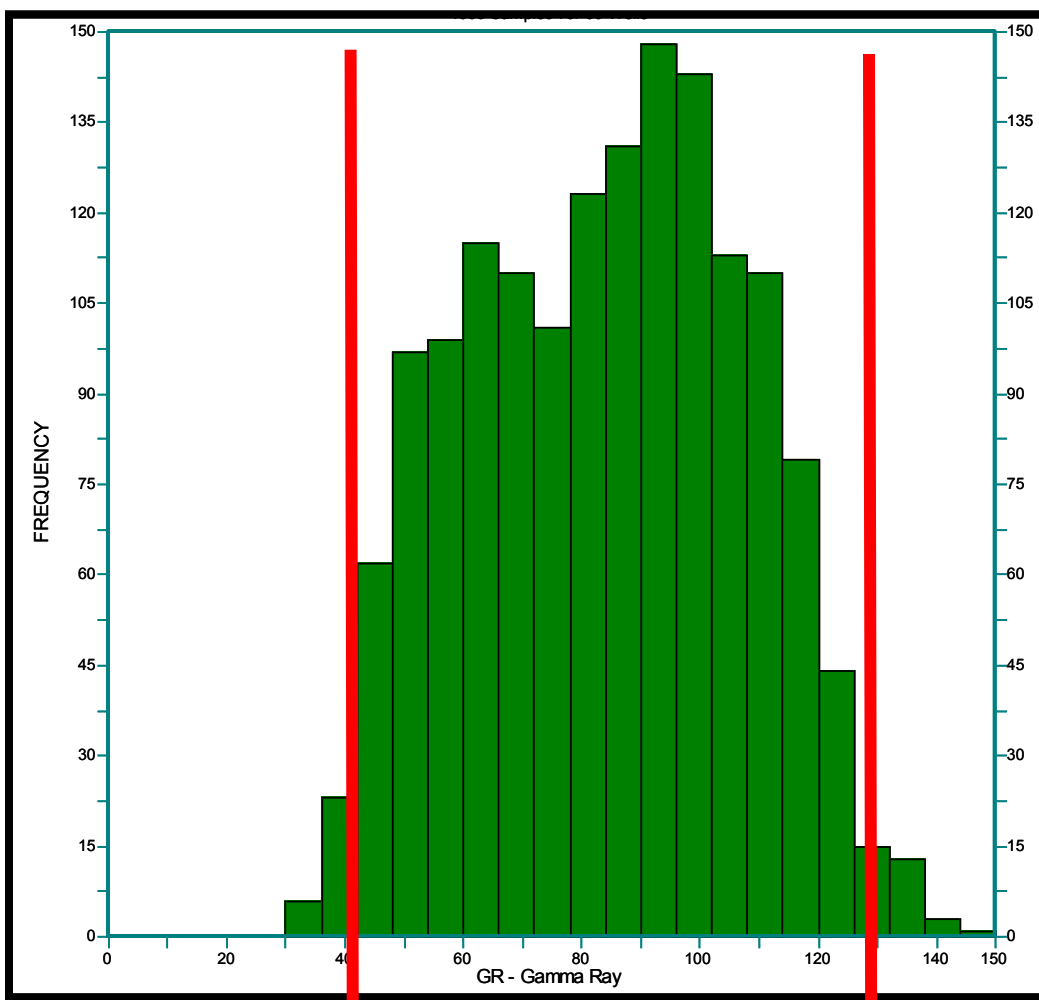


Figure 5.10: Composite gamma-ray histogram of Cleveland Sandstone in all wells evaluated in the study area. Red lines indicate 100% sandstone ( $GR_{Sandstone}$  42 API) and 100% shale ( $GR_{Shale}$ , 128 API).

## Porosity

For purposes of this study, total and effective porosity of the Cleveland Sandstone were calculated. Total porosity was computed by using only bulk-density logs; neutron porosity logs were not used. Density porosity was calculated as shown in Equation 5.3.

$$\phi_D = \frac{\rho_{ma} - \rho_{log}}{\rho_{ma} - \rho_{fl}}$$

Equation 5.3: Density-porosity calculation.  $\rho_{ma}$  is the density of the matrix;  $\rho_{log}$  signifies bulk density as recorded on density logs;  $\rho_{fl}$  signifies density of the fluid in pores. (Asquith, 2004, p. 39)

Based on grain-density data obtained from cores from the Cleveland Field (as described above), matrix density of Cleveland Sandstone was assumed to be 2.68 g/cm<sup>3</sup> within all four zones. Fluid density (i.e. density of drilling-mud filtrate) was assumed to be 1 g/cm<sup>3</sup>.

Bulk density was selected for computation of the total porosity because of its close correlation with the helium porosity measured from core plugs. Figure 5.11 is a graph of porosity measured from core as compared with calculated total porosity.

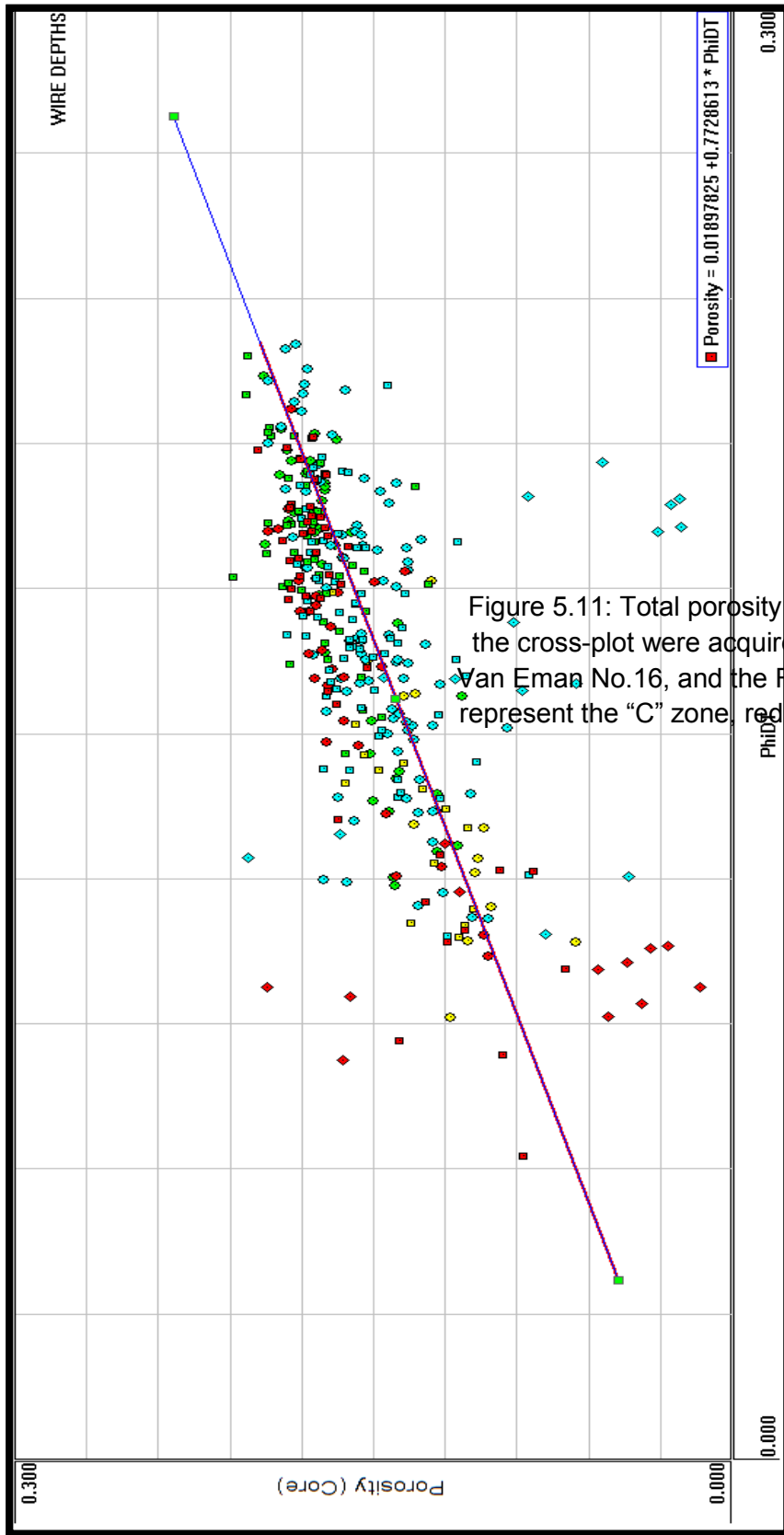


Figure 5.11: Total porosity (from logs) (x axis) and core porosity (y-axis) of the cross-plot were acquired from cores and from wireline logs, from the Van Eman No.16, and the Frazee No.22. Green squares represent the "B" zone, blue diamonds represent the "C" zone, red squares represent the "A" zone, and yellow circles represent the "D" zone.

The purpose of calculating effective porosity is to account for shale within pores. Measurement of effective porosity is used to calculate water saturation and to estimate oil-in-place. For this study, effective porosity was calculated by using core-calibrated total porosity and applying Equation 5.4.

$$\text{PhiE} = \text{PhiT} * (1 - \text{Vsh})$$

Equation 5.4: Calculation of effective porosity. PhiE = effective porosity, PhiT = total porosity (calculated by Equation 5.3, density porosity is equal to total porosity), Vsh = shale volume (calculated by Equation 5.2).

Alternatively, the Equation 5.5 can also be used to calculate effective porosity:

$$\text{PhiE} = \text{PhiT} * (\text{Vsh} * \text{PhiSh})$$

Equation 5.5: Alternative method for calculating effective porosity. PhiE = effective porosity; PhiT = total porosity (calculated by Equation 5.3); Vsh = shale volume (calculated by Equation 5.2), PhiSh = shale porosity (interpreted from the total porosity recorded within stratigraphically associated shale).

Primarily, Equation 5.4 was used, because it is a more conservative estimate of effective porosity within the Cleveland Sandstone than Equation 5.5.

### *Water Saturation*

Measuring water saturation from evidence extracted from wireline logs involves the integration of porosity, resistivity, formation water resistivity, and electrical data. Total porosity and resistivity were recorded directly from wireline logs. Water samples were collected from wells that produce only from the Cleveland Sandstone; these samples were analyzed to determine resistivity water in the Cleveland. Based on analyses obtained from Chemical Flooding Technologies ©, water resistivity of 0.059 ohm-meters was regarded as a reliable estimate. Parameters for basic equations in estimating of water saturation (by the Archie and Simandoux equations), namely, cementation, lithology, and saturation exponents, were

estimated by plotting true formation resistivity (Rt) against neutron density porosity (PhiND), a plot well known as a Pickett plot. Based on evidence from Pickett plots and from personal communication with Mid-Con Energy's petrophysical consultant John Kulha, the tortuosity factor (a) used was 1, the cementation exponent used was 1.73, and the saturation exponent (n) was 2 (Appendix C).

Traditionally, the Archie method is applicable when calculating the water saturation in clean sandstones (Kulha, J, 2014, Private Communication). The Archie method in the strictest sense does not take into account dispersed clay or thin beds of siltstone and shale within the formation being analyzed. The Simandoux equation, accounts for clay in sandstone and yields more accurate estimates of water saturation. Therefore, the Simandoux equation (Equation 5.6) was used to estimate water saturation based on petrographic data from cores and on measurements from produced water. The valuable guidance by John Kulha is acknowledged here.

$$S_w = \left[ \frac{.4R_w}{\phi_e^2} \right] \left[ \sqrt{\frac{5*\phi_e^2}{R_w*R_t} + \left( \frac{V_{sh}}{R_{sh}} \right)} - \left( \frac{V_{sh}}{R_{sh}} \right) \right]$$

Equation 5.6: Simandoux Water Saturation Equation.  $V_{sh}$  = Shale Volume,  $R_{sh}$  = True Formation Resistivity from shale,  $\phi_e$  = Effective porosity,  $R_w$  = Formation Water Resistivity,  $R_t$  = True Formation Resistivity.



Calculated average water saturation, effective porosity and electrical exponents are shown in Table 5.5.

Zone	Effective Porosity	Water Saturation (Simandoux)	Electrical Exponents (A,M,N)
A	15.7%	42.2%	1, 1.73, 2
B	16.2%	41.8%	1, 1.73, 2
C	17.5%	45.1%	1, 1.73, 2
D	13.2%	55.1%	1, 1.73, 2

Table 5.5: Summary of the petrophysical analysis. Parameters were used in estimate oil-in-place in the Cleveland Sandstone.

## **Chapter VI**

### **Petroleum Geology and Reservoir Geometry**

By integrating information derived from the geological and petrophysical models described in previous chapters, the spatial geometry and reservoir-storage volume of each of the four divisions of the Cleveland can be determined. The primary purpose in establishing reservoir geometry and storage capacity is to estimate the amount of oil-in-place. Previous estimations of oil in place for the Cleveland Sandstone reservoir have been as low as 10 MMBO. By incorporating data gained in this study, oil-in-place estimates, which have been generated, have drastically increased the estimated future oil production from the Cleveland Sandstone and enhance the overall value of the field. This chapter documents a quantitative estimate of oil-in-place.

#### **Reservoir Geometry: Thickness and Distribution**

To characterize spatial distribution of the Cleveland Sandstone properly, isopach maps were hand-contoured and loaded into Petra software. Stratigraphic cross-sections were of much value in preparation of the isopach maps. Appendix E contains a location map showing evidence of wells used to create each cross-section and the extent of each cross-section. These

cross-sections were useful in determining the boundary of each zone. Digital data (.LAS) for each well in the cross-sections were imported into HDS petrophysical evaluation software, along with the “tops” of the units (elevations of upper limits), petrophysical data and derived parameters (as described in Chapter V).

By use of the HDS software, gross sandstone (Figure 6.1), porous sandstone, and net-pay sandstone thicknesses were compiled, based on cut-off values shown in Table 6.1. An example of the qualitative evaluation generated from HDS software is shown in Appendix F.

Zone	Net Vshale	Net Porous Vshale+Phi	Net Pay Vshale+Phi+Sw
A	<50%	>12%	<60%
B	<50%	>12%	<60%
C	<40%	>15%	<60%
D	<60%	>10%	<60%

Table 6.1: Limiting values (cutoffs) for each unit of the Cleveland Sandstone, arranged according to type of map.

### **Net Pay, Petroleum Bearing Sandstone**

For oil-and-gas net-pay maps (Figures 6.2 - 6.5), shale volume, porosity, and water-saturation volumes were computed by use of the petrophysical model in Hydrocarbon Data Systems petrophysical evaluation software (Chapter IV). As an example of using net-pay cut-offs based on petrophysical data, analogues, and field-production data, for example, oil production from the “C” zone appears to be restricted to areas that have a minimum of 15% porosity and less than 60% water saturation.

## Estimation of Reserves

Oil-in-place estimates were based on equation 6.1 (below)

$$OIP = \frac{7758 * A * \phi * h * (1 - Sw)}{Boi}$$

Equation 6.1: Oil-in-place Equation. “A” signifies the reservoir area,  $\phi$  signifies the effective porosity used in calculating *OIP*; *h* represents reservoir thickness;  $(1-Sw)$  indicates the estimated oil saturation, *Boi* signifies the initial formation volume factor.

Estimated oil-in-place values were computed for each of the four divisions of the Cleveland Sand. In total, current oil-in-place is estimated to be nearly 50 million barrels of oil. Most of the oil is within the “C” zone (29 million barrels of oil).

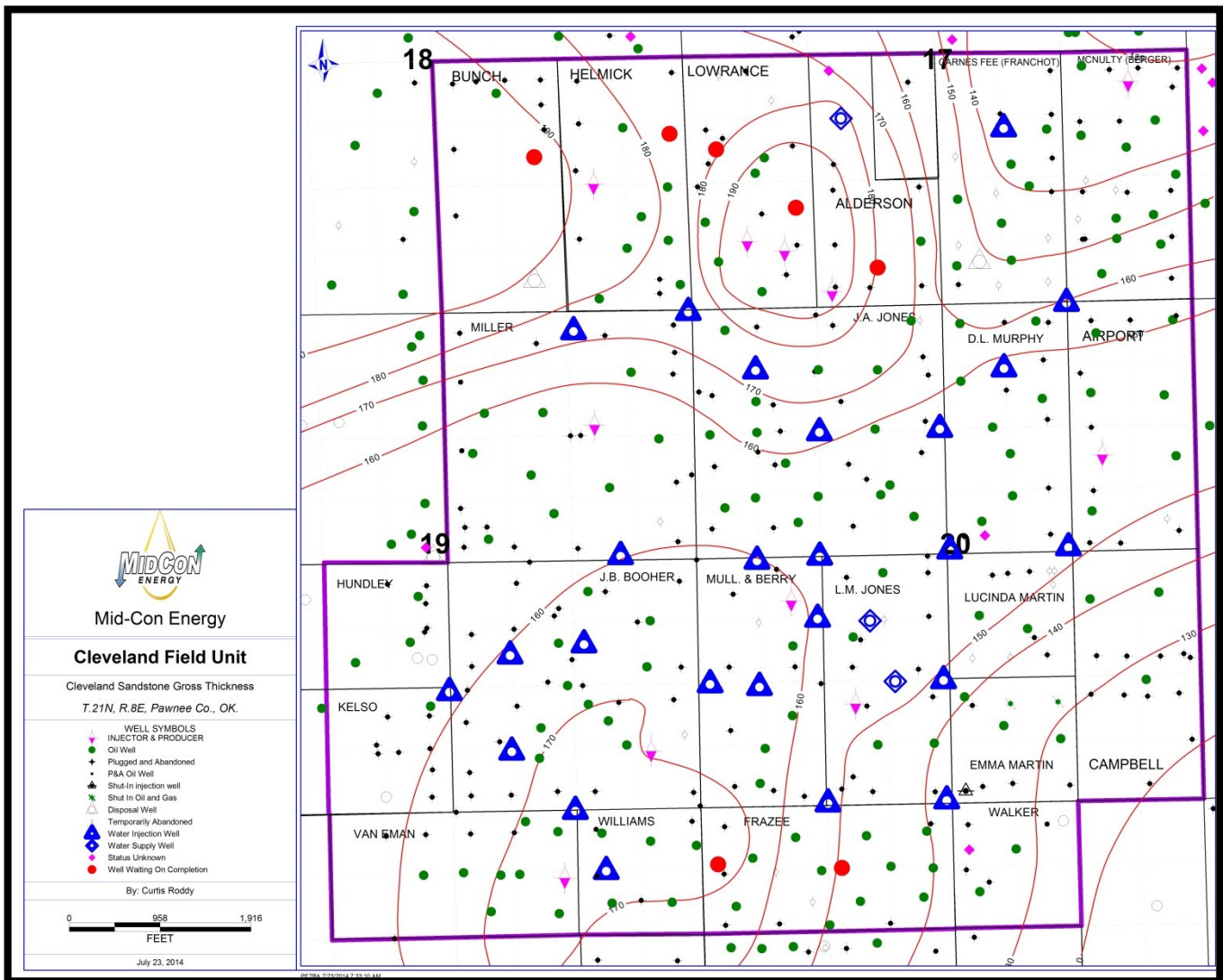


Figure 6.1: Thickness of the Cleveland Sandstone, showing overall thinning from 190 ft. in the northwest and north-center to approximately 120 ft. in the southeast and northeast of the Cleveland Field Unit. Numbers in black represent the well numbers. Contour interval: 10 ft.

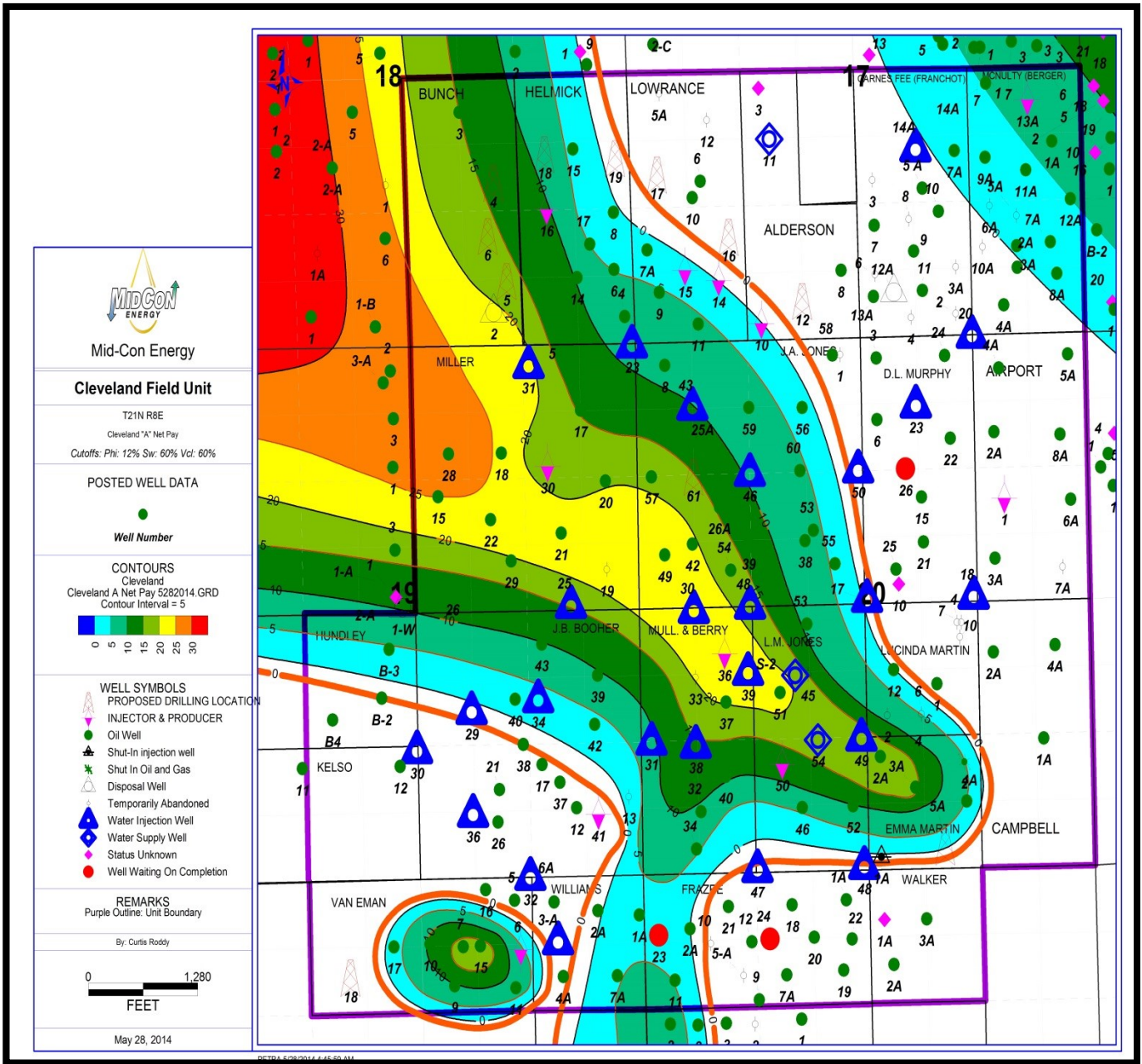


Figure 6.2: Cleveland “A” net pay sandstone map (total Phi >12%, Vsh<60%, Sw<60%). Thickest sand in the northwest thins along a southeast trend, with separate developments in the northeast and southwest. Contour interval 5 ft.

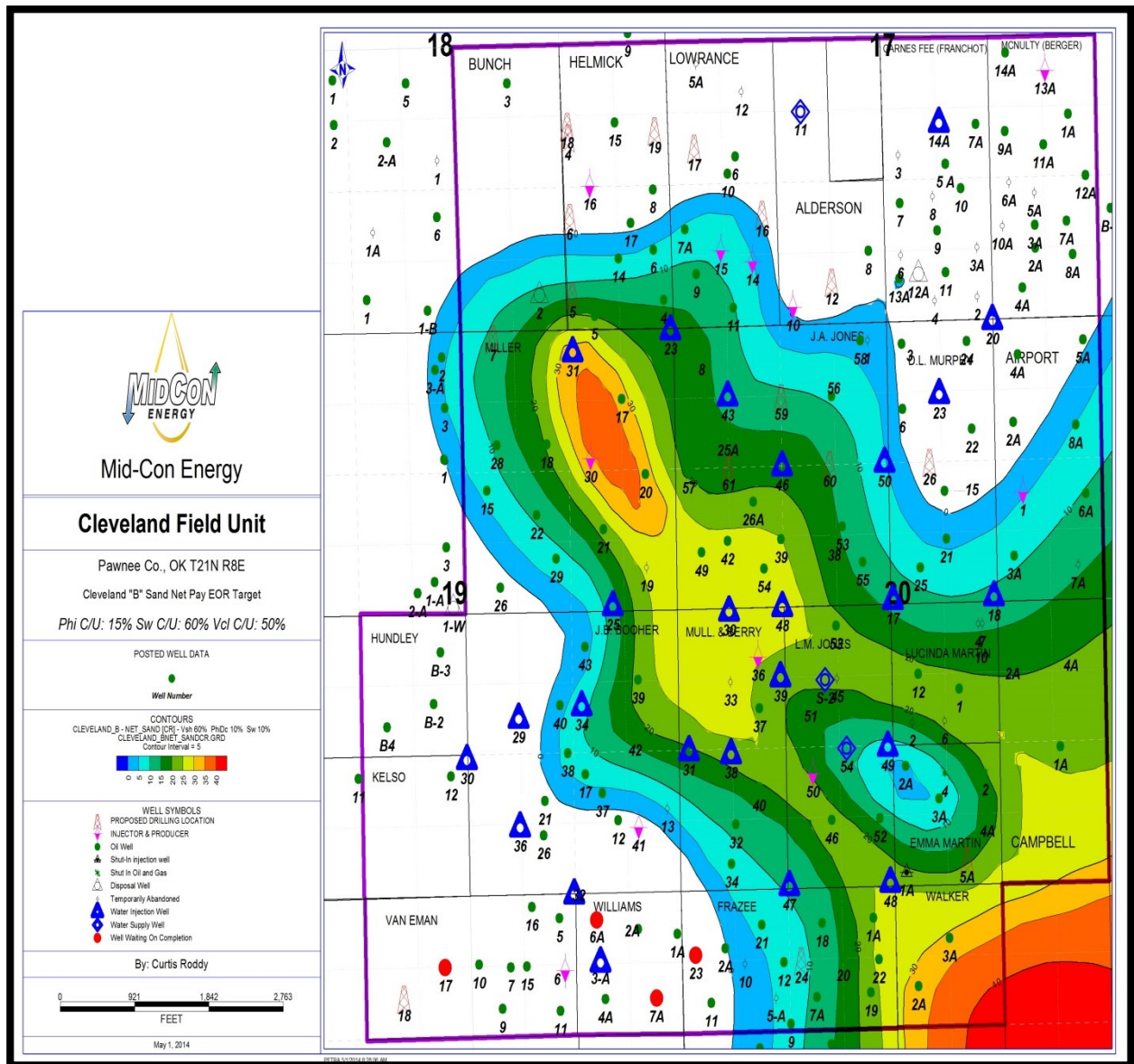


Figure 6.3: Cleveland "B" net pay sandstone map (total Phi >15%, Vsh<50%, Sw<60%). Sand trends to the northwest, with no pay in the north, and southwest. Contour interval 5 ft.

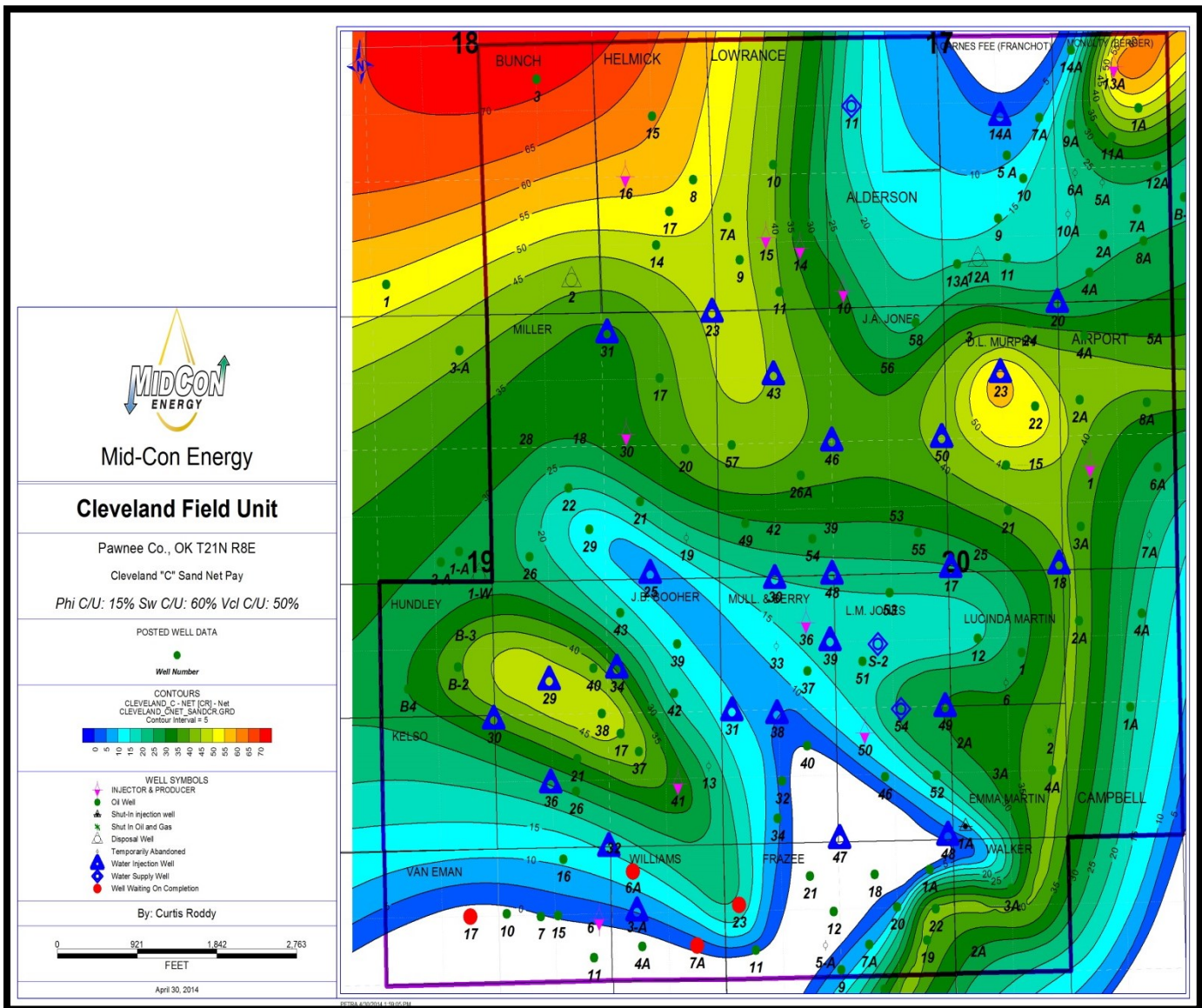


Figure 6.4: Cleveland "C" net pay sandstone map (total Phi >15%, Vsh <50%, Sw <60%). Sand is widespread, with greatest thickness in the northwest. Contour interval 5 ft.



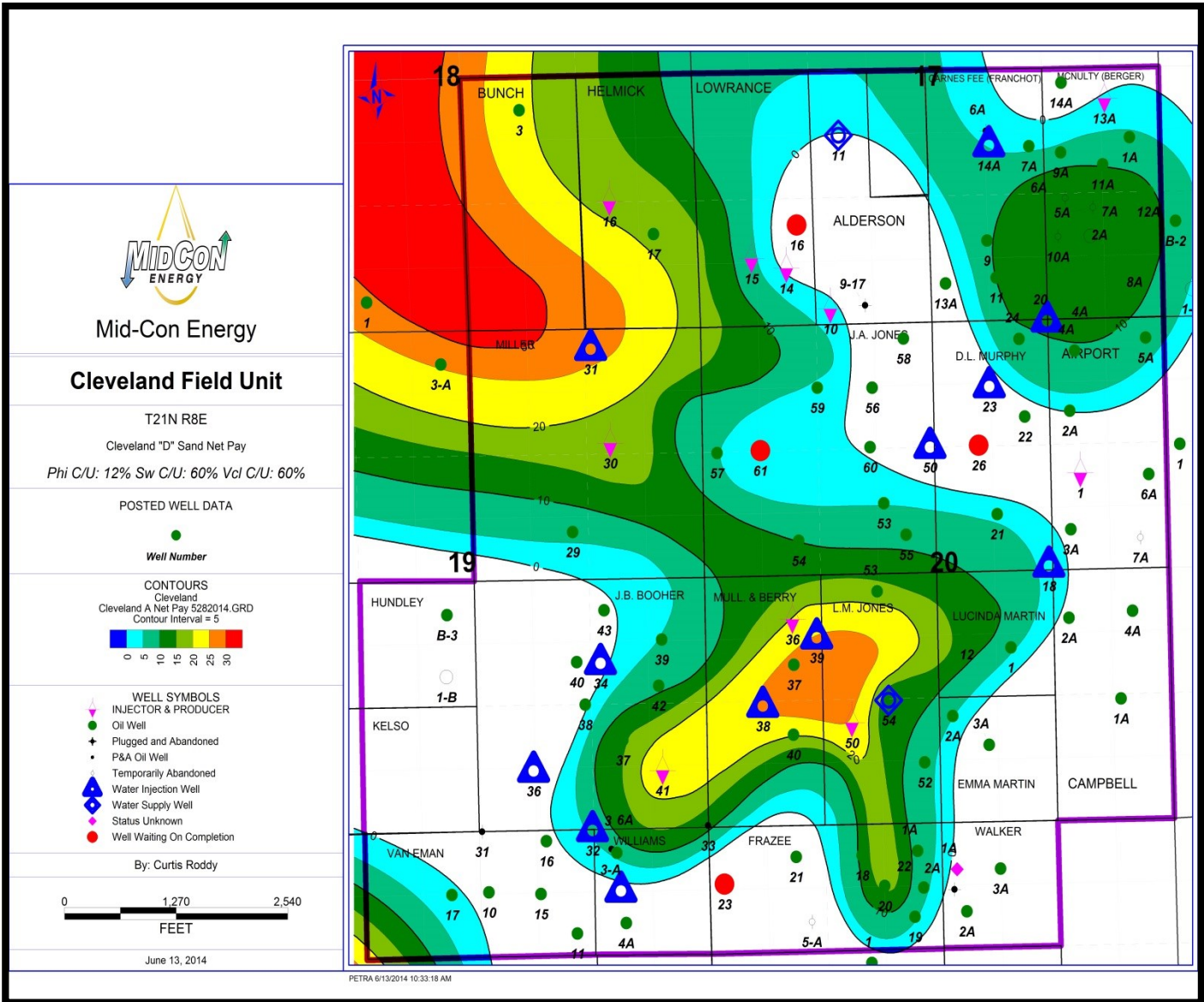


Figure 6.5: Cleveland "D" net pay sandstone map (total Phi >12%, Vsh<60%, Sw<60%). Irregular sand trend is northwest to southeast, with minor northeast trend in the south. Contour interval 5 ft.

## Chapter VII

### Discussion and Conclusions

#### Discussion

This study shows the value of detailed rock analysis (core examination and analysis) and its fluids (including water resistivity), of using modern tools (especially wireline logs), and of applying germane ideas (e.g., in petrophysical calculations) are valuable in finding and producing previously by –passed reservoirs. The Cleveland Field has been producing oil and gas from the Pennsylvanian sandstones since 1904. In the time since the discovery of the field eight companies have evaluated and operated the field. While the Cleveland Sandstone (Cleveland “B” zone) has been produced by earlier operators (operators other than Mid-Con Energy, LLC) the Cleveland “C” zone has never been targeted for oil and gas production. By applying nonconventional techniques and interpretation to old fields, new oil can be found and produced.

In attempting to determine the oil-in-place volume for each zone within the Cleveland Sandstone interval, the application of nonconventional equations were used. The use of the Simandoux equation was crucial in predicting the current oil saturations within the Cleveland interval. By accounting for the presence of silt and shale within the separate Cleveland Sandstone zones, the use of the Simandoux equation rendered a much more accurate estimate

of current oil saturation. Table 7.1 compares the water saturation calculated when using the Archie and Simandoux equations.

Zone	Archie Equation	Simandoux Equation	Saturation Difference
"A"	83.2%	42.2%	41.0%
"B"	46.48%	41.8%	4.68%
"C"	69.44%	45.1%	24.34%
"D"	84.85%	55.1%	29.75%

Table 7.1: Comparison of average water saturation calculations using the Archie and Simandoux equations.

Overall, the largest impact of the Simandoux equation is noticed in the "A" and "C" zones, the zones that are currently being targeted for oil production. It is also important to note the importance of using effective porosity, and not total porosity. Using the effective porosity accounts for any shale that may be in the zone and does not measure the area containing shale as porosity. Table 7.2, compares the differences between total porosity and effective porosity.

Zone	Total Porosity	Effective Porosity	Porosity Difference
"A"	16.83%	13.03%	3.80%
"B"	18.43%	14.70%	3.73%
"C"	18.13%	13.67%	4.46%
"D"	15.67%	10.30%	5.37%

After identifying the potential of oil production from the Cleveland, the next “hurdle” to overcome was completing and producing the oil from the “A” and “C” zones in the most efficient

Table 7.2: Comparison of average effective porosity and total porosity calculations.

manner. In completing the Cleveland zones, it is necessary to perform a relatively large hydraulic fracture in order to drain the entire targeted interval. On average, these “frac” jobs used 1,500 pounds of sand per foot of completion. Initially, Mid-Con Energy, LLC perforated the entire Cleveland interval with the hopes of contacting all four zones. After several of these completions the operator realized that the majority “frac” (98%) was going into the “B” zone of the Cleveland interval. This is due primarily to of the large permeability difference between the “A”, “B”, “C”, and “D” zones. The average permeability of the “B” zone averages three times that of the other three zones. In order to effectively target the “A” and “C” zones (the “B” zone appears to have already been effectively drained), a revised completion program was implemented. The largest change in this plan was to keep the perforations/completion zones at least fifteen feet away from the “B” zone. In implementing this program, the hydraulic fracture should be contained to the “A” and “C” zones, avoiding the “B” zone. In order to monitor the results of this design, radioactive tracers were injected during the end of each “frac” stage for the purpose of determining where the majority of the sand for each stage was temporarily residing. Iridium, a radioactive chemical, was/is used in the first stage of the “frac” and Scandium was/is used in the second stage of the “frac”. Following the hydraulic fracturing, a spectral gamma-ray tool was/is used to determine the amount of sand that has entered each zone during each stage of the completion (Figure 7.1). The valuable guidance from Mr. Ryan Logsdon (Petroleum Engineer, Mid-Con Energy Operating, LLC.) is acknowledged here.

In addition to using radioactive chemicals to monitor the success/failures of the completions process, injection profile tests were also used to determine the path and temporary residence of water injected into the Cleveland interval. When the “B” zone is perforated or fractured in Cleveland Sandstone injection wells, injection profile tests indicate that 99% of the injected water is entering the “B” zone. After comparing the injection profiles of wells that had been completed by means of hydraulic fracturing to wells that had been completed using acid

only, it was determined that wells that were not completed by hydraulic fracturing were able to inject water more efficiently into the “C” zone.

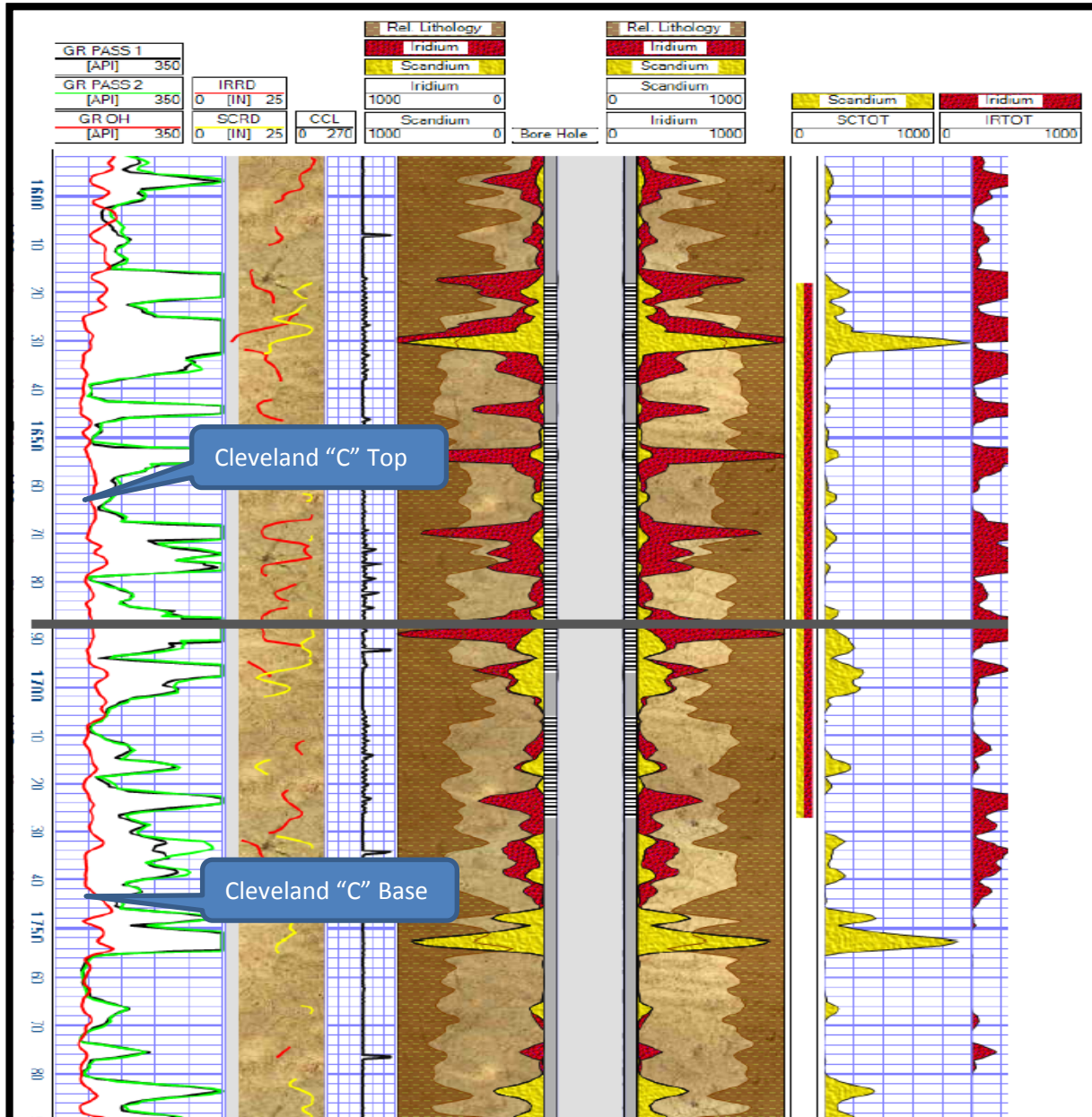


Figure 7.1: Spectrascan (Core Labs LLC., Houston, Texas) image from the J.A Jones #58 (Sec. 20, T.21N, R.8E). The results from this spectrascan indicate that both stages of hydraulic fracturing (1<sup>st</sup> stage red, 2<sup>nd</sup> stage yellow) contacted the majority of the Cleveland “C” zone and had little affect on the Cleveland “B” zone. The red log represents the first stage of the hydraulic fracture, the radioactive chemical measured is iridium. The yellow log represents the second stage of the hydraulic fracture, the radioactive chemical measured is scandium

## Conclusions

The data accumulated in this study, when analyzed, support the conclusion that the Cleveland Sandstone within the Cleveland Field Unit, Pawnee County, Oklahoma has additional potential for oil production in bypassed reservoirs. Besides this general conclusion, the following conclusions are proposed.

1. Correlations of the Cleveland stratigraphic interval provides evidence of four increments (zones/units) of deposition within the study area: "A", "B", "C", and "D". This is based on evidence gained from core analysis, wireline log examination, and past literature on the Cleveland Sandstone.
2. The Cleveland is interpreted as having been deposited within a fluvial-deltaic system, forming a multistoried complex in which deposition ranged from an active channel, represented by the lowermost part of the interval, to prodelta setting at the uppermost boundary of the interval ("A" zone).
3. Principal framework constituents of the Cleveland Sand vary only slightly from zone to zone, consisting primarily of quartz, feldspar, and muscovite.
4. Pickett plots were used to establish reliable values for  $a$ ,  $m$ , and  $n$  which are 1, 1.73, and 2, respectively. The Simandoux equation was used to identify bypassed pay.
5. Currently the Cleveland "A" and "C" stratigraphic units have the best reservoir quality for oil production.
6. Properties of the Cleveland "C" stratigraphic interval are the best for secondary oil recovery.
7. Selection of zones to perforate should consider keeping the "A" and "C" zones isolated from the high permeability, but practically depleted "B" zone.

## REFERENCES

- Asquith, G. B. (2004). *Basic well log analysis* (2nd ed.). Tulsa, Oklahoma: American Association of Petroleum Geologists. Baker, David Alan. *Subsurface geology of southwestern Pawnee County, Oklahoma*. unpublished M.S. thesis, Oklahoma University, Norman, Oklahoma.
- Berryhill, Richard A *Subsurface geology of south-central Pawnee County, Oklahoma*, 1960. Print.
- Bootle, R. J. R., Waugh, M., Bittar, M. S., Hveding, F., Hendricks, W. E., and Pancham, S. (2009, January 1). Laminated Sand Shale Formation Evaluation Using Azimuthal LWD Resistivity. Society of Petroleum Engineers. doi:10.2118/123890-MS
- Campbell, J. A., 1997, The Cleveland Play: Regional Geology: Oklahoma Geological Survey, Special Publication 97-5, p. 13-29.
- Clare, Patrick H. *Petroleum geology of Pawnee County, Oklahoma*. Norman: University of Oklahoma, 1963. Print.
- Eardley, A.J. "Tectonic Divisions of North America." *AAPG Bulletin* 19: 60-67. Print.
- Grace, M., 2014, Verbal communication.
- Krumme, G. J., 1981, Stratigraphic significance of limestones of the Marmaton Group (Pennsylvanian, Desmoinesian) in eastern Oklahoma: Oklahoma Geological Survey Bulletin 131.
- Krystinik, Lee, and Tony Lupo. "High-Resolution 3-D, Sequence Stratigraphy Delineate New Tight Oil Play." *The American Oil and Gas Reporter* 1 July 2011: Web.
- Krystinik, Lee. "Exploring for Tight Oil in the Pennsylvanian Cleveland Sandstone on the Nemaha Ridge Using High Resolution 3D Seismic & Stratigraphic Analysis: A New Play in an Old Area ." Applied Petroleum Geology Lecture. Oklahoma State University. , Stillwater. 2013. Lecture.
- Kulha, J., 2013-2014, Verbal communication.
- Logsdon, R, 2012-2014, Verbal communication
- Passey, Q. R. *Petrophysical evaluation of hydrocarbon pore-thickness in thinly bedded clastic reservoirs*. Tulsa, Okla.: American Association of Petroleum Geologists, 2006. Print.



Powers, Sidney. "Structural Geology of Northeastern Oklahoma." *The Journal of Geology* 39: 117-132. *JSTOR*. Web.

Rascoe, B., Jr., and Adler, F. J., 1983, Permo-Carboniferous hydrocarbon accumulations, Mid-Continent, U.S.A.: *AAPG Bulletin*, v. 67, no.6, p. 979-1001.

Roller, C., 2013-2014, Verbal Communication

## APPENDICES

### Appendix A – Core Sample Acquisition Procedures



## CMS-300 CONVENTIONAL PLUG ANALYSIS PROTOCOL

---

### Sample Preparation

1.5" and 1.0" diameter plugs were drilled with nitrogen gas and trimmed into right cylinders with a diamond-blade trim saw. All sample trims were archived.

### Core Extraction

Plugs selected for routine core analysis were placed in Dean Stark equipment using toluene, followed by Soxhlet extraction cycling between a chloroform / methanol (87:13) azeotrope and methanol.

### Sample Drying

Samples were oven dried at 240° F to weight equilibrium (+/- 0.001 g).

### Porosity

Porosity was determined using Boyle's Law technique by measuring grain volume at ambient conditions & pore volume at indicated net confining stresses (NCS)

### Grain Density

Grain density values were calculated by direct measurement of grain volume and weight on dried plug samples.  
Grain volume was measured by Boyle's Law technique.

### Permeability

Permeability to air was measured on each sample using unsteady-state method at indicated NCS.

### Fluid Saturations

Fluid saturations were determined by the Dean Stark technique using the following fluid properties:

Brine	1.032 g/cc (50000 ppm TDS)
Oil	0.845 g/cc (36° API)

Appendix A: Protocol for core plug extraction, preparation and testing from the Van Eman No.16. The same protocol was used for cores from the J.A Jones No.58 and Frazee No.22.

## APPENDICES

### Appendix B – Laser Particle-Size Analysis (LPSA) Results

Mid-Con Energy  
 J A Jones #58  
 Pawnee County, Oklahoma

File No. : HOU-140129  
 Date : Feb 18, 2014



**PARTSIZ<sup>SM</sup> ANALYSIS**

SMPL NO	DEPTH (ft)	SAND %			SILT %			CLAY (%)	Vsh (%)	Cs (m2/cc)	MEAN (μ)	LITHOLOGY*				
		GRVL	VCRS	CRS	MED	FINE	VFIN						CRS	MED	FINE	VFIN
49	1572.30	0.0	0.0	0.0	5.6	23.4	29.8	18.8	8.9	6.4	4.5	2.6	22	0.27	87	Sd vfg vsshy vshty
63	1588.70	0.0	0.0	0.0	7.3	30.8	32.0	11.2	6.4	6.1	3.8	2.3	19	0.24	106	Sd vfg vsshy
89	1614.40	0.0	0.0	0.0	2.5	24.6	31.3	18.2	9.8	6.7	4.5	2.5	23	0.27	82	Sd vfg vsshy
101	1626.30	0.0	0.0	1.5	28.4	37.0	12.4	5.1	4.7	4.3	3.6	3.0	16	0.22	181	Sd fg vsshy
124	1649.50	0.0	0.0	0.0	5.0	32.9	28.8	7.3	7.4	7.9	5.9	4.9	26	0.36	92	Sd vfg sshy
139	1664.50	0.0	0.0	0.0	5.9	32.5	27.6	8.5	7.2	7.6	5.8	4.8	25	0.35	95	Sd vfg sshy
141	1665.90	0.0	0.0	0.0	3.4	21.7	25.6	14.1	11.1	9.8	8.3	6.0	35	0.43	71	Sd vfg shy
146	1670.50	0.0	0.0	0.5	2.7	17.3	34.0	18.0	8.6	9.2	6.4	3.3	27	0.33	70	Sd vfg sshy
170	1694.70	0.0	0.0	1.1	18.1	33.1	18.0	6.7	7.5	7.5	5.2	2.7	23	0.26	130	Sd fg vsshy
183	1708.20	0.0	0.0	1.5	22.3	39.2	19.4	4.7	4.8	4.2	2.6	1.3	13	0.15	168	Sd fg cin
196	1720.30	0.0	0.0	4.8	28.7	28.0	13.2	7.0	7.1	5.7	3.6	1.9	18	0.20	179	Sd fg vsshy
209	1731.50	0.0	0.0	0.3	12.9	38.3	25.0	4.8	6.7	6.1	3.6	2.2	19	0.22	132	Sd fg vsshy
213	1736.20	0.0	0.0	0.0	7.5	26.4	32.1	13.3	6.4	6.4	4.7	3.2	21	0.27	97	Sd vfg vsshy
224	1750.50	0.0	0.0	0.9	12.4	32.0	25.3	7.6	7.4	7.1	4.4	3.0	22	0.27	117	Sd f-vfg vsshy
241	1767.50	0.0	0.0	0.0	9.5	32.7	28.0	8.1	7.5	7.2	4.2	2.7	22	0.26	109	Sd vfg vsshy
252	1778.50	0.0	0.0	0.9	18.4	39.9	22.9	3.7	5.2	5.1	2.7	1.1	14	0.16	156	Sd fg cin

A

B

C

D

**Footnotes:**

\* Lithology determined using laser particle size distribution.

Mid-Con Energy  
 Van Eman #16  
 Pawnee County, Oklahoma

File No. : HOU-131339  
 Date : Feb 7, 2014  
 : AC, WS



## PARTSIZ<sup>SM</sup> ANALYSIS

SMPL NO	DEPTH (ft)	SAND %			SILT %			CLAY (%)	Vsh (%)	Cs (m2/cc)	MEAN (μ)	LITHOLOGY*				
		GRVL	VCRS	CRS	CRS	VFIN	CRS						MED	FINE	VFIN	
94H	1617.15	0.0	0.0	0.0	3.6	13.8	23.6	21.1	13.5	9.9	7.9	6.7	38	0.48	57	Sd vfg shy
97H	1620.80	0.0	0.0	0.5	6.2	22.6	33.9	13.3	7.3	7.3	4.9	4.0	23	0.32	87	Sd vfg vsshy
102H	1625.50	0.0	0.0	0.7	18.5	36.9	23.0	5.1	4.8	4.8	3.5	2.7	16	0.22	149	Sd fg vsshy
107H	1630.05	0.0	0.0	0.7	31.9	46.7	10.9	2.4	3.5	1.8	1.3	0.7	7	0.10	208	Sd f-mg cin
112H	1635.30	0.0	0.0	0.0	14.8	42.4	20.0	4.0	6.2	5.1	4.1	3.4	19	0.25	141	Sd fg vsshy
115H	1638.45	0.0	0.0	0.6	22.4	37.4	15.0	4.9	6.1	5.5	4.5	3.7	20	0.27	153	Sd fg vsshy
118H	1641.60	0.0	0.0	3.6	27.6	33.7	15.2	5.3	4.8	4.2	3.2	2.5	15	0.20	185	Sd fg cin
123H	1646.55	0.0	0.0	0.3	1.6	14.1	31.2	21.7	10.3	8.5	6.7	5.6	31	0.42	61	Sd vfg sshy
130H	1653.85	0.0	0.0	1.5	21.9	40.6	19.8	3.4	4.0	3.8	2.8	2.2	13	0.18	169	Sd fg cin
135H	1658.70	0.0	0.0	0.0	3.9	24.1	31.5	12.7	8.1	8.5	6.1	5.2	28	0.39	79	Sd vfg sshy
141H	1664.60	0.0	0.0	0.0	11.3	33.7	24.2	8.7	6.7	6.3	5.0	4.0	22	0.30	114	Sd f-vfg vsshy
148H	1671.75	0.0	0.0	0.8	28.3	41.3	10.7	3.8	5.6	4.1	3.2	2.3	15	0.19	187	Sd fg vsshy
154H	1677.75	0.0	0.0	0.0	5.7	27.8	33.2	12.0	6.1	6.4	4.7	4.0	21	0.31	95	Sd v-fg vsshy
158H	1681.85	0.0	0.0	0.1	14.2	35.7	22.7	7.0	6.5	5.9	4.4	3.5	20	0.27	127	Sd f-vfg vsshy
161H	1684.45	0.0	0.0	0.0	9.9	29.3	23.8	9.6	8.0	8.0	6.3	4.9	27	0.36	98	Sd v-fg sshy
171H	1694.15	0.0	0.0	0.0	6.1	21.6	23.3	13.1	11.2	10.3	8.0	6.4	36	0.46	76	Sd vfg shy
178H	1701.50	0.0	0.0	3.3	8.2	20.3	29.9	15.8	6.5	6.4	5.2	4.4	22	0.33	93	Sd v-fg vsshy
187H	1710.60	0.0	0.0	0.0	1.5	11.0	24.3	24.4	14.5	9.4	7.7	7.1	39	0.51	51	Sd v-f-silt shy
194H	1717.70	0.0	0.0	0.0	2.7	25.5	36.8	13.5	5.9	6.9	4.8	3.9	21	0.31	88	Sd vfg vsshy
205H	1728.50	0.0	0.0	2.6	8.2	31.6	34.9	5.5	4.9	5.8	3.6	2.8	17	0.24	118	Sd f-vfg vsshy
206H	1729.35	0.0	0.0	0.0	6.9	34.8	30.0	8.0	6.5	6.2	4.3	3.3	20	0.27	110	Sd v-fg vsshy
219H	1742.55	0.0	2.2	8.0	23.4	31.4	13.1	4.6	5.8	5.3	3.7	2.5	17	0.21	193	Sd fg vsshy
235H	1758.15	0.0	0.0	0.1	4.9	26.8	27.0	11.5	9.7	9.2	6.3	4.5	30	0.36	83	Sd vfg sshy
238H	1761.80	0.0	0.0	0.0	8.6	30.4	20.5	7.2	9.5	10.2	7.9	5.7	33	0.41	93	Sd v-fg sshy
252H	1775.30	0.0	0.0	0.0	8.6	37.8	31.3	7.9	5.8	4.6	2.4	1.6	14	0.18	123	Sd f-vfg cin

A

B

\*

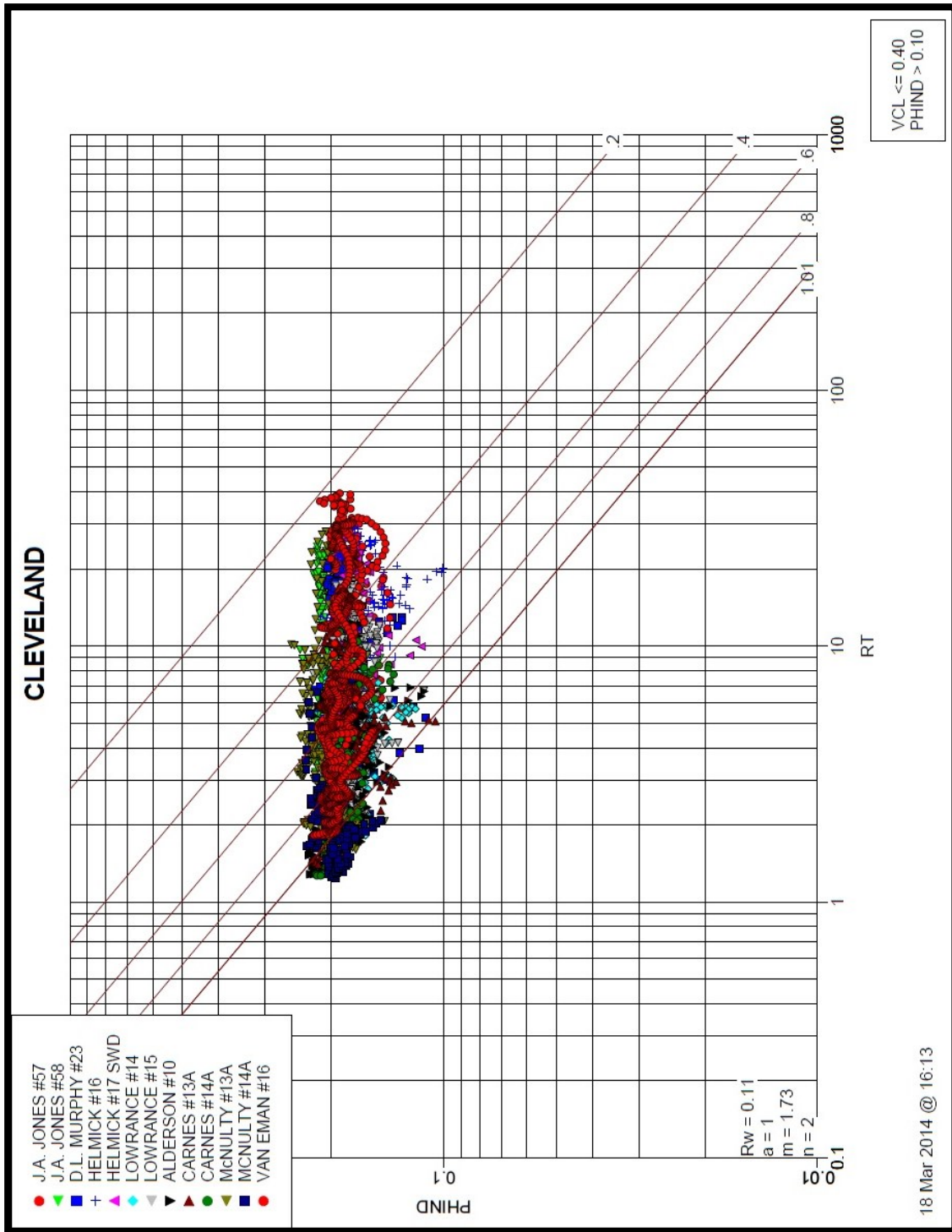
D

**Footnotes:**

\* Lithology determined using laser particle size distribution.

## APPENDICES

Appendix C – Pickett Plot, Cleveland Sandstone Interval



Appendix C: Pickett plot from the Cleveland Sand interval. This plot indicates that the Cleveland Sand has (for variables in Archie and Simandoux equations) a lithology constant value of 1, a cementation factor of 1.73, and a saturation exponent of 2. (From Kulha, J, 2014, Private Communication)



## APPENDICES

### Appendix D – Well Data

APPENDIX D  
GROSS AND NET SAND THICKNESS

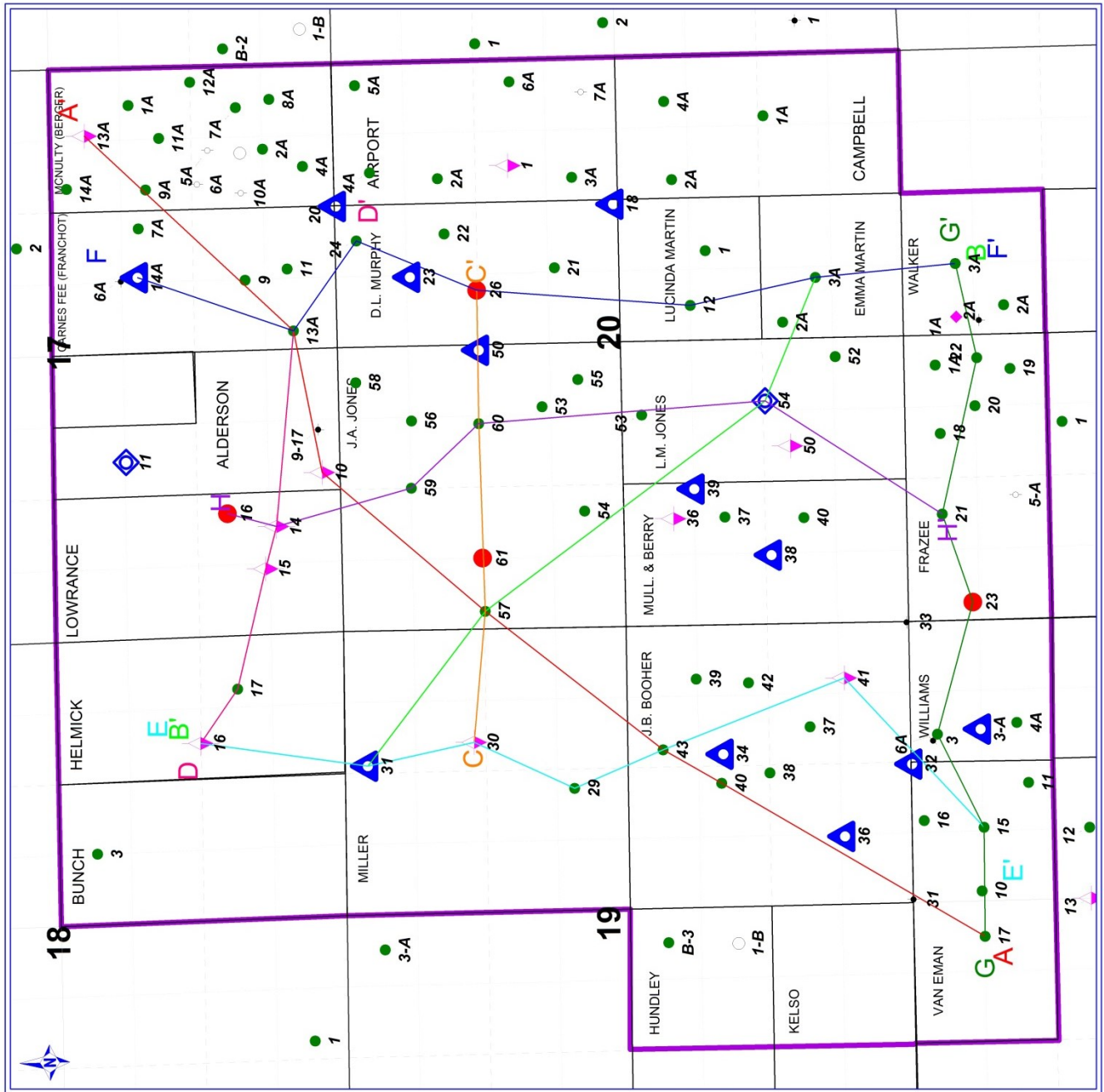
Well Label	Cleveland Gross	Cleveland "A" Net Pay	Cleveland "B" Net Pay	Cleveland "C" Net Pay	Cleveland "D" Net Pay
ALDERSON 10	198	3	0	31	3
ALDERSON 11	181	0	0	4	3
BOOHER 40	162	3	4	43	0
BOOHER 41	169	0	0	31	24
BOOHER 42	167	4	19	18	8
BOOHER 43	162	11	3	16	3
CARNES 13A	153	0	2	21	0
CARNES 14A	136	0	0	4	5
EMMA MARTIN 3A	136	16	5	32	0
FRAZEE 20	145	14	13	6	18
FRAZEE 21	158	0	8	0	0
FRAZEE 22	141	26	29	45	6
FRAZEE 23	177	3	0	20	0
HELMICK 16	189	11	0	58	18
HELMICK 17	185	4	0	54	19
JONES 57	158	21	19	44	5
JONES 58	170	4	4	24	0
JONES LM 54	157	18	11	27	14
LOWRANCE 14	196	2	5	33	0
LOWRANCE 15	195	4	9	42	5
MARTIN L 12	151	0	21	19	14
MCNULTY 13A	130	0	0	61	3
MCNULTY 14A	119	0	0	7	0
MILLER 29	152	19	9	11	6
MILLER 30	155	18	37	33	16
MILLER 31	173	21	37	34	27
MURPHY 22	154	0	0	55	0
MURPHY 23	157	0	0	56	0
MURPHY 24	162	0	0	33	9
VAN EMAN 12	179	0	0	0	0
VAN EMAN 13	163	0	0	0	0
VAN EMAN 14	160	0	0	30	0
VAN EMAN 15	174	17	0	12	0
VAN EMAN 16	170	0	0	10	0
VAN EMAN 17	163	4	0	2	0
WALKER 3A	133	0	31	30	0
WILLIAMS 4A	170	0	0	0	0
WILLIAMS 5A	163	5	0	0	0
WILLIAMS 6A	185	0	0	0	0

Appendix D: Gross and net pay sand thicknesses used to generate gross and net pay isopach maps. All wells listed above are located within the study area (T.21N, R.8E, Pawnee Co., Oklahoma).

Units of measurement: ft.

## APPENDICES

Appendix E – Cross-Section Location Map and Cross-Sections



PETRA 6/16/2014 1:17:52 PM

**Mid-Con Energy**  
**Cleveland Field Unit**

T21N R8E  
 Cross-Section Locator Map

POSTED WELL DATA

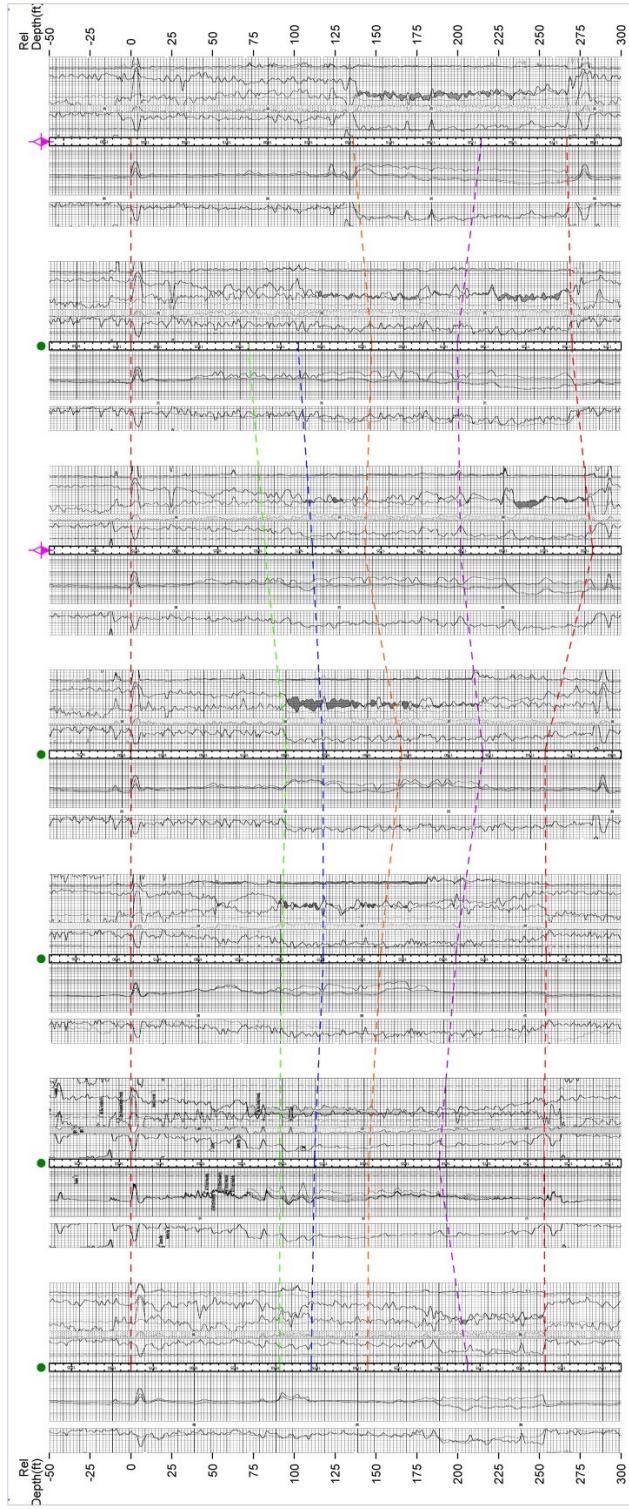
Well Number

WELL SYMBOLS  
 INJECTOR & PRODUCER  
 Oil Well  
 Plugged and Abandoned  
 P&A Oil Well  
 Temporarily Abandoned  
 Water Injection Well  
 Water Supply Well  
 Status Unknown  
 Well Waiting On Completion

By: Curtis Roddy

0 960 1,960  
 FEET

June 16, 2014



Mid-Con Energy  
Cleveland Field Unit

A to A'

Cleveland Sandstone

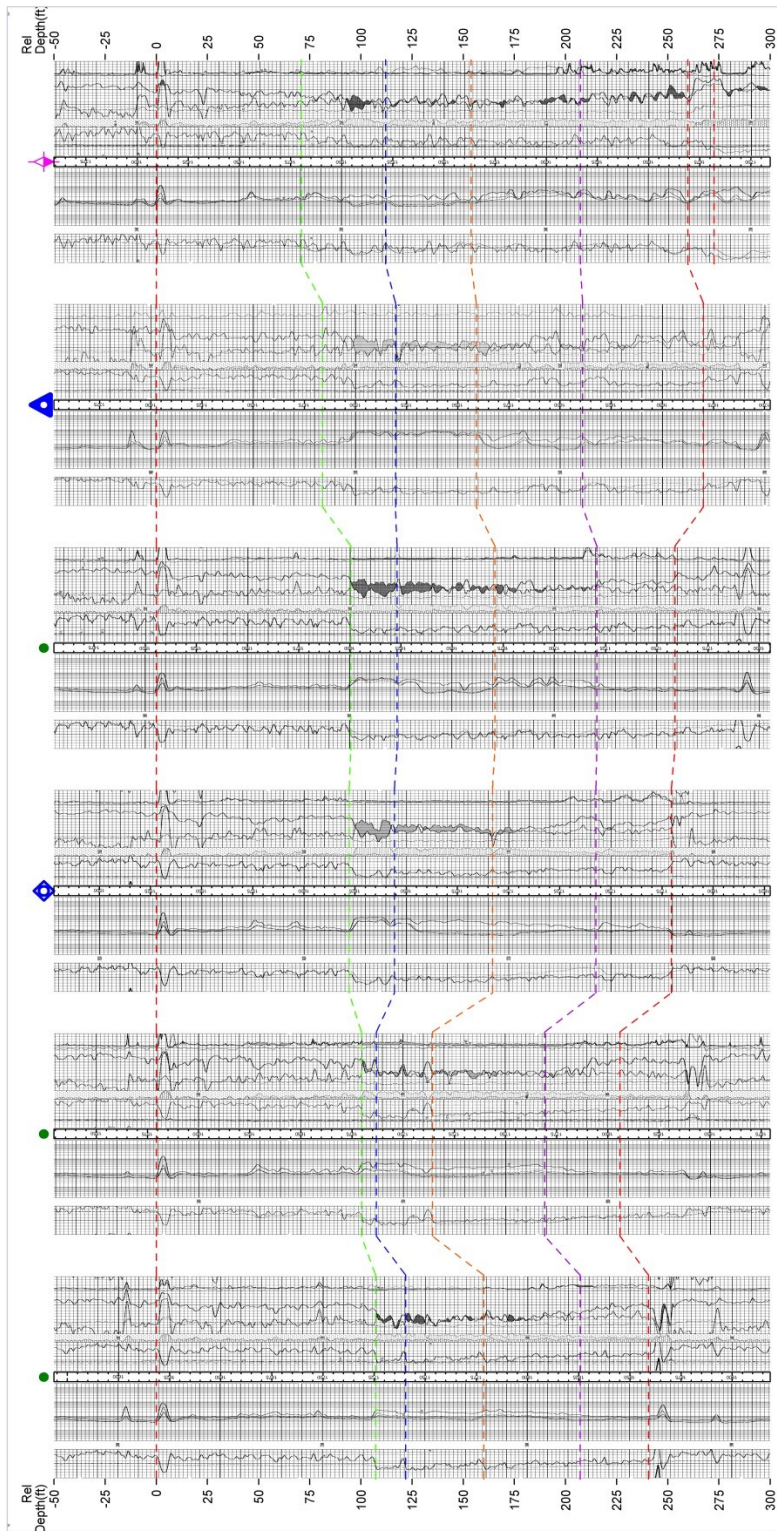
Horizontal Scale = 32.5  
Vertical Scale = 25 ft, 1s


TOPS AND MARKERS

- Cleveland A
- Cleveland B
- Cleveland C
- Cleveland Base
- Checkboard

By Curtis Rudy  
July 21, 2011 7:20 PM

MRN 12120117.2632 PM (New 031)

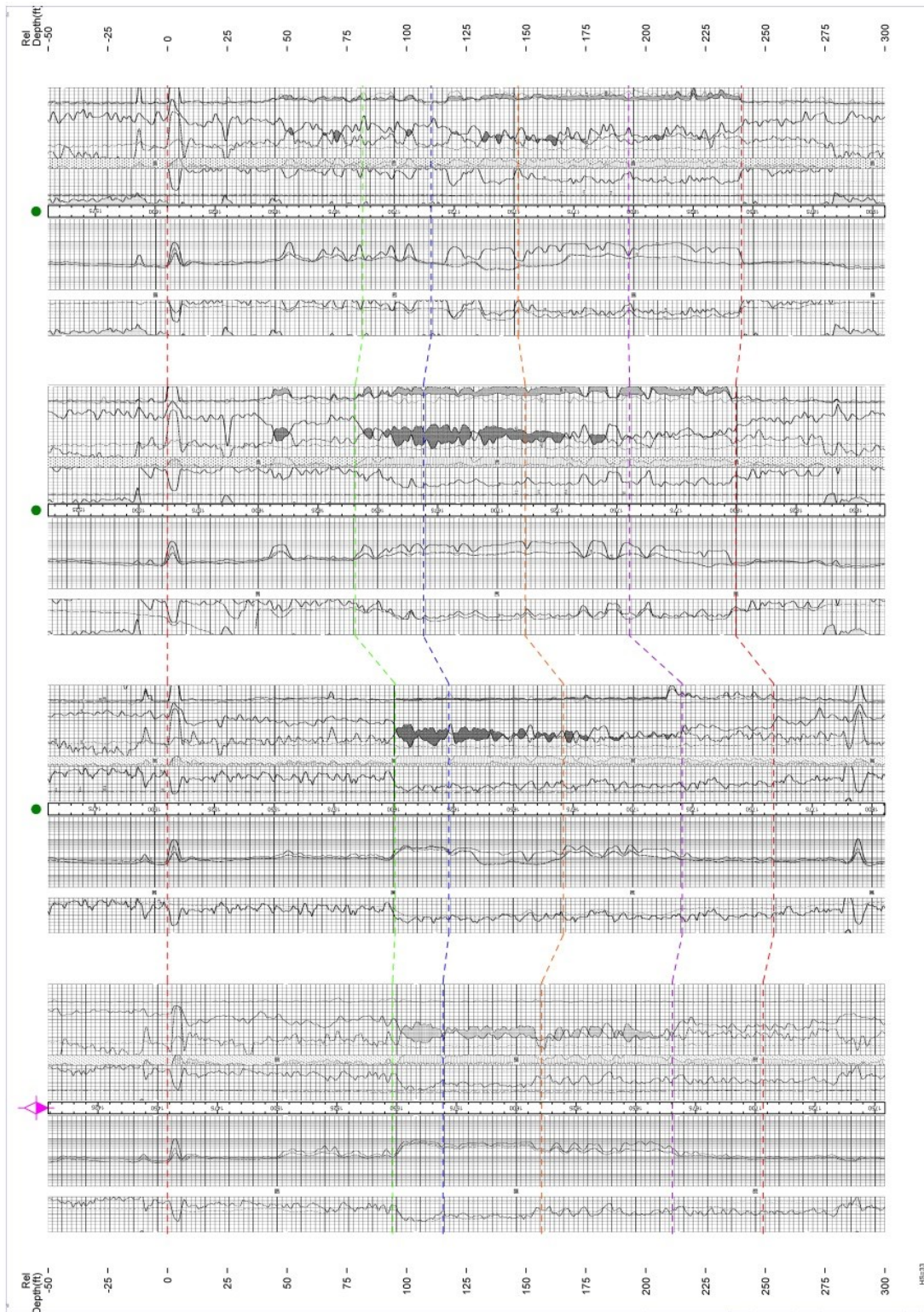


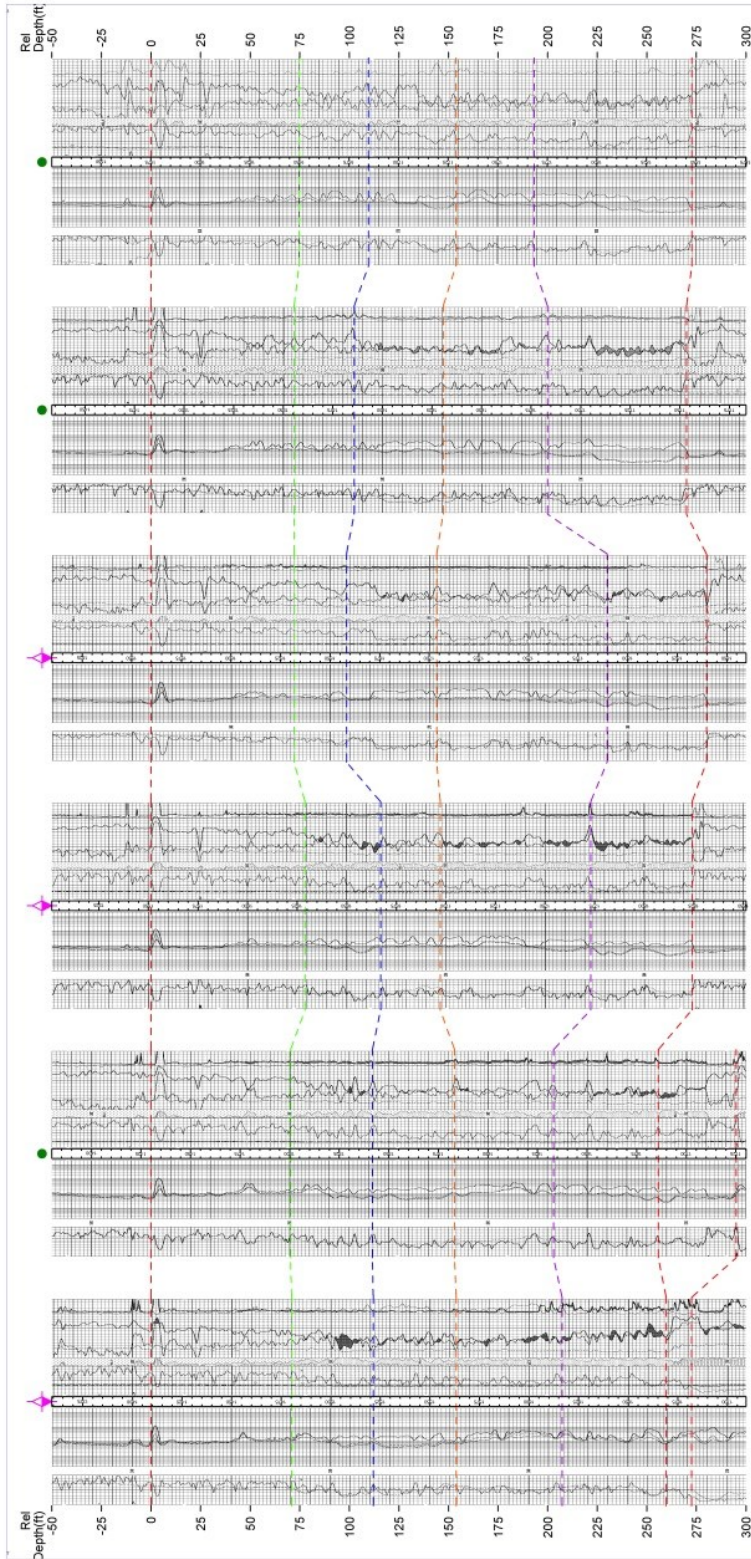

**Mid-Con Energy**  
 Cleveland Field Unit  
**B to B'**  
**Cleveland Sandstone**  
 Horizontal Scale = 32.5  
 Vertical Exaggeration = 1.3x  
**TOPS AND MARKERS**  
 --- BIG LINE  
 --- Cleveland A  
 --- Cleveland B  
 --- Cleveland C  
 --- Cleveland D  
 --- Cleveland Base  
 --- Checkboard  
 ---

By: Curtis Rudy

July 21, 2014 7:28 PM

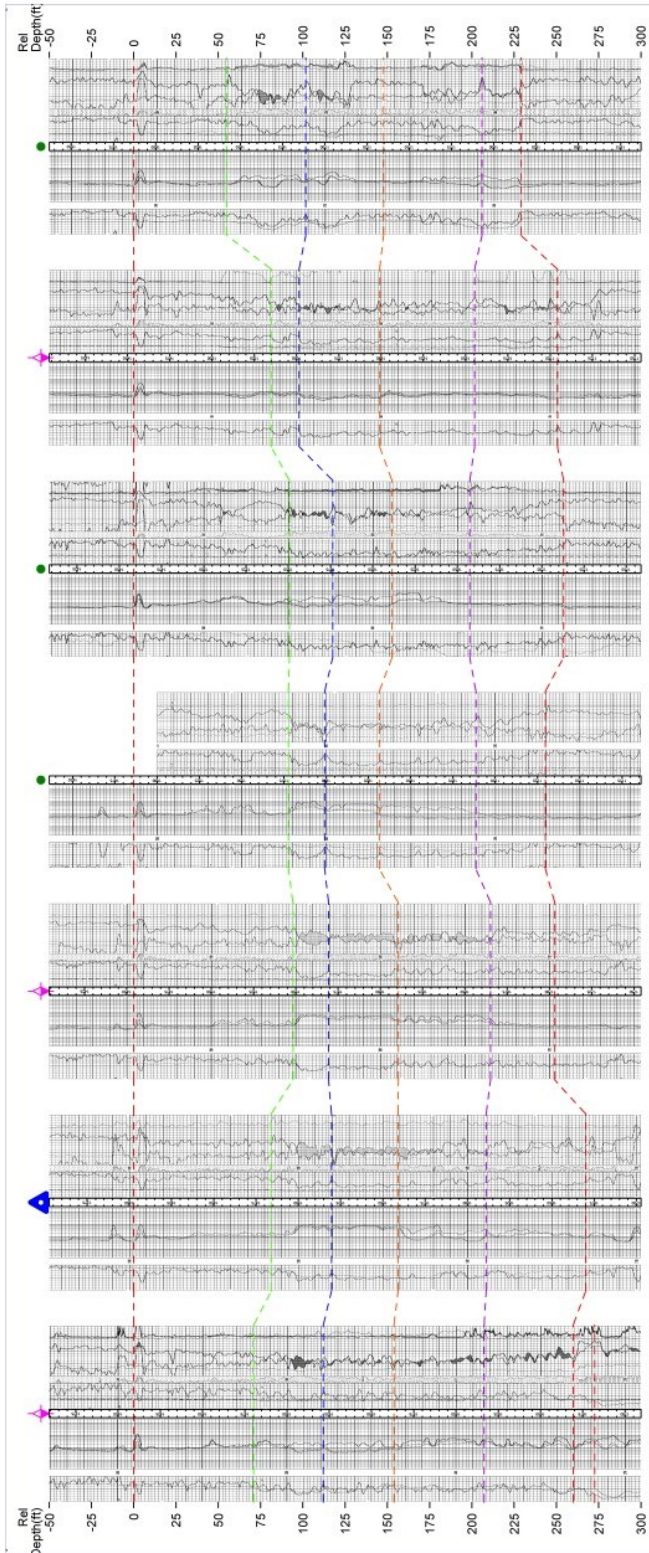
16033  
 P:\2014\07\21\2014-07-21-08 PM (Thurs CDT)





	
<b>Mid-Con Energy</b> Cleveland Field Unit	
<b>D to D'</b>	
<b>Cleveland Sandstone</b> Horizontal Scale = 12.5 Vertical Exaggeration = 1.2x	
<b>TOPS AND MARKERS</b>	
	BIG LINE
	Cleveland A
	Cleveland B
	Cleveland D
	Cleveland Base
	Cleveland
By: Curtis Roddy July 21, 2014 7:30 PM	





  
**Mid-Con Energy**  
 Cleveland Field Unit

**E to E'**

**Cleveland Sandstone**

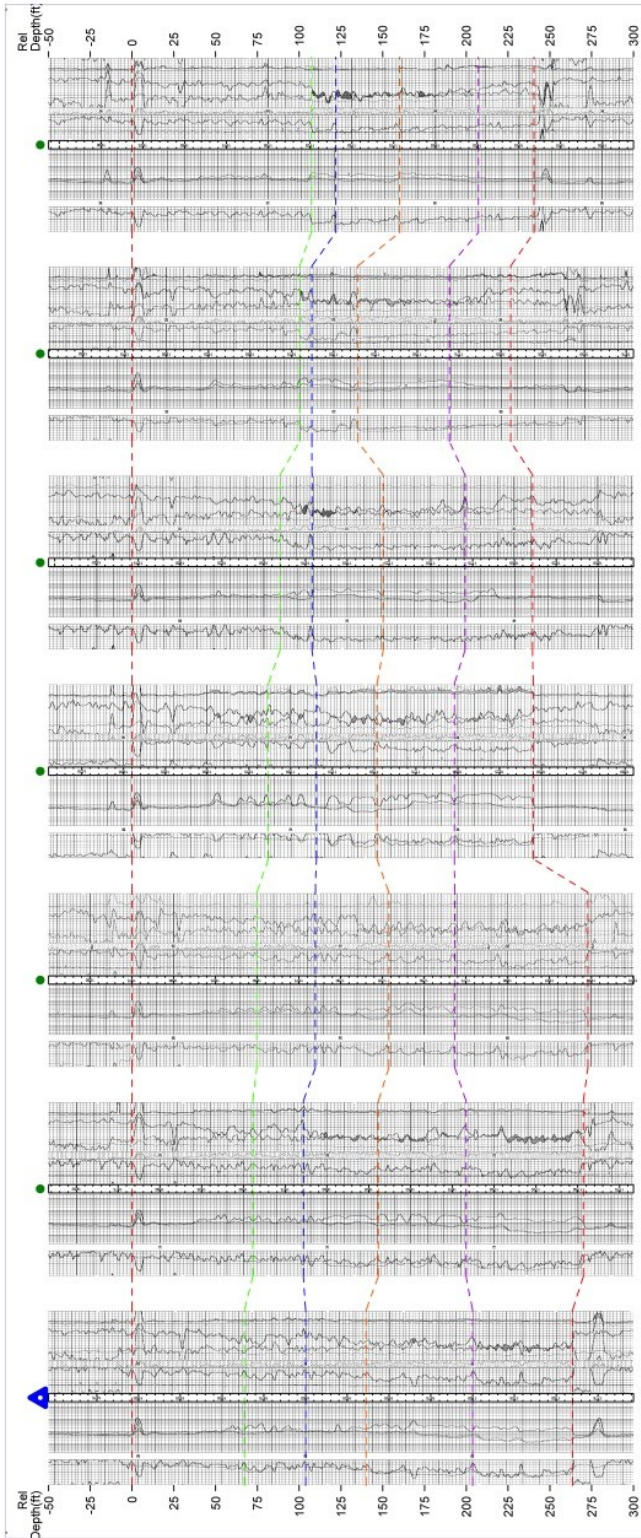
Horizontal Scale = 32.5  
 Vertical Exaggeration = 1.3x

**TOPS AND MARKERS**

- BIG LINE
- Cleveland A
- Cleveland B
- Cleveland C
- Cleveland D
- Cleveland Base
- Cleveland#1

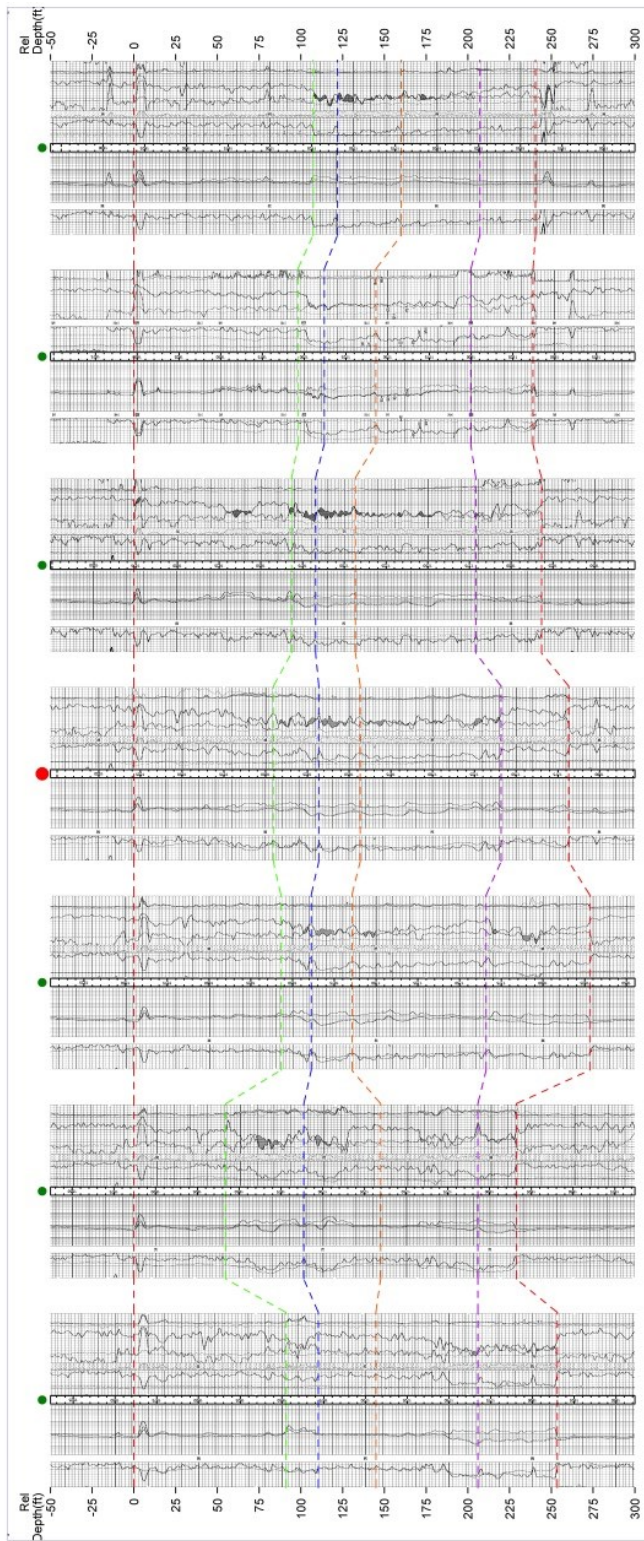
By: Curtis Rocky  
 JULY 21, 2014 7:31 PM

PETWA 12120641 3:13:30 PM (PHEAC.GST)

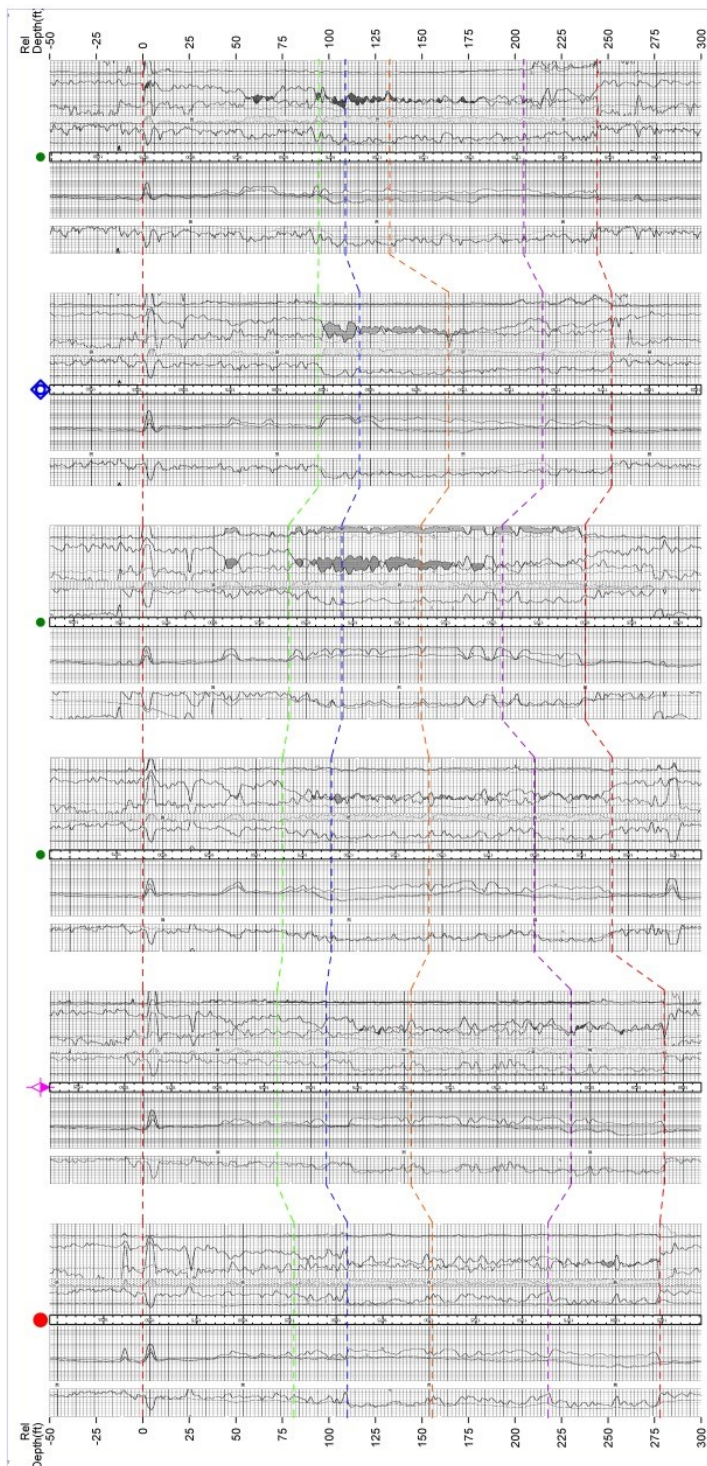


	
<b>Mid-Con Energy</b>	
Cleveland Field Unit	
F to F'	
<b>Cleveland Sandstone</b>	
Horizontal Scale = 32.5	
Vertical Exaggeration = 1.3x	
TOPS AND MARKERS	
—	Cleveland A
—	Cleveland B
—	Cleveland C
—	Cleveland D
—	Cleveland Base
—	Cleveland
By: Chris Rocky	
JUL 21 2014 7:52 AM	

PE:BNV17012014132511.MW (Theac.G37)



	
<b>Mid-Con Energy</b>	
Cleveland Field Unit	
<b>G to G'</b>	
<b>Cleveland Sandstone</b>	
Horizontal Scale = 32.5 Vertical Exaggeration = 1.3x	
TOPS AND MARKERS	
— Green —	Cleveland A
— Blue —	Cleveland B
— Orange —	Cleveland C
— Purple —	Cleveland D
— Red —	Cleveland Base
— Dashed —	Cleveland
By: Curtis Rocky JUN 23, 2014, 7:33 PM PETRA 7/21/2014 2:23:54 PM (Thea.CST)	



	<b>Mid-Con Energy</b>
	Cleveland Field Unit
<b>H to H'</b>	
<b>Cleveland Sandstone</b>	
Vertical Scale = 25.0	
Vertical Exaggeration = 1.5x	
<b>TOPS AND MARKERS</b>	
—	Cleveland A
—	Cleveland B
—	Cleveland C
—	Cleveland D
—	Cleveland E
—	Chickensound
By: Curtie Robby	
July 21, 2014 7:30 PM	

148308  
 P:\104\_101701614\_136\_12104 (ThruMid-CON)

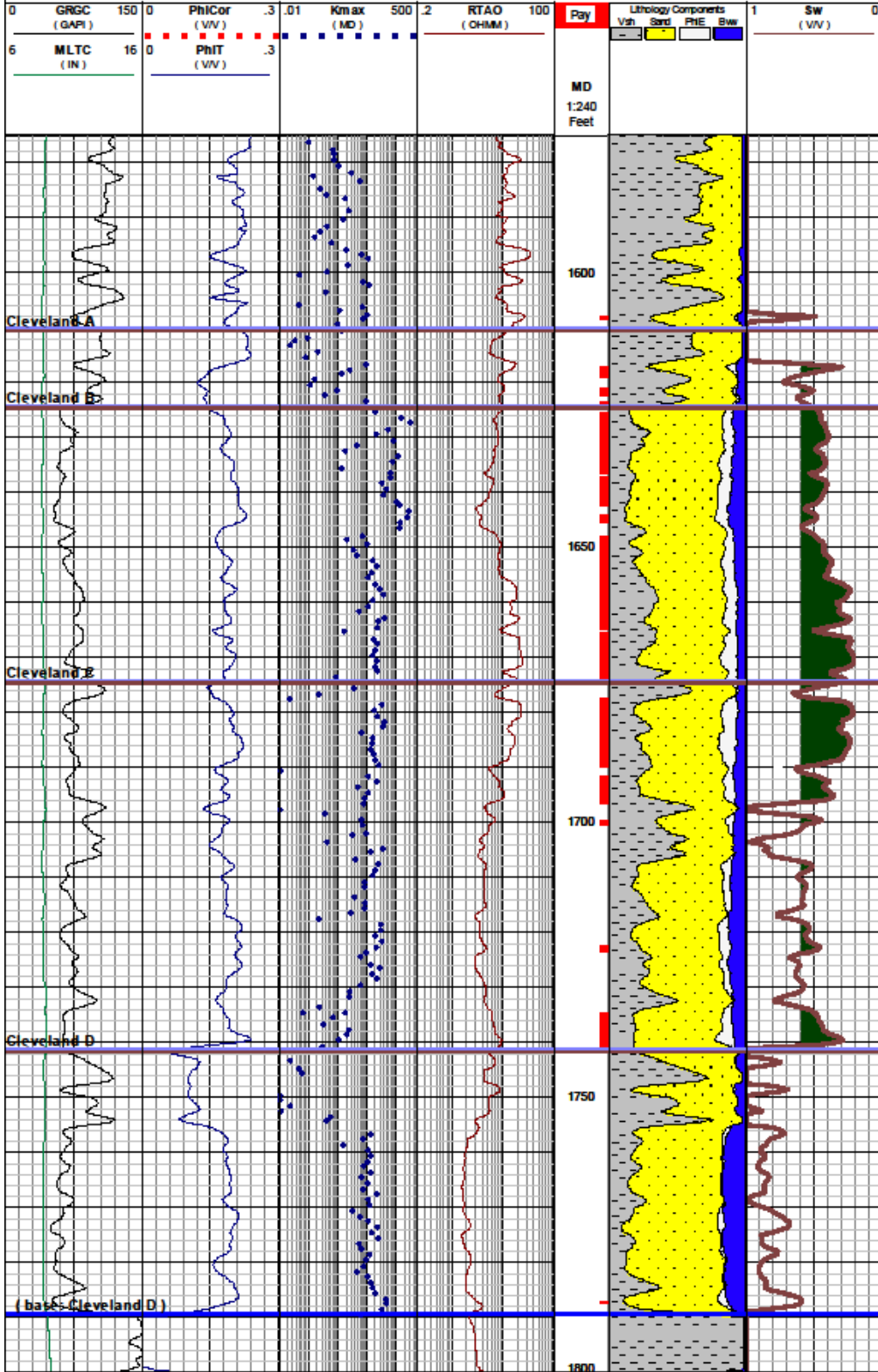
## APPENDICES

Appendix F – Petrophysical Evaluation of the J.A Jones #58

Operator: MID-CON ENERGY OPERATING  
 Well Name: J.A. JONES #58  
 Field Loc.: 165 FNL & 330 FEL NE-NE-NW  
 Field Name: CLEVELAND

KB: 822 feet  
 GL: 812 feet

Legal 1:  
 Legal 2: not available  
 County / Parish: PAWNEE  
 State / Province: PAWNEE/ OKLAHOMA



VITA

Curtis Martin Roddy

Candidate for the Degree of

Master of Science

Thesis: A RESERVOIR CHARACTERIZATION OF THE MIDDLE PENNSYLVANIAN CLEVELAND SANDSTONE, CLEVELAND FIELD UNIT, PAWNEE COUNTY, OKLAHOMA.

Major Field: Geology

Biographical:

Personal Data: Born in Dallas, Texas, on December 6, 1989, the son of George and Laura Roddy.

Education: Graduated from Faith Christian School, Grapevine, Texas in May 2008; received Bachelor of Science degree in Geology from Oklahoma State University in December 2012. Completed the requirements for the Masters of Science degree with a major in Geology in July 2014.

Experience: Employed by Weinkauf Petroleum as an intern geologist from April 2011 to August 2011. Employed by Mid-Con Energy as a full-time staff geologist from June 2013 to present

Professional Memberships: American Association of Petroleum Geologists, Society of Petroleum Engineers, Society of Petrophysicists and Well Log Analysts, Tulsa Geological Society, Chairman of Young Geology Professionals of Tulsa (part of Tulsa Geological Society).